

CONTENTS

Mathematics

Brahim Mittou. New properties of an arithmetic function	5
Bouharket Benaissa. Discussions on Hardy-type inequalities via Riemann-Liouville fractional integral inequality.....	12
E. Özkan T. Alp. B ₁ Gaussian Pell and Pell-Lucas polynomials	17
I. Laib, N. Rezzoug. On a sum over primitive sequences of finite degree	26
N. Yilmaz. The generalized bivariate Fibonacci and Lucas matrix polynomials.....	33

Mathematical physics

A.V. Kolesnichenko. Correct definition of internal energy at the phenomenological construction of model of multicomponent continuous medium by methods of nonequilibrium thermodynamics	45
-----------------------------------------------------------------------------------------------------------------------------------------------------------------------------------------------	----

Mathematical modeling

O.B. Feodoritova, M.M. Krasnov, N.D. Novikova, V.T. Zhukov. Multigrid method for numerical modelling of high temperature superconductors.....	72
V.I. Mazhukin, O.N. Koroleva, A.V. Shapranov, A.A. Aleksashkina, M.M. Demin. Molecular dynamics study of thermal hysteresis during melting-crystallization of noble metals	90

NEW PROPERTIES OF AN ARITHMETIC FUNCTION BRAHIM MITTOU

Department of Mathematics, University Kasdi Merbah Ouargla, Algeria
EDPNL & HM Laboratory of ENS Kouba, Algiers, Algeria
Corresponding author.E-mail: mathmittou@gmail.com

DOI:10.20948/mathmontis-2022-53-1

Summary. Recently the author and Derbal introduced and studied some elementary properties of arithmetic functions related the greatest common divisor. New properties of them are given in this paper.

1. INTRODUCTION

Throughout this paper, we let \mathbb{N}^* denote the set $\mathbb{N} \setminus \{0\}$ of positive integers and we let (m, n) and $[m, n]$ denote, respectively, the greatest common divisor and the least common multiple of any two integers m and n . A sequence of positive integers $(a_n)_{n \geq 1}$ is simply denoted by a . Let the prime factorization of the positive integer $n > 1$ be

$$n = \prod_{i=1}^r p_i^{e_i}$$

where r, e_1, e_2, \dots, e_r are positive integers and p_1, p_2, \dots, p_r are different primes.

In number theory, an arithmetic function, is a function whose domain is the positive integers and whose range is a subset of the complex numbers. Their various properties were studied by several authors (see e.g., [1-4]) and they still represent an important research topic up to now. Recently, the author and Derbal [5] introduced and studied some elementary properties of the following arithmetic function, for a positive integer α :

$$\left\{ \begin{array}{l} f_\alpha(1) = 1, \\ f_\alpha(n) = \prod_{i=1}^r p_i^{(e_i, \alpha)}, \end{array} \right.$$

which can be considered a generalization of the radical function, since

$$f_1(n) = \prod_{i=1}^r p_i = \text{rad}(n) \text{ for all } n.$$

In the present paper, we will discuss other properties of the functions f_α and will define new integer sequences related to them.

2010 Mathematics Subject Classification: 11A25, 11A05.

Key words and Phrases: Arithmetic function, Greatest common divisor, Strong divisibility sequence.

2. MAIN RESULTS

It can be easily seen that:

$$f_\alpha(mn) = f_\alpha(m)f_\alpha(n) \text{ whenever } (m, n) = 1 \quad (2.1)$$

which means that f_α is a multiplicative function, for all α . It is not completely multiplicative, since for a prime number p :

$$f_\alpha(p) = \begin{cases} p, & \text{if } \alpha \text{ is odd;} \\ p^2, & \text{if } \alpha \text{ is even.} \end{cases}$$

While

$$f_\alpha(p)f_\alpha(p) = p^2 \text{ for all } \alpha.$$

The next theorem gives a condition for m and n (which are not necessarily co-prime) to be satisfied the equation (2.1), for all even positive integers α .

Theorem 2.1 Let α be an even positive integers. Then

$$f_\alpha(mn) = f_\alpha(m)f_\alpha(n)$$

for all square-free positive integers m and n .

Proof. Let m and n be square-free positive integers. Then it follows that:

$$f_\alpha(mn) = \prod_{p|m, p \nmid n} p \prod_{q \nmid m, q|n} q \prod_{r|m, r|n} r^{(2, \alpha)}, \quad (2.2)$$

where p , q , and r are prime numbers. Also, we have

$$f_\alpha(m)f_\alpha(n) = mn = \prod_{p|m, p \nmid n} p \prod_{q \nmid m, q|n} q \prod_{r|m, r|n} r^2. \quad (2.3)$$

The right-hand sides of (2.2) and (2.3) are equal only if $(2, \alpha) = 2$, i.e., only if α is even, as claimed. The proof is complete.

Let α and k be positive integers. It is clear that if $(k, \alpha) = 1$, then $f_\alpha(n^k) = f_\alpha(n)$ for all $n \in \mathbb{N}^*$. In the general case we have the following theorem.

Theorem 2.2 Let the prime factorization of the positive integer $n > 1$ be $\prod_{i=1}^r p_i^{e_i}$. Let α and k be positive integers with $(k, \alpha) = d$. Then

$$f_\alpha(n^k) = \prod_{i=1}^r p_i^{\gamma_i d},$$

where $\gamma_i = \left(\frac{\alpha}{d}, e_i\right)$. In particular, if $(\alpha, e_i) = e$ ($1 \leq i \leq r$), then

$$f_\alpha(n^k) = f_\alpha(n)^l, \text{ with } l = \left(\frac{\alpha}{e}, k\right).$$

Proof. According to [6, Ex. 24, p. 22] we have the following multiplicative property of the greatest common divisor. If $a, b, h,$ and k be positive integers, then

$$(ah, bk) = (a, b)(h, k) \left(\frac{a}{(a, b)}, \frac{k}{(h, k)} \right) \left(\frac{b}{(a, b)}, \frac{h}{(h, k)} \right).$$

By taking $h = 1$ we obtain

$$(a, bk) = (a, b) \left(\frac{a}{(a, b)}, k \right).$$

It follows by using this fact that:

$$\begin{aligned} f_\alpha(n^k) &= f_\alpha \left(\prod_{i=1}^r p_i^{ke_i} \right) \\ &= p_1^{(ke_1, \alpha)} p_2^{(ke_2, \alpha)} \dots p_r^{(ke_r, \alpha)} \\ &= p_1^{(k, \alpha) \left(\frac{\alpha}{(a, k)}, e_1 \right)} p_2^{(k, \alpha) \left(\frac{\alpha}{(a, k)}, e_2 \right)} \dots p_r^{(k, \alpha) \left(\frac{\alpha}{(a, k)}, e_r \right)} \\ &= \prod_{i=1}^r p_i^{\gamma_i d}, \end{aligned}$$

where $\gamma_i = \left(\frac{\alpha}{d}, e_i \right)$, as claimed. The proof is finished.

Theorem 2.3 Let α be a positive integer. Then the following two systems of inequalities:

$$\left\{ \begin{array}{l} m < n \\ f_\alpha(m) < f_\alpha(n) \end{array} \right. \text{ and } \left\{ \begin{array}{l} m < n \\ f_\alpha(m) > f_\alpha(n) \end{array} \right.$$

hold for infinitely many positive integers m and n .

Proof. Let us distinguish the following two cases:

Case 1: If $\alpha = 1$. For the first system, let m be a positive integer and let n be any square-free number such that $m < n$. Then

$$f_\alpha(m) \leq m < n = f_\alpha(n),$$

which confirms the first system. For the second one, let p and q be prime numbers with $p < q$. Let

$$S := \{a \in \mathbb{N}^*; p^a > q\}.$$

Clearly $S \neq \emptyset$ and it contains infinitely many elements. We put $m = q$ and $n = p^s$, where $s \in S$. From which $m < n$ and

$$f_\alpha(q) = q > p = f_\alpha(p^s) \Rightarrow f_\alpha(m) > f_\alpha(n),$$

this confirms the second system.

Case 2: If $\alpha > 1$. Let M be the set of the positive multiples of α and let $k \in M$. So $(k, \alpha) = \alpha$, $k - 1 \notin M$ since $\alpha > 1$, and $(k - 1, \alpha) < \alpha$. Now we put $m = \varphi(2^k) = 2^{k-1}$, where φ is the totient's Euler function (see e.g., [6, Chapter 2]) and $n = 2^k$. Clearly, $m < n$ and we have

$$\begin{aligned}
 f_\alpha(\varphi(2^k)) &= f_\alpha(2^{k-1}) \\
 &= 2^{(k-1, \alpha)} \\
 &< 2^\alpha \quad (\text{since } (k-1, \alpha) < \alpha) \\
 &= 2^{(k, \alpha)} \quad (\text{since } k \in M) \\
 &= f_\alpha(2^k) \\
 &\Rightarrow f_\alpha(m) < f_\alpha(n),
 \end{aligned}$$

from which the validity of the first system follows. Next, let us choose an integer k such that $k-1 \in M$. So $k \notin M$, $(k-1, \alpha) = \alpha$ and $(k, \alpha) < \alpha$. If we put $m = \varphi(p^k)$ and $n = p^k$, where p is an odd prime, then we have $m < n$ and

$$\begin{aligned}
 f_\alpha(\varphi(p^k)) &= f_\alpha((p-1)p^{k-1}) \\
 &= f_\alpha(p-1)f_\alpha(p^{k-1}) \quad (\text{since } (p-1, p^{k-1}) = 1) \\
 &= f_\alpha(p-1)p^{(k-1, \alpha)} \\
 &> p^{(k-1, \alpha)} \quad (\text{since } f_\alpha(p-1) > 1) \\
 &> 2^{(k, \alpha)} \quad (\text{since } (k-1, \alpha) = \alpha > (k, \alpha)) \\
 &= f_\alpha(p^k) \\
 &\Rightarrow f_\alpha(m) > f_\alpha(n),
 \end{aligned}$$

which confirms the second system and completes this proof.

Theorem 2.4 Let $n > 1$ be an integer and let d be a proper positive divisor of n . Then we have

1. If n is a square-free number, then $f_\alpha(d)|f_\alpha(n)$ ($\forall \alpha \in \mathbb{N}^*$).
2. If d is a square-free number, then $f_\alpha(d)|f_\alpha(n)$ ($\forall \alpha \in \mathbb{N}^*$).
3. If n and d are not square-free number, then there are infinitely many positive integers α such that $f_\alpha(d)|f_\alpha(n)$.

Proof. Let the prime factorization of the positive integer $n > 1$ be $\prod_{i=1}^r p_i^{e_i}$. It is well known that the positive divisors of n are all integers of the form $\prod_{i=1}^r p_i^{h_i}$ with $0 \leq h_i \leq e_i$ ($1 \leq i \leq r$).

1. If n is a square-free integer, then d must itself to be a square-free. According to [5, Theorem 2.1] we can write

$$f_\alpha(d) = d|n = f_\alpha(n) \quad (\forall \alpha \in \mathbb{N}^*),$$

which proves the first property.

2. Suppose that d is a square-free number, i.e., $h_i \leq 1$ ($1 \leq i \leq r$). Then

$$(h_i, \alpha) = 1 \leq (e_i, \alpha) \quad (1 \leq i \leq r \text{ and } \forall \alpha \in \mathbb{N}^*).$$

Therefore $f_\alpha(d) = d|f_\alpha(n)$ ($\forall \alpha \in \mathbb{N}^*$), as required.

3. We let e denote the least common multiple of e_1, e_2, \dots, e_r . Then it is well known [1, Theorem 2.3] that f_α is e -periodic function as a function of α , in other words $f_{\alpha+e}(n) = f_\alpha(n)$, for all α . It follows by taking $\alpha = ke, (k \in \mathbb{N}^*)$ that:

$$(h_i, \alpha) \leq h_i \leq e_i = (e_i, \alpha) \quad (1 \leq i \leq r),$$

from which the validity of the last property follows. The proof of the theorem is complete.

A sequence of positive integers $\mathbf{a} = (a_n)_{n \geq 1}$ is said to be a divisibility sequence if it satisfies, for all $n, m \geq 1$, the property:

$$n|m \Rightarrow a_n | a_m.$$

It is said to be a strong divisibility sequence if it satisfies, for $n, m \geq 1$, the stronger property:

$$(a_m, a_n) = a_{(m,n)}.$$

For any positive integer α we define \mathfrak{f}_α to be the sequence of integer such that $\mathfrak{f}_\alpha = \{f_\alpha(n); n \in \mathbb{N}^*\}$. For examples:

$$\mathfrak{f}_1 = \{1, 2, 3, 2, 5, 6, 7, 2, 3, 10, 11, 6, 13, 14, 15, 2, 17, 6, 19, 10, \dots\},$$

which is the sequence A007947 in the *On-Line Encyclopedia of Integer Sequences* (OEIS, see [7]).

$$\mathfrak{f}_2 = \{1, 2, 3, 4, 5, 6, 7, 2, 9, 10, 11, 12, 13, 14, 15, 4, 17, 18, 19, 20, \dots\},$$

which is the sequence A066990 in the (OEIS).

$$\mathfrak{f}_3 = \{1, 2, 3, 2, 5, 6, 7, 8, 3, 10, 11, 6, 13, 14, 15, 2, 17, 6, 19, 10, \dots\},$$

which is the sequence A331737 in the (OEIS).

$$\mathfrak{f}_4 = \{1, 2, 3, 4, 5, 6, 7, 2, 9, 10, 11, 12, 13, 14, 15, 16, 17, 18, 19, 20, \dots\}.$$

Theorem 2.5 Let $\mathfrak{F} := \{\mathfrak{f}_\alpha, \alpha \in \mathbb{N}^*\}$. Then \mathfrak{f}_1 is the only strong divisibility sequence in \mathfrak{F} .

Proof. It easy to show that \mathfrak{f}_1 is a strong divisibility sequence, since

$$(f_1(m), f_1(n)) = (m, n) = f_1((m, n)),$$

for all $m, n \in \mathbb{N}^*$. Now we assume that $\alpha \geq 2$ and we wish to prove that \mathfrak{f}_α is not a strong divisibility sequence. To do so, it suffices to prove that \mathfrak{f}_α is not a divisibility sequence, since every strong divisibility sequence is divisibility sequence. For a prime number p we have $p|p^{\alpha+1}$ but

$$f_\alpha(p^\alpha) = p^\alpha \nmid p = f_\alpha(p^{\alpha+1}),$$

which means that \mathfrak{f}_α is not a divisibility sequence. The proof is finished.

Definition 2.6 Let $A \subset \mathbb{N}$ be an infinite set. Then \mathbf{a} is said to be a A -strong divisibility sequence if it satisfies

$$(a_m, a_n) = a_{(m,n)} \text{ whenever } m, n \in A.$$

Theorem 2.7 Let $\alpha \geq 2$ be an integer. Then

1. f_α is a f_1 -strong divisibility sequence.
2. f_α is a \mathbb{P} -strong divisibility sequence, where \mathbb{P} is the set of all primes.

Proof.

1. The first item follows at once from [5, Theorem 2.1] which states that the square-free positive integers are the only integers satisfying $f_\alpha(n) = n$ for all positive integers α , so

$$f_\alpha((m, n)) = (m, n) = (f_\alpha(m), f_\alpha(n)) \quad (\forall m, n \in f_1 \text{ and } \forall \alpha \geq 2).$$

2. The second item follows from the following elementary property:

$$(m, n) = 1 \Rightarrow (f_\alpha(m), f_\alpha(n)) = 1.$$

This completes the proof of the theorem.

Remark 2.8 The second item of Theorem 2.7 remains true even when we replace \mathbb{P} with any infinite subset of \mathbb{N} which elements are pairwise co-prime.

We close the paper with the following theorem which proves existing, under some conditions on m and n , of a positive integer α such that $(f_\alpha(m), f_\alpha(n)) \neq f_\alpha((m, n))$.

Theorem 2.9 Let m and n be positive integer such that $p^r \parallel m$ and $p^s \parallel n$ for a prime p and positive integers r and s with $2 \leq r < s$ and $r \nmid s$. Then

$$(f_r(m), f_r(n)) \neq f_r((m, n))$$

Proof. On one hand

$$\begin{aligned} \begin{cases} p^r \parallel m \\ p^s \parallel n \end{cases} &\Rightarrow \begin{cases} p^{(r,r)} = p^r \parallel f_r(m) \\ p^{(s,r)} = p^{sr/[s,r]} \parallel f_r(n) \end{cases} \\ &\Rightarrow p^{\min(r, sr/[s,r])} \parallel (f_r(m), f_r(n)). \end{aligned}$$

We have $s < [s, r]$, since $r \nmid s$, so $\frac{sr}{[s,r]} < r$. Thus

$$p^{sr/[s,r]} \parallel (f_r(m), f_r(n)). \quad (2.4)$$

On the other hand,

$$\begin{aligned} p^r \parallel m &\Rightarrow p^r \parallel (m, n) \quad (\text{since } r < s) \\ &\Rightarrow p^r = p^{(r,r)} \parallel f_r((m, n)). \end{aligned} \quad (2.5)$$

Consequently, (2.4) and (2.5) show that $(f_r(m), f_r(n)) \neq f_r((m, n))$, which concludes this proof.

3. CONCLUSION

In this paper, we give some new interesting properties of the arithmetic functions f_α . For example we prove (Theorem 2.3) that the sequence $f_\alpha(n)$ ($n \in \mathbb{N}^*$) can not be monotonically increasing or decreasing for all α . Also, we show (Theorem 2.5) that the sequence f_1 (see A007947 in the OEIS) is a strong divisibility sequence. On the other hand, the purpose of our next papers will be the study their relationship with some other well-studied arithmetic functions. Also, we will try to find asymptotic formulas for the Dirichlet series associated with f_α and other sums related to them.

Acknowledgements: The author would like to thank the anonymous referee for their careful reading and valuable suggestions.

REFERENCES

- [1] H. N. Shapiro, "An arithmetic function arising from the φ function", *Amer. Math. Monthly*, **50**, 18-30 (1943).
- [2] R. Bellman and H.N. Shapiro, "On the normal order of arithmetic functions", *Proc. Nat. Acad. Sci.*, **38**, 884-886 (1952).
- [3] A. Derbal and M. Karras, "Valeurs moyennes d'une fonction liée aux diviseurs d'un nombre entier", *C. R. Acad. Sci. Paris, Ser. I*, **354**, 555-558 (2016).
- [4] R. Zurita, "Generalized alternating sums of multiplicative arithmetic functions", *J. Integer Sequences*, **23**, (2020).
- [5] B. Mittou and A. Derbal, "On new arithmetic function relative to a fixed positive integer. Part 1", *Notes on Number Theory and Discrete Mathematics*, **27**, 22-26 (2021).
- [6] T. M. Apostol, *Introduction to Analytic Number Theory*, Springer-Verlage, New York, (1976).
- [7] N. J. A. Sloane et al., "*The On-Line Encyclopedia of Integer Sequences*". Published electronically at <https://oeis.org/>, (Last modified April 18 06:51 EDT 2022).

Received, January 4, 2022

DISCUSSIONS ON HARDY-TYPE INEQUALITIES VIA RIEMANN-LIOUVILLE FRACTIONAL INTEGRAL INEQUALITY

BOUHARKET BENAÏSSA

Faculty of Material Sciences, University of Tiaret-Algeria.
Laboratory of Informatics and Mathematics, University of Tiaret. Algeria
Corresponding author-mail: Bouharket.benaïssa@univ-tiaret.dz

DOI: 10.20948/mathmontis-2022-53-2

Summary. In this paper, we have shown that in the article entitled “New Riemann-Liouville generalizations for some inequalities of Hardy type” the Theorem 3.3 is false and that a necessary condition on the order α must be in Theorem 3.1 and Theorem 3.2. Additionally, the correct Theorem 3.3 and a new result with negative parameter are given; these results will prove using the Hölder inequality, and reverse Hölder inequality.

1 INTRODUCTION

Hardy-type inequalities and inverse Hardy-type inequalities have an important place in analysis and its applications, they have given rise to various extensions and generalizations in recent years, see for example [1]-[2]. So much paper appeared in different form of calculus mathematics, with functions of two variables [3], through the Steklov operator [4], on time scales [5]-[6]. In 2016, the authors have obtained some new results about Hardy type inequalities via Riemann-Liouville fractional integral operators [7]. In Theorem 3.1, the passing from the inequality (3.15) to inequality (3.16) and in Theorem 3.2, the passing from the inequality (3.27) to inequality (3.28), for $a < t \leq x \leq b$ we have

$$x - t \leq b - t,$$

if we take the order $0 < \alpha < 1$, then

$$\int_a^b (x - t)^{\alpha-1} dt \geq \int_a^b (b - t)^{\alpha-1} dt,$$

if $\alpha \geq 1$, we get

$$\int_a^b (x - t)^{\alpha-1} dt \leq \int_a^b (b - t)^{\alpha-1} dt.$$

So, it is necessary to mentioned that $\alpha \geq 1$ in Theorem3.1, Corollary3.1 and Theorem3.2. Now, let show the Theorem3.3 is not correct. In the inequalities (3.35) and (3.36) the following formulas are given:

Let f, g be positive functions on $[a; b]$ and for $\alpha > 0$, $a < t \leq x \leq b$, we have the integral

$$\int_a^b (a - t)^{\alpha-1} g^{-q}(t) f^p(t) dt.$$

2010 Mathematics Subject Classification: 26A33, 26D10, 26D15.

Key words and Phrases: Integral inequalities, Riemann-Liouville integral, Hardy inequality.

So, we deduce that $(a - t) < 0$, then

for $0 < \alpha < 1$, we set $\alpha = \frac{1}{2}$, hence we get $(a - t)^{\alpha-1} = (a - t)^{-\frac{1}{2}}$ (contradiction) for $\alpha \geq 1$, we set $\alpha = \frac{3}{2}$, hence we get $(a - t)^{\alpha-1} = (a - t)^{\frac{1}{2}}$ (contradiction).

This implies that there existed errors in the proof of the inequalities (3.35) and (3.36) and that the Theorem 3.3 is not necessarily true. The correct versions of Theorem 3.3 will be proved in Section 2.

2 MAIN RESULTS

We present the correct version of the Theorem 3.3 according the right Riemann-Liouville fractional integral operator of order $\alpha > 0$, for a continuous function f on $[a, b]$ defined as

$$j_{a^+}^{\alpha} f(x) = \frac{1}{\Gamma(\alpha)} \int_a^x (x-t)^{\alpha-1} f(t) dt, \quad a < x \leq b. \quad (1)$$

Theorem 2.1. Let $f \geq 0$ and $g > 0$ on $[a; b] \subseteq [0; +\infty[$ such that g is non-decreasing. Then, for all $0 < p < 1$, $q > 0$, $0 < \alpha < \frac{1}{1-p}$, we have

$$\int_a^b \frac{(j_{a^+}^{\alpha} f(x))^p}{g^q(x)} dx \geq \frac{\Gamma^{1-p}(\alpha + 1)}{(\alpha(1-p) + 1)g^q(b)} [(b-a)^{\alpha(1-p)+1} j_{a^+}^{\alpha} f^p(b) - j_{a^+}^{\alpha} (f^p(b)(b-a)^{\alpha(1-p)+1})]. \quad (2)$$

Proof. (i) For $0 < p < 1$, Apply the reverse Hölder inequality for $\frac{1}{p} + \frac{1}{p'} = 1$, we get

$$\begin{aligned} \int_a^b \frac{(j_{a^+}^{\alpha} f(x))^p}{g^q(x)} dx &= \int_a^b g^{-q}(x) \left(\int_a^x \left[\frac{(x-t)^{\alpha-1}}{\Gamma(\alpha)} \right]^{\frac{1}{p'}} \left[\frac{(x-t)^{\alpha-1}}{\Gamma(\alpha)} \right]^{\frac{1}{p}} f(t) dt \right)^p dx \\ &\geq \frac{1}{\Gamma(\alpha)\Gamma^{p-1}(\alpha + 1)} \int_a^b g^{-q}(x)(x-a)^{\alpha(p-1)} \left(\int_0^x (x-t)^{\alpha-1} f^p(t) dt \right) dx, \end{aligned}$$

since g is non-decreasing function on $[t, b]$ and by using Fubini Theorem, we obtain

$$\begin{aligned} \int_a^b \frac{(j_{a^+}^{\alpha} f(x))^p}{g^q(x)} dx &\geq \frac{\Gamma^{1-p}(\alpha + 1)}{g^q(b)} \int_a^b \frac{f^p(t)}{\Gamma(\alpha)} (b-t)^{\alpha-1} \left(\int_t^b (x-a)^{\alpha(p-1)} dx \right) dt, \\ &= \frac{\Gamma^{1-p}(\alpha + 1)}{(\alpha(1-p) + 1)g^q(b)} \int_a^b \frac{f^p(t)}{\Gamma(\alpha)} (b-t)^{\alpha-1} ((b-a)^{\alpha(p-1)+1} - (t-a)^{\alpha(p-1)+1}) dt. \end{aligned}$$

Therefore

$$\int_a^b \frac{(j_{a^+}^{\alpha} f(x))^p}{g^q(x)} dx \geq \frac{\Gamma^{1-p}(\alpha + 1)}{(\alpha(1-p) + 1)g^q(b)} \left[\frac{(b-a)^{\alpha(p-1)+1}}{\Gamma(\alpha)} \int_a^b (b-t)^{\alpha-1} f^p(t) dt \right]$$

$$\begin{aligned}
 & -\frac{1}{\Gamma(\alpha)} \int_a^b (b-t)^{\alpha-1} f^p(t) (t-a)^{\alpha(p-1)+1} dt \Big] \\
 & = \frac{\Gamma^{1-p}(\alpha+1)}{(\alpha(1-p)+1)g^q(b)} \left[(b-a)^{\alpha(p-1)+1} j_{a^+}^\alpha f^p(b) - j_{a^+}^\alpha (f^p(b))(b-a)^{\alpha(p-1)+1} \right].
 \end{aligned}$$

This ends the proof.

Now we present a new result according the left Riemann-Liouville fractional integral operator of order $\alpha > 0$, for a continuous function f on $[a, b]$ defined as

$$j_{b^-}^\alpha f(x) = \frac{1}{\Gamma(\alpha)} \int_x^b (t-x)^{\alpha-1} f(t) dt, \quad a \leq x < b. \quad (3)$$

We need the following reverse Hölder inequality (see [8]):

If $p < 0$, $\frac{1}{p} + \frac{1}{p'} = 1$, $\Phi, \Psi > 0$ and $\Phi \in L_p(a, b)$, $\Psi \in L_{p'}(a, b)$, then

$$\int_a^b \Phi(t) \Psi(t) dt \geq \left(\int_a^b \Phi^p(t) dt \right)^{\frac{1}{p}} \left(\int_a^b \Psi^{p'}(t) dt \right)^{\frac{1}{p'}}. \quad (4)$$

Theorem 2. 2. Let $f \geq 0$ and $g > 0$ on $[a; b] \subseteq [0; +\infty[$ such that g is non-increasing. Then, for all $p < 0$, $\frac{1}{1-p} < \alpha$, we have

$$\begin{aligned}
 \int_a^b \frac{(j_{b^-}^\alpha f(x))^p}{g(x)} dx & \geq \frac{\Gamma^{1-p}(\alpha+1)}{(\alpha(1-p)-1)g(a)} \\
 [j_{b^-}^\alpha (f^p(a))(b-a)^{\alpha(p-1)+1} - (b-a)^{\alpha(p-1)+1} j_{b^-}^\alpha f^p(a)]. & \quad (5)
 \end{aligned}$$

Proof. (i) For $p < 0$, Apply the reverse Hölder inequality (4), we get

$$\begin{aligned}
 j_{b^-}^\alpha f(x) & = \int_x^b \left[\frac{(t-x)^{\alpha-1}}{\Gamma(\alpha)} \right]^{\frac{1}{p'}} \left[\frac{(t-x)^{\alpha-1}}{\Gamma(\alpha)} \right]^{\frac{1}{p}} f(t) dt \\
 & \geq \left(\frac{1}{\Gamma(\alpha+1)} (b-x)^\alpha \right)^{\frac{1}{p'}} \left(\frac{1}{\Gamma(\alpha)} \int_x^b (t-x)^{\alpha-1} f^p(t) dt \right)^{\frac{1}{p}}.
 \end{aligned}$$

Since $p < 0$, we get

$$\int_a^b \frac{(j_{b^-}^\alpha f(x))^p}{g(x)} dx \leq \frac{\Gamma^{1-p}(\alpha+1)}{\Gamma(\alpha)} \int_a^b g^{-1}(x) (b-x)^{\alpha(p-1)} \left(\int_x^b (t-x)^{\alpha-1} f^p(t) dt \right) dx,$$

Since g is non-increasing function on $[a; t]$ and by using Fubini Theorem, we obtain

$$\int_a^b \frac{(j_{b^-}^\alpha f(x))^p}{g(x)} dx \leq \frac{\Gamma^{1-p}(\alpha+1)}{g(a)} \int_a^b \frac{f^p(t)}{\Gamma(\alpha)} (t-a)^{\alpha-1} \left(\int_a^t (b-x)^{\alpha(p-1)} dx \right) dt,$$

$$= \frac{\Gamma^{1-p}(\alpha + 1)}{(\alpha(1-p) - 1)g(a)} \int_a^b \frac{f^p(t)}{\Gamma(\alpha)} (t-a)^{\alpha-1} ((b-t)^{\alpha(p-1)+1} - (b-a)^{\alpha(p-1)+1}) dt.$$

This gives us that

$$\begin{aligned} \int_a^b \frac{(j_{b^-}^\alpha f(x))^p}{g(x)} dx &\leq \frac{\Gamma^{1-p}(\alpha + 1)}{(\alpha(1-p) - 1)g(a)} \left[\frac{1}{\Gamma(\alpha)} \int_a^b (t-a)^{\alpha-1} f^p(t) (b-t)^{\alpha(p-1)+1} dt \right. \\ &\quad \left. - \frac{(b-a)^{\alpha(p-1)+1}}{\Gamma(\alpha)} \int_a^b (t-a)^{\alpha-1} f^p(t) dt \right] \\ &= \frac{\Gamma^{1-p}(\alpha + 1)}{(\alpha(1-p) - 1)g(a)} [j_{b^-}^\alpha (f^p(a)(b-a)^{\alpha(p-1)+1}) - (b-a)^{\alpha(p-1)+1} j_{b^-}^\alpha f^p(a)]. \end{aligned}$$

So, the proof of Theorem 3.2. is complete.

Putting $\alpha = 1$ in above Theorem 2.2, we obtain the following Corollary.

Corollary 2.1. Let $f \geq 0$ and $g > 0$ on $[a; b] \subseteq [0; +\infty[$ such that g is non-increasing and $F(x) = \int_x^b f(t)dt$. Then, for all $p < 0$, we have

$$-p \int_a^b \frac{F^p(x)}{g(x)} dx \geq \frac{1}{g(a)} \left(\int_a^b (b-x)^p f^p(x) dx - (b-a)^p \int_a^b f^p(x) dx \right). \quad (6)$$

Remark4.1 The inequality (6) for negative parameter coincides with inequality (4.26) in [5].

3 CONCLUSIONS

In this paper, we present the correction of Theorem3.3 with the right-sided Riemann-Liouville operator with positive parameter $0 < p < 1$, we also introduced a new version using the left-sided Riemann-Liouville operator with the negative parameter. These results have been obtained by applying the Hölder’s inequality and the reverse Hölder’s inequality.

Acknowledgements: The authors also thank the anonymous referees for their valuable comments and suggestions which lead to the final version of this paper. This work was supported by the Directorate-General for Scientific Research and Technological Development (DGRSDT). Algeria.

REFERENCES

- [1] B. Benaissa, M.Z. Sarikaya, A. Senouci “On some new Hardy-type inequalities”, *Math. Meth. Appl.Sci*, **43**, 8488-8495 (2020). <https://doi.org/10.1002/mma.6503>
- [2] B. Benaissa, A. Benguassoum, “Reverses Hardy-type inequalities via Jensen integral inequality”, *Math. Montis.*, **52**, 43 - 51 (2021).
- [3] B. Benaissa, M.Z. Sarikaya, “Some Hardy-type integral inequalities involving functions of two independent variables”, *Positivity*, **25**, 853-866 (2021). <https://doi.org/10.1007/s11117-020-00791-5>
- [4] B. Benaissa, A. Senouci “Some new integral inequalities through the Steklov operator”, *Math. Montis.*, **49**, 49 - 56 (2020).
- [5] B. Benaissa, “Some Inequalities on Time Scales Similar to Reverse Hardy’s Inequality”, *Rad Hrvat. Akad. Znan. Umjet. Mat. Znan*, (2022), *Forthcoming papers (with pdf preview)*.

- [6] B. Benaissa, “More on Minkowski and Hardy integral inequality on time scales”, *Ric. di Mat.*, (2021). <https://doi.org/10.1007/s11587-021-00595-z>
- [7] A. Khameli, Z. Dahmani, K. Freha, and M. Z .Sarikaya, “New Riemann-Liouville generalizations for some inequalities of Hardy type”, *Malaya J. Mat.*, **4**(2), 277-283 (2016).
- [8] B. Benaissa, “On the Reverse Minkowski’s Integral Inequality”, *Kragujevac. J. Math.*, **46** (3), 407–416 (2022).

Received, March 3, 2022

BIGAUSSIAN PELL AND PELL-LUCAS POLYNOMIALS

E. ÖZKAN^{1*} AND T. ALP²

¹ Department of Mathematics, Faculty of Arts and Sciences, Erzincan Binali Yıldırım University.
Erzincan, Turkey.

² Graduate School of Natural and Applied Sciences, Erzincan Binali Yıldırım University. Erzincan,
Turkey.

*Corresponding author. E-mail: eozkan@erzincan.edu.tr or eozkanmath@gmail.com

DOI: 10.20948/mathmontis-2022-53-3

Summary. In this paper, we define biGaussian Pell and Pell-Lucas Polynomials. We give Binet's formulas, generating functions, Catalan's identities, Cassini's identities for these polynomials. Matrix presentations of biGaussian Pell and Pell-Lucas polynomials are found. Also, NegabiGaussian Pell and Pell-Lucas Polynomials are defined. Finally, we give some properties for these polynomials.

1 INTRODUCTION

Number sequences have a very important place in the world of science. Mankind has enabled the definition and development of new number systems in line with some needs over time. It appears not only in mathematics but also in nature, electromagnetic waves, quantum mechanics, series analysis, stock market, aesthetics and many other fields.

The most well-known of these number sequences is Fibonacci sequences which first appeared in Leonardo Fibonacci's book with a rabbit problem. This sequence, which is obtained by adding the two numbers before it; It continues as 1,1,2,3,5,8,13,21,34,55,89,144, 233, 377,... Fibonacci sequences appear in many branches of mathematics. These include calculus, group theory, applied mathematics, linear algebra, etc. [2, 3, 7, 8, 11, 12]

Many sequences have been defined by generalizing these number sequences. In addition to these numbers, appeared similar number sequences as Lucas numbers, Pell numbers and Jacobsthal numbers. [1, 14, 20, 23]

Koshy gave important relations about Fibonacci numbers, Lucas numbers and Pell numbers. Also, he gave the relations among these numbers. [9, 10]

Polynomials of sequences of numbers have also been studied by scientists. [6, 13, 15-17, 19, 22, 24]

Horadam, and Mahon [6] defined Pell and Pell - Lucas polynomials and gave their properties. Yağmur [25] defined the Gaussian Pell-Lucas polynomials and gave some properties of these polynomials. Özkan and Taştan [18] described Gauss Fibonacci and Gauss Pell polynomials and show that there is a relation between Gauss Fibonacci and Gauss Lucas polynomials. Halıcı and Öz [5] defined the Gaussian Pell and Pell-Lucas sequences and obtained some important identities involving the Gaussian Pell and Pell-Lucas numbers. Saba and Baussayoud [21] gave the new generating functions for the products of (p, q)-modified Pell numbers with Gaussian Jacobsthal and Gaussian Jacobsthal Lucas polynomials, Gaussian Pell and Gaussian Pell Lucas polynomials.

2010 Mathematics Subject Classification: 11B39, 11K31.

Key words and Phrases: BiGaussian Polynomials, Catalan's identity, Pell and Pell-Lucas polynomials, Generating functions.

One of the latest works in this area is [4] where Gökbaşı described a new type of Pell and Pell-Lucas numbers which are called biGaussian Pell and Pell-Lucas numbers.

In this work, we will introduce biGaussian Pell and Pell-Lucas Polynomials. In the following sections, biGaussian Pell and Pell-Lucas Polynomials will be defined. Some identities will be given for biGaussian Pell and Pell-Lucas Polynomials such as Binet's formulas, generating functions, Catalan's identities, Cassini's identities. Matrix presentations of biGaussian Pell and Pell-Lucas polynomials will be given. Also, NegabiGaussian Pell and Pell-Lucas Polynomials will be defined.

2 DEFINITIONS

2.1 Definition

The Pell Numbers P_n are defined by

$$P_n = 2P_{n-1} + P_{n-2}, n \geq 2$$

with $P_0 = 0$ and $P_1 = 1$.

2.2 Definition

The Pell-Lucas Numbers Q_n are given by

$$Q_n = 2Q_{n-1} + Q_{n-2}, n \geq 2$$

with $Q_0 = 2$ and $Q_1 = 2$.

2.3 Definition

The Pell Polynomials $P_n(x)$ are described by

$$P_n(x) = 2xP_{n-1}(x) + P_{n-2}(x), n \geq 2$$

with $P_0(x) = 0$ and $P_1(x) = 1$.

2.4 Definition

The Pell-Lucas Polynomials $Q_n(x)$ are described by

$$Q_n(x) = 2xQ_{n-1}(x) + Q_{n-2}(x), n \geq 2$$

with $Q_0(x) = 2$ and $Q_1(x) = 2x$.

2.5 Definition

BiGaussian Pell Numbers BGP_n [4] are defined as follows

$$BGP_n = \{P_n + iP_{n-1} + jP_{n-2} + ijP_{n-3} | P_n, nth \text{ Pell number}\}$$

$$BGP_n = 2BGP_{n-1} + BGP_{n-2}$$

where i and j satisfy the conditions $i^2 = -1$, $j^2 = -1$, $ij = ji$.

2.6 Definition

BiGaussian Pell-Lucas Numbers BGQ_n [4] are defined as follows

$$BGQ_n = \{Q_n + iQ_{n-1} + jQ_{n-2} + ijQ_{n-3} \mid Q_n, nth \text{ Pell - Lucas number}\}$$

$$BGQ_n = 2BGQ_{n-1} + BGQ_{n-2}.$$

3 MAIN RESULTS

3.1 Definition

BiGaussian Pell Polynomials $BGP_n(x)$ are defined as follows

$$BGP_n(x) = \{P_n(x) + iP_{n-1}(x) + jP_{n-2}(x) + ijP_{n-3}(x) \mid P_n(x), nth \text{ Pell polynomial}\}$$

$$BGP_n(x) = 2xBGP_{n-1}(x) + BGP_{n-2}(x).$$

3.2 Definition

BiGaussian Pell-Lucas Polynomials $BGQ_n(x)$ are defined as follows:

$$BGQ_n(x) = \{Q_n(x) + iQ_{n-1}(x) + jQ_{n-2}(x) + ijQ_{n-3}(x) \mid Q_n(x), nth \text{ Pell polynomial}\}$$

$$BGQ_n(x) = 2xBGQ_{n-1}(x) + BGQ_{n-2}(x).$$

3.3 Theorem

Binet formula for biGaussian Pell polynomials is given by

$$BGP_n(x) = \frac{\hat{\alpha}\alpha^{n-3}(x) - \hat{\beta}\beta^{n-3}(x)}{\alpha(x) - \beta(x)}$$

where $\hat{\alpha} = \alpha^3 + i\alpha^2 + j\alpha + ij$, $\alpha = x + \sqrt{x^2 + 1}$ and $\hat{\beta} = \beta^3 + i\beta^2 + j\beta + ij$,
 $\beta = x - \sqrt{x^2 + 1}$.

Proof.

$$\begin{aligned} BGP_n(x) &= P_n(x) + iP_{n-1}(x) + jP_{n-2}(x) + ijP_{n-3}(x) \\ &= \frac{\alpha^n(x) - \beta^n(x)}{\alpha(x) - \beta(x)} + i \frac{\alpha^{n-1}(x) - \beta^{n-1}(x)}{\alpha(x) - \beta(x)} + j \frac{\alpha^{n-2}(x) - \beta^{n-2}(x)}{\alpha(x) - \beta(x)} + ij \frac{\alpha^{n-3}(x) - \beta^{n-3}(x)}{\alpha(x) - \beta(x)} \\ &= \frac{\alpha^{n-3}(\alpha^3 + i\alpha^2 + j\alpha + ij) - \beta^{n-3}(\beta^3 + i\beta^2 + j\beta + ij)}{\alpha(x) - \beta(x)} = \frac{\hat{\alpha}\alpha^{n-3}(x) - \hat{\beta}\beta^{n-3}(x)}{\alpha(x) - \beta(x)}. \end{aligned}$$

In addition, we can indicate a matrix generator for the biGaussian Pell polynomials:

$$\begin{bmatrix} 2 & 1 \\ 1 & 0 \end{bmatrix}^n \begin{bmatrix} BGP_2(x) & BGP_1(x) \\ BGP_1(x) & BGP_0(x) \end{bmatrix} = \begin{bmatrix} BGP_{n+2}(x) & BGP_{n+1}(x) \\ BGP_{n+1}(x) & BGP_n(x) \end{bmatrix}$$

for $n \geq 1$.

We give the first 5 terms of biGaussian Pell polynomials in Table 1.

	$BGP_n(x)$
$n = 0$	$i - 2xj + (4x^2 + 1)ij$
$n = 1$	$1 + j - 2xij$
$n = 2$	$2x + i + ij$
$n = 3$	$4x^2 + 1 + 2xi + j$
$n = 4$	$8x^3 + 4x + (4x^2 + 1)i + 2xj + ij$

Table 1. Some terms of biGaussian Pell polynomials.

3.4 Theorem

Binet's formula for biGaussian Pell-Lucas polynomials is given by

$$BGQ_n(x) = \hat{\alpha}\alpha^{n-3}(x) + \hat{\beta}\beta^{n-3}(x).$$

Proof.

Binet's formula for biGaussian Pell-Lucas polynomials is obtained like the proof of Theorem 3.3.

Also, we can indicate a matrix generator for the biGaussian Pell-Lucas polynomials:

$$\begin{bmatrix} 2 & 1 \\ 1 & 0 \end{bmatrix}^n \begin{bmatrix} BGQ_2(x) & BGQ_1(x) \\ BGQ_1(x) & BGQ_0(x) \end{bmatrix} = \begin{bmatrix} BGQ_{n+2}(x) & BGQ_{n+1}(x) \\ BGQ_{n+1}(x) & BGQ_n(x) \end{bmatrix}$$

for $n \geq 1$.

We give some terms of biGaussian Pell-Lucas polynomials in Table 2.

	$BGQ_n(x)$
$n = 0$	$2 - 2xi + (4x^2 + 2)j - (8x^3 + 6x)ij$
$n = 1$	$2x + 2i - 2xj + (4x^2 + 2)ij$
$n = 2$	$4x^2 + 2 + 2xi + 2j - 2xij$
$n = 3$	$8x^3 + 6x + (4x^2 + 2)i + 2xj + 2ij$
$n = 4$	$16x^4 + 16x^2 + 2 + (8x^3 + 6x)i + (4x^2 + 2)j + 2xij$
$n = 5$	$32x^5 + 40x^3 + 10x + (16x^4 + 16x^2 + 2)i + (8x^3 + 6x)j + (4x^2 + 2)ij$

Table 2. Some terms of biGaussian Pell-Lucas polynomials.

3.5 Theorem

Catalan's identities for biGaussian Pell polynomials $BGP_n(x)$ and biGaussian Pell-Lucas polynomials $BGQ_n(x)$ are as follows, respectively.

- i. $(BGP_n(x))^2 - BGP_{n+r}(x)BGP_{n-r}(x) = 2(-1)^{n-r}[P_{r+2}(x) + P_{r-2}(x)]jP_r(x) + (-1)^{n-r}[P_{r-3}(x) - P_{r+3}(x) + P_{r+1}(x) - P_{r-1}(x)]ijP_r(x).$
- ii. $(BGQ_n(x))^2 - BGQ_{n+r}(x)BGQ_{n-r}(x) = 16(-1)^{n-r+1}[P_{r+2}(x) + P_{r-2}(x)]jP_r(x) + 8(-1)^{n-r}[P_{r+3}(x) - P_{r-3}(x) + P_{r-1}(x) - P_{r+1}(x)]ijP_r(x).$

Proof.

- i.
$$\begin{aligned} \text{LHS} &= (P_n(x) + iP_{n-1}(x) + jP_{n-2}(x) + ijP_{n-3}(x))(P_n(x) + iP_{n-1}(x) + jP_{n-2}(x) + ijP_{n-3}(x)) - \\ &\quad (P_{n+r}(x) + iP_{n+r-1}(x) + jP_{n+r-2}(x) + ijP_{n+r-3}(x))(P_{n-r}(x) + iP_{n-r-1}(x) + jP_{n-r-2}(x) + ijP_{n-r-3}(x)) \\ &= 2(-1)^{n-r}[P_{r+2}(x) + P_{r-2}(x)]jP_r(x) \\ &\quad + (-1)^{n-r}[P_{r-3}(x) - P_{r+3}(x) + P_{r+1}(x) - P_{r-1}(x)]ijP_r(x) \end{aligned}$$
- ii.
$$\begin{aligned} \text{LHS} &= (Q_n(x) + iQ_{n-1}(x) + jQ_{n-2}(x) + ijQ_{n-3}(x))(Q_n(x) + iQ_{n-1}(x) + jQ_{n-2}(x) + ijQ_{n-3}(x)) - \\ &\quad (Q_{n+r}(x) + iQ_{n+r-1}(x) + jQ_{n+r-2}(x) + ijQ_{n+r-3}(x))(Q_{n-r}(x) + iQ_{n-r-1}(x) + jQ_{n-r-2}(x) + ijQ_{n-r-3}(x)) \\ &= 16(-1)^{n-r+1}[P_{r+2}(x) + P_{r-2}(x)]jP_r(x) \\ &\quad + 8(-1)^{n-r}[P_{r+3}(x) - P_{r-3}(x) + P_{r-1}(x) - P_{r+1}(x)]ijP_r(x) \end{aligned}$$

3.6 Result

Cassini's identities for $BGP_n(x)$ and $BGQ_n(x)$ are as follows, respectively.

- i. $BGP_{n+1}(x)BGP_{n-1}(x) - (BGP_n(x))^2 = (-1)^n(8x^2 + 4)j - (-1)^n(8x^3 + 4x)ij$
- ii. $BGQ_{n+1}(x)BGQ_{n-1}(x) - (BGQ_n(x))^2 = (-1)^{n+1}(64x^2 + 32)j - (-1)^{n+1}(64x^3 + 32x)ij.$

Proof.

If it is taken $r = 1$ in the Catalan's identities, Cassini's identities are obtained.

3.7 Theorem

Generating functions for $BGP_n(x)$ and $BGQ_n(x)$ polynomials are as follows, respectively.

$$\begin{aligned}
 \text{i.} \quad h(t) &= \frac{i-2xj+(4x^2+1)ij+[1-2i+(4x^2+1)j-(8x^3+4x)ij]t}{1-2xt-t^2} \\
 \text{ii.} \quad m(t) &= \frac{2-2xi+(4x^2+2)j-(8x^3+6x)ij+[-2x+(4x^2+2)i-(8x^3+6x)j+(16x^4+16x^2+2)ij]t}{1-2xt-t^2}.
 \end{aligned}$$

Proof.

Let $h(t)$ be the generating function for biGaussian Pell polynomials as

$$h(t) = \sum_{n=0}^{\infty} BGP_n(x) t^n$$

Using $h(t)$, $2xth(t)$ and $t^2h(t)$, we get following equations

$$2xth(t) = \sum_{n=0}^{\infty} 2xBGP_n(x) t^{n-1}, \quad t^2h(t) = \sum_{n=0}^{\infty} BGP_n(x) t^{n+2}.$$

After needed calculations, the generating function for biGaussian Pell polynomials is obtained as

$$\begin{aligned}
 h(t) &= \frac{BGP_0(x) + [BGP_1(x) - 2xBGP_0(x)]t}{1 - 2xt - t^2} \\
 h(t) &= \frac{i - 2xj + (4x^2 + 1)ij + [1 - 2i + (4x^2 + 1)j - (8x^3 + 4x)ij]t}{1 - 2xt - t^2}
 \end{aligned}$$

Similarly, the generating function for biGaussian Pell-Lucas polynomials can be obtained.

3.8 Theorem

D’Ocagne’s identities for $BGP_n(x)$ and $BGQ_n(x)$ polynomials are as follows, respectively.

$$\begin{aligned}
 \text{i.} \quad & BGP_m(x)BGP_{n+1}(x) - BGP_{m+1}(x)BGP_n(x) = 12(-1)^{n-1}iP_{m-n+2}(x) + \\
 & 6jP_{m-n}(x)[(-1)^{2m-n} + (-1)^n] + 12(-1)^{n-1}ijP_{m-n+2}(x) \\
 \text{ii.} \quad & BGQ_m(x)BGQ_{n+1}(x) - BGQ_{m+1}(x)BGQ_n(x) = \\
 & 12[(-1)^{2m-n} + (-1)^n]iP_{m-n}(x) - 48j[(-1)^{2m-n} + (-1)^n]P_{m-n}(x) + \\
 & 96(-1)^n ijP_{m-n}(x).
 \end{aligned}$$

Proof.

$$\begin{aligned}
 \text{i.} \quad & BGP_m(x)BGP_{n+1}(x) - BGP_{m+1}(x)BGP_n(x) = (P_m(x) + iP_{m-1}(x) + \\
 & jP_{m-2}(x) + ijP_{m-3}(x))(P_{n+1}(x) + iP_n(x) + jP_{n-1}(x) + ijP_{n-2}(x)) - \\
 & (P_{m+1}(x) + iP_m(x) + jP_{m-1}(x) + ijP_{m-2}(x))(P_n(x) + iP_{n-1}(x) + jP_{n-2}(x) + \\
 & ijP_{n-3}(x)) \\
 & = 12(-1)^{n-1}iP_{m-n+2}(x) + 6jP_{m-n}(x)[(-1)^{2m-n} + (-1)^n] + 12(-1)^{n-1}ijP_{m-n+2}(x)
 \end{aligned}$$

$$\begin{aligned}
 \text{ii. } & BGQ_m(x)BGQ_{n+1}(x) - BGQ_{m+1}(x)BGQ_n(x) = (Q_m(x) + iQ_{m-1}(x) + \\
 & jQ_{m-2}(x) + ijQ_{m-3}(x))(Q_{n+1}(x) + iQ_n(x) + jQ_{n-1}(x) + ijQ_{n-2}(x)) - \\
 & (Q_{m+1}(x) + iQ_m(x) + jQ_{m-1}(x) + ijQ_{m-2}(x))(Q_n(x) + iQ_{n-1}(x) + \\
 & jQ_{n-2}(x) + ijQ_{n-3}(x)) \\
 & = 12[(-1)^{2m-n} + (-1)^n]iP_{m-n}(x) - 48j[(-1)^{2m-n} + (-1)^n]P_{m-n}(x) \\
 & \quad + 96(-1)^n ijP_{m-n}(x)
 \end{aligned}$$

3.9 Definition

NegabiGaussian Pell $BGP_{-n}(x)$ and negabiGaussian Pell-Lucas Polynomials $BGQ_{-n}(x)$ are defined as follows, respectively.

$$\begin{aligned}
 BGP_{-n}(x) &= \{P_{-n}(x) + iP_{-n-1}(x) + jP_{-n-2}(x) \\
 & \quad + ijP_{-n-3}(x) | P_{-n}(x), -nth \text{ Pell polynomial}\} \\
 BGQ_{-n}(x) &= \{Q_{-n}(x) + iQ_{-n-1}(x) + jQ_{-n-2}(x) \\
 & \quad + ijQ_{-n-3}(x) | Q_{-n}(x), -nth \text{ Pell polynomial}\}.
 \end{aligned}$$

3.10 Theorem

The following relations are satisfied for $BGP_n(x)$ and $BGQ_n(x)$ polynomials

- i. $2(xBGP_{n+1}(x) + BGP_n(x)) = BGQ_{n+1}(x)$
- ii. $2(BGP_{n+1}(x) - xBGP_n(x)) = BGQ_n(x)$
- iii. $BGP_{n+1}(x) + BGP_{n-1}(x) = BGQ_n(x)$
- iv. $BGP_{n+1}(x) - BGP_{n-1}(x) = 2xBGP_n(x)$
- v. $BGP_{n+2}(x) + BGP_{n-2}(x) = (4x^2 + 2)BGP_n(x)$
- vi. $BGP_{n+2}(x) - BGP_{n-2}(x) = 2xBGQ_n(x)$
- vii. $xBGQ_{n+1}(x) + BGQ_n(x) = (2x^2 + 2)BGP_{n+1}(x)$
- viii. $BGQ_{n+1}(x) - xBGQ_n(x) = (2x^2 + 2)BGP_n(x)$
- ix. $BGQ_{n+1}(x) + BGQ_{n-1}(x) = (4x^2 + 4)BGP_n(x)$
- x. $BGQ_{n+1}(x) - BGQ_{n-1}(x) = 2xBGQ_n(x)$
- xi. $BGQ_{n+2}(x) + BGQ_{n-2}(x) = (4x^2 + 2)BGQ_n(x)$
- xii. $BGQ_{n+2}(x) - BGQ_{n-2}(x) = (8x^3 + 8x)BGP_n(x)$

Proof:

They can be easily proven using the necessary definitions.

4 CONCLUSIONS

In this paper, we defined biGaussian Pell and Pell-Lucas Polynomials. We gave some terms of biGaussian Pell and Pell-Lucas polynomials in a table. NegabiGaussian Pell and Pell-Lucas Polynomials are defined. We also gave the Binet's formula, generating function, Catalan's identity, Cassini's identity. Moreover, matrix presentations of biGaussian Pell and Pell-Lucas polynomials are found. Finally, we gave some properties of these polynomials. In the future, this topic can be applied to other number sequences. Also, their polynomials, some identities, and properties of the number sequences can be defined.

Acknowledgements: The authors thank the editor and referees for helpful comments and advice.

REFERENCES

- [1] S. Çelik, E. Durukan, and E. Özkan, "New Recurrences on Pell Numbers, Pell-Lucas Numbers, Jacobsthal Numbers and Jacobsthal-Lucas Numbers", *Chaos, Solitons & Fractals*, 150, 111173 (2021).
- [2] Ö. Deveci, S. Hulku, A.G. Shannon, "On the Co-complex Type k-Fibonacci Numbers", *Chaos, Solutions & Fractals*, 153, 111522 (2021).
- [3] R.A. Dunlap, *The Golden Ratio and Fibonacci Numbers*, World Scientific, Canada, (1997).
- [4] H.A. Gökbaşı, "Note on biGaussian Pell and Pell-Lucas Numbers", *J. sci. arts*, **56**, 669-680 (2021).
- [5] S. Halıcı, and S. Öz, "On Some Gaussian Pell and Pell-Lucas numbers", *Ordu Univ. J. Sci. Tech.*, **6**(1), 8–18 (2016).
- [6] A.F. Horadam, and Bro. J. M. Mahon, "Pell and Pell - Lucas polynomials", *Fibonacci Q.*, **23**(1), 7–20 (1985).
- [7] A.F. Horadam, "A Generalized Fibonacci Sequence", *American Math. Monthly*, **68**, 455-459 (1961).
- [8] S.O. Karkuş and F.K. Aksoyak, "Generalized Bicomplex Numbers and Lie Groups", *Adv. In Appl. Clifford Algebras*, **25**, 943-963(2015).
- [9] T. Koshy, *Fibonacci and Lucas Numbers with Applications*, Canada: John Wiley & sons, inc. (2001).
- [10] T. Koshy, *Pell and Pell-Lucas Numbers with Applications*, New York: Springer (2014).
- [11] E. Özkan, "3-Step Fibonacci Sequences in Nilpotent Groups", *Appl. Math. Comput.*, **144**, 517-527 (2003).
- [12] E. Özkan, "On General Fibonacci Sequences in Groups", *Turk. J. Math.*, **27**, 525-537 (2003).
- [13] E. Özkan, İ. Altun, "Generalized Lucas Polynomials and Relationships between the Fibonacci Polynomials and Lucas Polynomials", *Commun. Algebra*, **47**, 10-12 (2019).
- [14] E. Özkan, A. Aydoğdu, İ. Altun, "Some Identities for A Family of Fibonacci and Lucas Numbers", *J. Math. Stat. Sci.*, **3**(10), 295-303 (2017).

- [15] E. Özkan, M. Taştan, “On A New Family of Gauss k-Lucas Numbers and Their Polynomials”, *Asian-Eur. J. Math.*, **14**, 2150101 (2021).
- [16] E. Özkan, M. Taştan, “On Gauss Fibonacci Polynomials, Gauss Lucas Polynomials and their Applications”, *Commun. Algebra*, **48**, 952-960 (2020).
- [17] E. Özkan, M. Taştan, “On Gauss k-Fibonacci Polynomials”, *EJMAA*, **9**, 124-130 (2021).
- [18] E. Özkan, M. Taştan and A. Aktaş, “On the new families of k-Pell numbers and k-PellLucas numbers and their polynomials”, *J. Contemp. Appl. Math.*, **11**(1), 16–30 (2021).
- [19] E. Özkan, M. Taştan, A. Aydoğdu, “2-Fibonacci Polynomials in the Family of Fibonacci Numbers”, *NNTDM*, **24**, 47-55 (2018).
- [20] E. Özkan, N.Ş. Yılmaz, and A. Wloch, “On $F_3(k, n)$ -Numbers of Fibonacci Type”, *Bol. Soc. Mat. Mex.*, **27**, 1-17 (2021).
- [21] N. Saba, and A. Baussayoud, “Generating functions of binary products of (p,q)-modified Pell numbers with Gaussian numbers and polynomials”, *Nonlinear Stud.*, **28**(4), 1311-1327 (2021).
- [22] A.G. Shannon, Ö. Deveci, “A Note On Coefficient Array of a Generalized of Fibonacci Polynomial”, *NNTDM*, **26**, 206-212 (2020).
- [23] A.G. Shannon, Ö. Erdağ, Ö. Deveci, “On Connections Between Pell Numbers and Fibonacci p-Numbers”, *NNTDM*, **27**(1), 148-160 (2021).
- [24] M. Taştan, E. Özkan, and A.G. Shannon, “The Generalized k-Fibonacci polynomials and Generalized k-Lucas Polynomials”, *NNTDM*, **27**(2), 148-158 (2021).
- [25] T. Yağmur, “Gaussian Pell-Lucas Polynomials”, *CMA*, **10**(4), 673-679 (2019).

Received, February 24, 2022

ON A SUM OVER PRIMITIVE SEQUENCES OF FINITE DEGREE

I. LAIB¹, N. REZZOUG^{2*}

¹ENSTP, GaridiKouba, 16051, Algiers, and Laboratory of Equations with Partial Non
Linear Derivatives, ENS Vieux Kouba, Algiers, Algeria.

²University of Tiaret, Computer and Mathematics Laboratory and University of Sidi Bel Abbes, Algeria.

*Corresponding author. E-mail: nadir793167115@gmail.com

DOI: 10.20948/mathmontis-2022-53-4

Summary. A sequence of strictly positive integers is said to be primitive if none of its terms divides the others and is said to be homogeneous if the number of prime factors of its terms counted with multiplicity is constant. In this paper, we construct primitive sequences A of degree d , for which the Erdős's analogous conjecture for translated sums is not satisfied.

1 INTRODUCTION

A sequence A of strictly positive integers is said to be primitive if there is no term of A which divides any other. We can see directly that the set of primes $P = (p_n)_{n \geq 1}$ is primitive. We define the degree of an integer, to be the number of prime factors counted with multiplicity and the degree of a sequence A is defined as the maximum degree of its terms. Erdős [1] showed that for any primitive sequence $A \neq \{1\}$, the series $\sum_{a \in A} \frac{1}{a \log a}$ converges. Later, in [2], he conjectured that if $A \neq \{1\}$, is a primitive sequence, then

$$\sum_{a \in A} \frac{1}{a \log a} \leq \sum_{p \in P} \frac{1}{p \log p}.$$

Based on the primitive sequences A of finite degree, in [3], Zhang proved this conjecture when the degree of A is at most 4 and in [4], he proved it for the particular case of primitive sequences when the degree of its terms is constant. In [5] the authors simplified the proof of [3] and Laib [6] improved this result up to degree 5. Recently, in [7], the authors studied translated sums of the form:

$$S(A, x) = \sum_{a \in A} \frac{1}{a (\log a + x)}, \quad x \in \mathbb{R}$$

and they constructed primitive sequences A of degree 2, such that $S(A, x) > S(P, x)$ for all $x \geq 81$ and in [8] the authors prove that $S(A, x) \gg S(P, x)$ for x large enough. In this note, we present a general case for any degree d , that is, we prove the following:

Theorem. Let $d \geq 2$ be an integer, $x_0 = \frac{d!e^{d+1}}{(d+1)^{d-1-d!}}$ and let k_0 be the greatest integer such that $p_{k_0} \leq e^{e^{d+1}}$. Then for any $k \geq k_0$ and any primitive sequence

$$B_d^k = \{p_1^{\alpha_1} p_2^{\alpha_2} \dots p_k^{\alpha_k}, \alpha_1 \dots \alpha_k \in \mathbb{N}, \alpha_1 + \dots + \alpha_k = d\} \cup \{p_n \mid p_n \in P, n > k\}$$

2010 Mathematics Subject Classification: Primary 11B73, Secondary 11B37, 11B13.

Key words and Phrases: Primitive Sequence, Prime Number, Erdős Conjecture, Degree.

we have $S(B_d^k, x) > S(P, x)$ for $x \geq x_0$.

2 MAIN RESULTS

Lemma 2.1. [9] For $x \geq 3275$ there exists a prime number p such that

$$x < p < x \left(1 + \frac{1}{2 \ln^2 x}\right).$$

Lemma 2.2. For any integer $n > 1$, we have

$$n! \leq n^n e^{1-n} \sqrt{n}, \quad (1)$$

$$2.5 n^n e^{1-n} \sqrt{n} < n! \leq n^{n-1}, \quad (2)$$

$$n! \leq 2(n+1)^{n-2}, \quad (3)$$

$$n! < n^{n-2} (n \geq 5). \quad (4)$$

Proof. For $n = 2$, the inequalities (1) and (2) is verified, for $n > 2$, it comes from the inequality [10]

$$n^n e^{-n} \sqrt{2\pi n} e^{\frac{1}{12n+1}} < n! < n^n e^{-n} \sqrt{2\pi n} e^{\frac{1}{12n}},$$

and we can prove (3) and (4) by induction.

Lemma 2.3. Let $n \geq 2$ be an integer and x be a reel number such that $x \geq n - 1$. The function

$$x \mapsto f_n(x) = \frac{nn! e^x}{x^{n-1} - n!}$$

reaches its minimum x_n in the interval $]n - 1, n + 1]$, moreover $x_2 = 2$, $x_3 = \sqrt{7} + 1$, $x_4 \simeq 4.298$ and $x_n < n$ for $n \geq 5$.

Proof. Let $n \geq 2$ be an integer and let f_n be the function defined on the interval $I =]n - 1; +\infty[$

$$f_n(x) = \frac{nn! e^x}{x^{n-1} - n!}$$

f is differentiable on I and

$$f'_n(x) = \frac{nn! e^x (x^{n-1} - (n-1)x^{n-2} - n!)}{(x^{n-1} - n!)^2}.$$

For $x > n - 1$, put $g_n(x) = x^{n-1} - (n-1)x^{n-2} - n!$

then

$$g'_n(x) = x^{n-1} - (n-1)x^{n-2} > 0, x \in I,$$

hence g_n increases on I . On the other hand, since g_n is continuous then by lemma 2.2, we have

$$\lim_{x \rightarrow n-1} g_n(x) = -n! < 0,$$

$$g_n(n) = n^{n-2} - n! > 0 \text{ for } n \geq 5,$$

$$g_n(n+1) = 2(n+1)^{n-2} - n! \geq 0,$$

therefore, there exists only one root $x_n \in]n-1, n+1]$, where for $n \geq 5$ $x_n \in]n-1, n]$, such that $f'_n(x_n) = 0$. Since $g_n(x) < 0$ for $x < x_n$ and $g_n(x) > 0$ for $x > x_n$ then f_n strictly decreases on $]n-1, x_n]$ and strictly increases on $[x_n, +\infty[$, so we have

$$f_n(x) \geq f_n(x_n) \text{ where } x_n \in]n-1, n+1].$$

It is clear that, for $n = 2, 3, 4$ the equation $x^{n-1} - (n-1)x^{n-2} - n! = 0$ gives $x_2 = 2$, $x_3 = \sqrt{7} + 1$ and $x_4 \simeq 4.298$. This completes the proof.

Lemma 2.4. For any integer $d \geq 2$, there exists a prime p such that

$$e^{e^{x_d}} < p \leq e^{e^{d+1}}, \quad (5)$$

moreover $\max\{p : p \in]e^{e^{x_d}}, e^{e^{d+1}}]\} > e^{e^d}$, where $(x_d)_{d \geq 2}$ is the sequence defined in lemma 2.3.

Proof. The inequality (5) is easy to verify for $d = 2, 3, 4$. By lemma 2.3, we have, for $d \geq 5$

$$d-1 \leq x_d \leq d, \quad (6)$$

therefore $e^{e^{x_d}} > 3275$, then from lemma 1.1 there exists a prime p such that

$$e^{e^{x_d}} < p \leq e^{e^{x_d}} \left(1 + \frac{1}{2e^{2x_d}}\right).$$

From (6) we get $4 \leq x_d \leq d$, then $1 + \frac{1}{2e^{2x_d}} < 2$ and $e^{e^{x_d}} < e^{e^d}$, thus $\left(1 + \frac{1}{2e^{2x_d}}\right) < 2e^{e^d} < e^{e^{d+1}}$. Since $4e^{e^d} < (e^{e^d})^2 < e^{e^{d+1}}$, then according to the Bertrand's postulate there exists a prime number in $[2e^{e^d}, 4e^{e^d}]$, thus, the greatest prime number in $[e^{e^{x_d}}, e^{e^{d+1}}]$ is greater than e^{e^d} . Which finishes the proof.

Lemma 2.5. [7] For any integer $k \geq 1$ and any integer $d \geq 2$, we define

$$A_d^k = \{p_1^{\alpha_1} p_2^{\alpha_2} \dots p_k^{\alpha_k}, \alpha_1, \dots, \alpha_k \in \mathbb{N}, \alpha_1 + \dots + \alpha_k = d\}$$

then we have the disjoint union

$$A_d^{k+1} = A_d^k \cup \{ap_{k+1} : a \in A_{d-1}^{k+1}\}.$$

Lemma 2.6. [11] For any real number $x > 1$, we have

$$\sum_{p \in P, p \leq x} \frac{1}{p} > \log \log x.$$

Lemma 2.7. Let $d \geq 2$ and let k' be the integer such that $p_{k'} \geq \exp \exp(d)$. For any real number $x > 0$ the sequence $\left(S(A_d^k, x)\right)_{k \geq k'}$ strictly increases.

Proof. For any integer $k \geq 1$ and any integer $d \geq 2$, the multinomial formula ensures that

$$\begin{aligned} \sum_{a \in A_d^k} \frac{1}{a} &= \sum_{\alpha_1 + \dots + \alpha_k = d} \frac{1}{p_1^{\alpha_1} p_2^{\alpha_2} \dots p_k^{\alpha_k}} \\ &\geq \sum_{\alpha_1 + \dots + \alpha_k = d} \frac{(1/p_1)^{\alpha_1}}{\alpha_1!} \dots \frac{(1/p_k)^{\alpha_k}}{\alpha_k!} \\ &= \frac{1}{d!} \left(\sum_{n=1}^k \frac{1}{p_n} \right)^d \end{aligned}$$

therefore

$$\sum_{a \in A_d^k} \frac{1}{a} \geq \frac{1}{d!} \left(\sum_{n=1}^k \frac{1}{p_n} \right)^d. \quad (7)$$

Put $A_d^k = \{p_n/p_n \in P, n > k\}$, then from lemma 2.5 we have

$$B_d^{k+1} = A_d^{k+1} \cup A^{k+1} = A_d^k \cup \{ap_{k+1} : a \in A_{d-1}^{k+1}\} \cup A^{k+1}$$

so,

$$S(B_d^{k+1}, x) = S(B_d^k, x) + E$$

where

$$E = \frac{1}{p_{k+1}} \left(S(A_{d-1}^{k+1}, \log p_{k+1} + x) - \frac{1}{\log p_{k+1} + x} \right).$$

Since p_{k+1}^{d-1} is the greatest element of A_{d-1}^{k+1} , we have

$$\begin{aligned} S(A_{d-1}^{k+1}, \log p_{k+1} + x) &= \sum_{a \in A_{d-1}^{k+1}} \frac{1}{a(\log a + \log p_{k+1} + x)} \\ &\geq \sum_{a \in A_{d-1}^{k+1}} \frac{1}{a((d-1)\log p_{k+1} + \log p_{k+1} + x)} \\ &\geq \frac{1}{d \log p_{k+1} + x} \sum_{a \in A_{d-1}^{k+1}} \frac{1}{a} \end{aligned}$$

and by lemma 2.6 we obtain

$$\begin{aligned} \sum_{a \in A_{d-1}^{k+1}} \frac{1}{a} &\geq \frac{1}{(d-1)!} \left(\sum_{n=1}^{k+1} \frac{1}{p_n} \right)^{d-1} \\ &\geq \frac{1}{(d-1)!} (\log \log p_{k+1})^{d-1} \end{aligned}$$

$$\begin{aligned} &\geq \frac{d^{d-1}}{(d-1)!} \\ &\geq \frac{d^{d-1}}{d!} d \text{ for } k \geq k', \end{aligned}$$

and according to lemma 2.2 we have $d! \leq d^{d-1}$, then

$$\sum_{a \in A_{d-1}^{k+1}} \frac{1}{a} \geq d \text{ for } k \geq k',$$

which implies

$$\begin{aligned} S(A_{d-1}^{k+1}, \log p_{k+1} + x) - \frac{1}{\log p_{k+1} + x} &> \frac{1}{d \log p_{k+1} + x} - \frac{1}{\log p_{k+1} + x} \\ &= \frac{dx - x}{(d \log p_{k+1} + x)(\log p_{k+1} + x)} > 0 \end{aligned}$$

thus $S(B_d^{k+1}, x) - S(B_d^k, x) > 0$. Which ends the proof.

Proof of theorem.

From [7], for any integer $k \geq 1$ and any integer $d \geq 2$, we have

$$\begin{aligned} \sum_{a \in B_d^k} \frac{1}{a(\log a + x)} &= \sum_{a \in A_d^k \cup A^k} \frac{1}{a(\log a + x)} = \sum_{a \in A_d^k} \frac{1}{a(\log a + x)} + \sum_{a \in A^k} \frac{1}{a(\log a + x)} \\ &\geq \frac{1}{d \log p_k + x} \sum_{a \in A_d^k} \frac{1}{a} + \sum_{n > k} \frac{1}{p_n(\log p_n + x)}. \end{aligned}$$

Using (7) and lemma 2.6, we get

$$\sum_{a \in A_d^k} \frac{1}{a} > \frac{(\log \log p_k)^{d-1}}{d!} \sum_{n=1}^k \frac{1}{p_n},$$

therefore

$$\begin{aligned} \sum_{a \in B_d^k} \frac{1}{a(\log a + x)} &\geq \frac{x(\log \log p_k)^{d-1}}{d!(d \log p_k + x)} \sum_{n=1}^k \frac{1}{x p_n} + \sum_{n > k} \frac{1}{p_n(\log p_n + x)} \\ &\geq \frac{x(\log \log p_k)^{d-1}}{d!(d \log p_k + x)} \sum_{n=1}^k \frac{1}{p_n(\log p_n + x)} + \sum_{n > k} \frac{1}{p_n(\log p_n + x)}. \end{aligned}$$

To obtain the inequality required in theorem, we must choose k and x so that

$$\frac{x(\log \log p_k)^{d-1}}{d!(d \log p_k + x)} > 1. \quad (8)$$

Since the function

$$x \mapsto h_{k,d}(x) = \frac{x(\log \log p_k)^{d-1}}{d!(d \log p_k + x)} \text{ for } d \geq 2, k > 1$$

strictly increases for $x > 0$, let x_0 the smallest value for which the inequality (8) is verified. That is

$$\frac{(\log \log p_k)^{d-1} - d!}{dd! \log p_k} > \frac{1}{x_0}. \quad (9)$$

Since $x_0 > 0$, we need to find k such that $(\log \log p_k)^{d-1} - d! > 0$, then by lemma 2.2, we just take $\log \log p_k > d$, and if we put $\log \log p_k = z$, then (9) becomes

$$\frac{dd! e^z}{z^{d-1} - d!} < x_0.$$

Now, we must choose z so that the number $\frac{dd! e^z}{z^{d-1} - d!}$ is the smallest possible. According to lemma 2.3, the function

$$x \mapsto f_d(x) = \frac{dd! e^x}{x^{d-1} - d!}$$

reaches its minimum x_d in

$$]d - 1, d + 1],$$

then we can take $z \in]x_d, d + 1[$ and $x_0 = \frac{dd! e^{d+1}}{(d+1)^{d-1} - d!}$, from lemma 2.4, there exists a prime integer p_k such that

$$x_d < \log \log p_k < d + 1.$$

Choose $p_{k_0} = \max \{p_k : \log \log p_k \in]x_d, d + 1]\}$ and $z = \log \log p_{k_0}$, then we obtain $S(B_d^{k_0}, x) > S(P, x)$ for $x \geq x_0$. Finally, by lemma 2.4, we have $e^{e^d} \leq p_{k_0} \leq e^{e^{d+1}}$ and from lemma 2.7, we get for $k \geq k_0, x \geq x_0$,

$$S(B_d^{k_0}, x) > S(P, x).$$

And the proof is achieved.

3 CONCLUSIONS

In this work, we obtain a generalization of result introduced in [7], concerning primitive sequences of finite degree, thus, if we take $d = 2$ in the theorem we get $S(B_2^k, x) > S(B_1^k, x)$, for $k \geq 27775592$ and $x \geq 81$, which apply to improve the results of [3,6]. Since for x is sufficiently large, we have $S(B_d^k, x) > S(P, x)$, so we can ask if it is true: for any $d \geq 1$ there exists k_0 such that $S(B_{d+1}^k, x) > S(B_d^k, x), k \geq k_0, x > 0$.

Acknowledgements: The Authors would like to thank the reviewers for their comments that helped us to improve this article.

REFERENCES

- [1] P. Erdős, “Note on sequences of integers no one of which is divisible by any other”, *J. Lond. Math. Soc.*, **10**, 126-128 (1935).
- [2] P. Erdős & Z. Zhang, “Upper bound of $\sum 1/a_i \log a_i$ for primitive sequences”, *Math. Soc.*, **117**, 891-895 (1993).
- [3] Z. Zhang, “On a conjecture of Erdős on the sum $\sum 1/(\log p)$ ”, *J. Number Theory*, **39**, 14-17 (1991).
- [4] Z. Zhang, “On a problem of Erdős concerning primitive sequences”, *Math. Comput.*, **60**(202), 827-34 (1993).
- [5] I. Laib, A. Derbal, R. Mechik and N. Rezzoug, “Note on a theorem of Zehxiang Zhang”, *Math. Montis.*, **50**, 44-50 (2021).
- [6] I. Laib, “The degree of primitive sequences and Erdős conjecture”, *Math. Montis.*, **52**, 37-42 (2021).
- [7] I. Laib A. Derbal et R. Machik, “Somme translatée sur des suites primitives et la conjecture d’Erdős C. R. Acad. Sci. Paris, Ser.I 357 p. 413-417 (2019).
- [8] N. Rezzoug, I. Laib , & K. Guenda, “On a translated sum over primitive sequences related to a conjecture of Erdős”, *NNTDM*, **26** (4), 68-73 (2020).
- [9] P. Dusart, *Autour de la fonction qui compte le nombre de nombres premiers*, Thèse de doctorat, université de Limoges, 17 (1998).
- [10] H. Robbins, “A remark on Stirling’s formula”, *Amer. Math. Monthly*, **62**, 26-29 (1955).
- [11] J. -P. Massias & G. Robin, “Bornes effectives pour certaines fonctions concernant les nombres premiers”, *J. Théorie. Nombres Bordeaux*, **8**, 215-242 (1996).

Received, February 8, 2022

THE GENERALIZED BIVARIATE FIBONACCI AND LUCAS MATRIX POLYNOMIALS

N. YILMAZ*

University of Karamanoglu Mehmetbey. Karaman, Turkey.

*Corresponding author. E-mail: yilmaznzmy@gmail.com

DOI: 10.20948/mathmontis-2022-53-5

Summary. The main object of the present paper is to consider the matrix polynomials for the generalized bivariate Fibonacci and Lucas polynomials. Working with matrix properties for these new matrix polynomials, some identities of the generalized bivariate Fibonacci and Lucas polynomials will be researched. Finally, we build the relationships between the generalized bivariate Fibonacci and Lucas matrix polynomials

1 INTRODUCTION

As with any very well-studied subject in mathematics, the Fibonacci, Lucas, Pell, Chebyshev numbers possess many kinds of generalizations. One of the most important generalizations is the Fibonacci polynomial [1-3, 8, 12, 15, 16, 18-21, 26, 29, 31]. Because of the common usage of this polynomial in the applied sciences, its some generalizations have been defined in the literature. In [14] and its references, concerned readers may find a short history and comprehensive information about the Fibonacci polynomial. The Fibonacci numbers are defined as

$$F_n = F_{n-1} + F_{n-2}, F_0 = 0, F_1 = 1 \quad (1.1)$$

for $n \geq 2$. In [13], the authors gave a new generalization of the Fibonacci and Lucas polynomials which are called generalized bivariate Fibonacci and Lucas polynomials. For $n \geq 2$ and $p(x, y)$, $q(x, y)$ polynomials with real coefficients, the generalized bivariate Fibonacci and Lucas polynomials are described by

$$H_n(x, y) = p(x, y)H_{n-1}(x, y) + q(x, y)H_{n-2}(x, y) \quad (1.2)$$

and

$$K_n(x, y) = p(x, y)K_{n-1}(x, y) + q(x, y)K_{n-2}(x, y), \quad (1.3)$$

where $H_0(x, y) = 0, H_1(x, y) = 1, K_0(x, y) = 2, K_1(x, y) = p(x, y)$ and $p^2(x, y) + 4q(x, y) > 0$. The relation of generalized bivariate Fibonacci and Lucas polynomials is (see[13])

$$K_n(x, y) = H_{n+1}(x, y) + q(x, y)H_{n-1}(x, y). \quad (1.4)$$

For the different $p(x, y)$ and $q(x, y)$, we obtain different polynomial sequences by using recursive relation. These polynomial sequences are given in Table 1 below:

2010 Mathematics Subject Classification: 11B39, 15A24.

Key words and Phrases: bivariate Fibonacci polynomials, bivariate Lucas polynomials, Fibonacci matrix polynomials, Lucas matrix polynomials.

$p(x, y)$	$q(x, y)$	$H_n(x, y)$	$K_n(x, y)$
x	y	Bivariate Fibonacci, $F_n(x, y)$	Bivariate Lucas, $L_n(x, y)$
x	1	Fibonacci, $F_n(x)$	Lucas, $L_n(x)$
$2x$	1	Pell, $P_n(x)$	Pell-Lucas, $Q_n(x)$
1	$2x$	Jacobsthal, $J_n(x)$	Jacobsthal-Lucas, $j_n(x)$
$2x$	-1	Chebyshev of the second kind, $U_{n-1}(x)$	Chebyshev of the first kind, $2T_n(x)$
$3x$	-2	Fermat, $F_n(x)$	Fermat-Lucas, $F_n(x)$

Table 1: Special conditions of the generalized bivariate Fibonacci and Lucas polynomials (see [13])

But then, the matrix sequences have received attention from many authors ([4-7, 9-11, 17, 22-25, 27, 28, 30, 32, 33]). In [6],[7], the authors established the bi-periodic Fibonacci and Lucas matrix sequences and acquired n th general term of these matrix sequences.

Therefore, the key purpose of this study is to examine the relations between the generalized bivariate Fibonacci and Lucas matrix polynomials. Firstly, we determine the generalized bivariate Fibonacci and Lucas matrix polynomials. Then, we obtain the generating functions, Binet formulas and summation formulas for these matrix polynomials. By considering the results in Section 2, we have a big chance to get new properties in Section 3.

2 THE MATRIX POLYNOMIALS OF GENERALIZED BIVARIATE FIBONACCI AND LUCAS POLYNOMIALS

In this part of the study, the relations and properties for the matrix polynomials of the generalized bivariate Fibonacci and Lucas polynomials are investigated.

Then, we will first give the definition of the generalized bivariate Fibonacci and Lucas matrix polynomials.

Definition 2.1 For $n \in \mathbb{N}$, the generalized bivariate Fibonacci (H_n) and Lucas matrix polynomials (K_n) are satisfy the following recurrence relations

$$H_{n+2}(x, y) = p(x, y)H_{n+1}(x, y) + q(x, y)H_n(x, y), \quad (2.1)$$

and

$$K_{n+2}(x, y) = p(x, y)K_{n+1}(x, y) + q(x, y)K_n(x, y), \quad (2.2)$$

respectively, with initial conditions

$$H_0(x, y) = \begin{pmatrix} 1 & 0 \\ 0 & 1 \end{pmatrix}, H_1(x, y) = \begin{pmatrix} p(x, y) & 1 \\ q(x, y) & 0 \end{pmatrix},$$

and

$$\mathbf{K}_0(x, y) = \begin{pmatrix} p(x, y) & 2 \\ 2q(x, y) & -p(x, y) \end{pmatrix}, \mathbf{K}_1(x, y) = \begin{pmatrix} p^2(x, y) + 2q(x, y) & p(x, y) \\ p(x, y)q(x, y) & 2q(x, y) \end{pmatrix}.$$

We would like mention hereafter that, we write $H_n(x, y) = H_n$, $K_n(x, y) = K_n$ and $p = p(x, y), q = q(x, y)$ for brevity. We obtain the n th general terms of the matrix polynomials in (2.1) and (2.2) by the generalized Fibonacci and Lucas polynomials as in the following.

Theorem 2.2 We have

$$\mathbf{H}_n(x, y) = \begin{pmatrix} H_{n+1} & H_n \\ qH_n & qH_{n-1} \end{pmatrix} \quad (2.3)$$

and

$$\mathbf{K}_n(x, y) = \begin{pmatrix} K_{n+1} & K_n \\ qK_n & qK_{n-1} \end{pmatrix}, \quad (2.4)$$

where $n \geq 0$.

Proof. The proof will be done by induction. For $n = -1$, we obtain the equality $H_{-1} = 1/q$ by using equation (1.2) which gives the first step of the finite induction.

$$\mathbf{H}_0 = \begin{pmatrix} H_1 & H_0 \\ qH_0 & qH_{-1} \end{pmatrix} = \begin{pmatrix} 1 & 0 \\ 0 & 1 \end{pmatrix}.$$

Let assume that the equation in (2.3) satisfies all the conditions $n = k \in \mathbb{Z}^+$. Then, by considering (1.2) and (2.1), we need to present that the part also holds for $n = k + 1$. So we obtain

$$\begin{aligned} \mathbf{H}_{k+1} &= p\mathbf{H}_k + q\mathbf{H}_{k-1} \\ &= p \begin{pmatrix} H_{k+1} & H_k \\ qH_k & qH_{k-1} \end{pmatrix} + q \begin{pmatrix} H_k & H_{k-1} \\ qH_{k-1} & qH_{k-2} \end{pmatrix} \\ &= \begin{pmatrix} H_{k+2} & H_{k+1} \\ qH_{k+1} & qH_k \end{pmatrix}. \end{aligned}$$

For another part of the proof, we require the following nearly like approximation by using (1.3). Similarly, as in the above part, the end step of the induction can be acquired by $\mathbf{K}_{k+1} = p\mathbf{K}_k + q\mathbf{K}_{k-1}$ as in the following

$$\mathbf{K}_{k+1} = \begin{pmatrix} K_{k+2} & K_{k+1} \\ qK_{k+1} & qK_k \end{pmatrix}.$$

This completes the proof.

The generating functions for the generalized bivariate Fibonacci and Lucas matrix polynomials play a vital role to find out many important identities for these matrix

polynomials. In the following theorem, we construct the generating functions for these matrix polynomials.

Theorem 2.3 For the generalized bivariate Fibonacci and Lucas matrix polynomials, we have the generating functions

$$\sum_{i=0}^{\infty} H_i t^i = \frac{1}{1-pt-qt^2} \begin{pmatrix} 1 & t \\ qt & 1-pt \end{pmatrix}$$

and

$$\sum_{i=0}^{\infty} K_i t^i = \frac{1}{1-pt-qt^2} \begin{pmatrix} p+2qt & 2-pt \\ 2q-pqt & -p+(p^2+2q)t \end{pmatrix},$$

respectively.

Proof. We will disregard the proof for Fibonacci because it will be similar. Accept that $G(t)$ is the generating function for the $\{K_n\}_{n \in \mathbb{N}}$. Then we obtain

$$\begin{aligned} G(t) &= \sum_{i=0}^{\infty} K_i t^i \\ &= K_0 + K_1 t + \sum_{i=2}^{\infty} K_i t^i. \end{aligned}$$

From Definition 2.1, we get

$$\begin{aligned} G(t) &= K_0 + K_1 t + pt \sum_{i=2}^{\infty} K_{i-1} t^{i-1} + qt^2 \sum_{i=0}^{\infty} K_i t^i \\ &= K_0 + K_1 t + pt(G(t) - K_0) + qt^2 G(t). \end{aligned}$$

Now, rearrangement of the above equation will show that

$$G(t) = \frac{K_0 + K_1 t - ptK_0}{1-pt-qt^2}$$

which match to the $\sum_{i=0}^{\infty} K_i t^i$ in theorem.

In [13], the authors obtain the generating functions for the generalized bivariate Fibonacci and Lucas polynomials. However, here, we will get these functions in terms of the generalized bivariate Fibonacci and Lucas matrix polynomials as a result of Theorem 2.3.

Corollary 2.4 There always exist

$$\sum_{i=0}^{\infty} H_i t^i = \frac{t}{1-pt-qt^2}$$

and

$$\sum_{i=0}^{\infty} K_i t^i = \frac{2-pt}{1-pt-qt^2}.$$

Theorem 2.5 We can note the Binet formulas for the generalized bivariate Fibonacci and Lucas matrix polynomials

$$H_n = A_1\alpha^n + B_1\beta^n \quad \text{and} \quad K_n = A_2\alpha^n + B_2\beta^n,$$

where

$$A_1 = \frac{H_1 - \beta H_0}{\alpha - \beta}, B_1 = \frac{\alpha H_0 - H_1}{\alpha - \beta}$$

and

$$A_2 = \frac{K_1 - \beta K_0}{\alpha - \beta}, B_2 = \frac{\alpha K_0 - K_1}{\alpha - \beta}$$

such that α, β are roots of equations of (2.1) and (2.2), $n \in \mathbb{N}$.

Proof. We omit the generalized bivariate Lucas matrix polynomial case since the proof is quite similar. The proof will be done by Theorem 2.3. Let α, β are roots of equations of (2.1), it is easily seen that

$$\begin{aligned} \sum_{n=0}^{\infty} H_n t^n &= \frac{1}{1-pt-qt^2} \begin{pmatrix} 1 & t \\ qt & 1-pt \end{pmatrix} \\ &= \frac{1}{\alpha-\beta} \begin{pmatrix} \frac{\alpha}{1-\alpha t} - \frac{\beta}{1-\beta t} & \frac{1}{1-\alpha t} - \frac{1}{1-\beta t} \\ \frac{q}{1-\alpha t} - \frac{q}{1-\beta t} & \frac{-\beta}{1-\alpha t} + \frac{\alpha}{1-\beta t} \end{pmatrix} \\ &= \frac{1}{\alpha-\beta} \begin{pmatrix} \sum_{n=0}^{\infty} (\alpha^{n+1} - \beta^{n+1}) t^n & \sum_{n=0}^{\infty} (\alpha^n - \beta^n) t^n \\ q \sum_{n=0}^{\infty} (\alpha^n - \beta^n) t^n & q \sum_{n=0}^{\infty} (\alpha^{n-1} - \beta^{n-1}) t^n \end{pmatrix} \\ &= \sum_{n=0}^{\infty} \alpha^n t^n \begin{pmatrix} \frac{\alpha}{\alpha-\beta} & \frac{1}{\alpha-\beta} \\ \frac{q}{\alpha-\beta} & \frac{q}{\alpha(\alpha-\beta)} \end{pmatrix} + \sum_{n=0}^{\infty} \beta^n t^n \begin{pmatrix} \frac{-\beta}{\alpha-\beta} & \frac{-1}{\alpha-\beta} \\ \frac{-q}{\alpha-\beta} & \frac{-q}{\beta(\alpha-\beta)} \end{pmatrix} \\ &= \sum_{n=0}^{\infty} (A_1 \alpha^n + B_1 \beta^n) t^n. \end{aligned}$$

Thus, by the equality of generating function, we obtain $H_n = A_1\alpha^n + B_1\beta^n$.

In [13], the writers find the Binet formulas for the generalized bivariate Fibonacci and Lucas polynomials. Now as a different approximation and so as a result of Theorems 2.2 and 2.5, we will show these formulas by matrix polynomials in the following corollary.

Corollary 2.6 The Binet formulas for the generalized bivariate Fibonacci and Lucas polynomials in terms of their matrix polynomials are given by

$$H_n = \frac{\alpha^n - \beta^n}{\alpha - \beta},$$

and

$$K_n = \alpha^n + \beta^n,$$

where $n \geq 0$.

Proof. Firstly, by considering Definition 2.1 and Theorem 2.5, we can write

$$\begin{aligned} H_n &= A_1 \alpha^n + B_1 \beta^n \\ &= \frac{H_1 - \beta H_0}{\alpha - \beta} \alpha^n + \frac{\alpha H_0 - H_1}{\alpha - \beta} \beta^n \\ &= \frac{\alpha^n}{\alpha - \beta} \begin{pmatrix} p - \beta & 1 \\ q & \frac{q}{\alpha} \end{pmatrix} + \frac{\beta^n}{\alpha - \beta} \begin{pmatrix} \alpha - p & -1 \\ -q & \frac{-q}{\beta} \end{pmatrix}. \end{aligned}$$

Here, by Theorem 2.2 and α, β are roots of the equation $\lambda^2 - p\lambda - q = 0$, we clearly have

$$\begin{pmatrix} H_{n+1} & H_n \\ qH_n & qH_{n-1} \end{pmatrix} = \frac{\alpha^n}{\alpha - \beta} \begin{pmatrix} \alpha & 1 \\ q & \frac{q}{\alpha} \end{pmatrix} + \frac{\beta^n}{\alpha - \beta} \begin{pmatrix} -\beta & -1 \\ -q & \frac{-q}{\beta} \end{pmatrix}.$$

Now, if we compare the 1st row and 2nd column entries with the matrices in the above equation, so we get

$$H_n = \frac{\alpha^n - \beta^n}{\alpha - \beta}.$$

Secondly, similarly, by using Theorem 2.2, Theorem 2.5 and Definition 2.1, we can write

$$\begin{aligned} K_n &= A_2 \alpha^n + B_2 \beta^n \\ &= \frac{K_1 - \beta K_0}{\alpha - \beta} \alpha^n + \frac{\alpha K_0 - K_1}{\alpha - \beta} \beta^n \\ &= \frac{\alpha^n}{\alpha - \beta} \begin{pmatrix} p^2 + 2q - p\beta & p - 2\beta \\ pq - 2q\beta & 2q + p\beta \end{pmatrix} + \frac{\beta^n}{\alpha - \beta} \begin{pmatrix} p\alpha - p^2 - 2q & 2\alpha - p \\ 2q\alpha - pq & -p\alpha - 2q \end{pmatrix}. \end{aligned}$$

In here, by Theorem 2.2 and α, β are roots of the equation $\lambda^2 - p\lambda - q = 0$, we have

$$\begin{pmatrix} K_{n+1} & K_n \\ qK_n & qK_{n-1} \end{pmatrix} = \alpha^n \begin{pmatrix} \alpha & 1 \\ q & \frac{q}{\alpha} \end{pmatrix} + \beta^n \begin{pmatrix} \beta & 1 \\ q & \frac{q}{\beta} \end{pmatrix}.$$

Finally, if we compare the 1st row and 2nd column entries with the matrices in above equation, then we acquire

$$K_n = \alpha^n + \beta^n.$$

Now, for the generalized bivariate Fibonacci and Lucas matrix polynomials, we give the summations by determining principles.

Theorem 2.7 For $j \geq m > 0$ and $n \geq 1$, we have

$$\sum_{i=0}^{n-1} H_{mi+j} = \frac{(-q)^m H_{mn+j-m} - H_{mn+j} + H_j - (-q)^m H_{j-m}}{(-q)^m - K_m + 1} \quad (2.5)$$

and

$$\sum_{i=0}^{n-1} K_{mi+j} = \frac{(-q)^m K_{mn+j-m} - K_{mn+j} + K_j - (-q)^m K_{j-m}}{(-q)^m - K_m + 1}. \quad (2.6)$$

Proof. We will consider the proof over the generalized bivariate Lucas matrix polynomials and will disregard the part of Fibonacci. From Theorem 2.5, we have

$$\begin{aligned} \sum_{i=0}^{n-1} K_{mi+j} &= \sum_{i=0}^{n-1} (A_2 \alpha^{mi+j} + B_2 \beta^{mi+j}) \\ &= A_2 \alpha^j \left(\frac{\alpha^{mn} - 1}{\alpha^m - 1} \right) + B_2 \beta^j \left(\frac{\beta^{mn} - 1}{\beta^m - 1} \right). \end{aligned}$$

Here, by simplification the last equation, is implied equation (2.6), as claimed.

3 RELATIONSHIPS BETWEEN NEW MATRIX POLYNOMIALS

The following proposition presents us that there exist some relations between the generalized bivariate Fibonacci and Lucas matrix polynomials.

Proposition 3.1 We obtain the following identities:

- i. $K_n = H_{n+1} + qH_{n-1}$,
- ii. $K_0 H_n = H_n K_0 = K_n$,
- iii. $K_0 K_n = K_n K_0 = pK_n + 2qK_{n-1}$,

where $n \in \mathbb{N}$.

Proof. The proof can be easily done by the equations (1.2),(1.3), Definition 2.1 and Theorem 2.2.

Theorem 3.2 The following identities are satisfied:

- i. $H_m H_n = H_{m+n}$,
- ii. $H_m K_n = K_n H_m = K_{m+n}$,
- iii. $K_m K_n = pK_{m+n} + 2qK_{m+n-1}$,

where $m, n \in \mathbb{N}$.

Proof.

i. From Theorem 2.5 with its assumptions, we can have

$$\begin{aligned} H_m H_n &= (A_1 \alpha^m + B_1 \beta^m)(A_1 \alpha^n + B_1 \beta^n) \\ &= A_1^2 \alpha^{m+n} + A_1 B_1 \alpha^m \beta^n + B_1 A_1 \beta^m \alpha^n + B_1^2 \beta^{m+n}. \end{aligned}$$

Here, since $\alpha + \beta = p$ and $\alpha\beta = -q$, a simple matrix calculations imply that $A_1^2 = A_1$, $B_1^2 = B_1$ and

$$A_1 B_1 = B_1 A_1 = [0].$$

Then we obtain

$$H_m H_n = A_1 \alpha^{m+n} + B_1 \beta^{m+n} = H_{m+n}.$$

ii. Here, we will just prove the correctness of the $H_m K_n = K_{m+n}$ since the other can be performed nearly the same. Now, by Proposition 3.1-ii., we get

$$H_m K_n = H_m H_n K_0.$$

Finally, by the above i. and again Proposition 3.1-ii, we obtain

$$H_m K_n = H_{m+n} K_0 = K_{m+n}.$$

iii. By Theorem 3.2-i., Proposition 3.1-ii. and iii., we have

$$\begin{aligned} K_m K_n &= K_0 H_m H_n K_0 \\ &= K_{m+n} K_0 \\ &= p K_{m+n} + 2q K_{m+n-1} \end{aligned}$$

as desired.

In [13, 20], the authors obtain the relations for the generalized bivariate Fibonacci and Lucas polynomials. Even so, comparing matrix entries and then utilizing Theorems 2.2 and 3.2, we find the next result.

Corollary 3.3 We have the following equalities for the generalized bivariate Fibonacci and Lucas polynomials:

i. $H_{m+1} H_n + q H_m H_{n-1} = H_{m+n},$

ii. $H_{m+1} K_n + q H_m K_{n-1} = K_{m+n},$

iii. $K_{m+1} K_n + q K_m K_{n-1} = K_{m+n}.$

We get the powers of the generalized bivariate Fibonacci and Lucas matrix polynomials in the following theorems.

Theorem 3.4 The following identities are satisfied:

i. $H_n^m = H_{mn}$,

ii. $H_{n+1}^m = H_1^m H_{nm}$,

iii. $H_{n-r} H_{n+r} = H_n^2 = H_2^n$,

where $r, m, n \in \mathbb{N}$ and $n \geq r$.

Proof.

i. We can write $H_n^m = H_n H_n \dots H_n$ (m -times). Then, we get H_{mn} by Theorem 3.2-i.

ii. Similar to i., we obtain

$$\begin{aligned} H_{n+1}^m &= H_{n+1} H_{n+1} \dots H_{n+1} \\ &= H_{m(n+1)} \\ &= H_m^m H_{nm}. \end{aligned}$$

From this Theorem i. , we can write $H_m = H_1^m$. Then, we acquire

$$H_{n+1}^m = H_1^m H_{nm}.$$

iii. The proof can be done similarly to ii..

Theorem 3.5 The equalities always hold:

$$K_{n-r} K_{n+r} = K_n^2 \quad \text{and} \quad K_n^m = K_0^m H_{mn},$$

where $r, m, n \in \mathbb{N}$ and $n \geq r$.

Proof. Firstly, we are using Theorem 2.5. Thus we have

$$K_{n-r} K_{n+r} - K_n^2 = (A_2 \alpha^{n-r} + B_2 \beta^{n-r})(A_2 \alpha^{n+r} + B_2 \beta^{n+r}) - (A_2 \alpha^n + B_2 \beta^n)^2,$$

where A_2 , B_2 and α, β are as given in Theorem 2.5. By applying the elementary calculations, we get

$$K_{n-r} K_{n+r} - K_n^2 = A_2 B_2 \alpha^{n-r} \beta^{n+r} + B_2 A_2 \beta^{n-r} \alpha^{n+r} - 2A_2 B_2 \alpha^n \beta^n.$$

Ultimately, by $A_2 B_2 = B_2 A_2 = [0]_{3 \times 3}$, we obtain $K_{n-r} K_{n+r} = K_n^2$, as claimed.

In the second case of the proof, let us take the right-hand side of the equality $K_n^m = K_0^m H_{mn}$. By Theorem 3.4-i., we get

$$K_0^m H_{mn} = \underbrace{K_0 K_0 \dots K_0}_{m \text{ times}} \underbrace{H_n H_n \dots H_n}_{m \text{ times}}.$$

By iterating usage of Proposition 3.1-ii., we finally obtain

$$K_0^m H_{mn} = K_0 H_n K_0 H_n \dots K_0 H_n = K_n K_n \dots K_n = K_n^m.$$

The result is obtained.

4 CONCLUSIONS

In this paper, we define the generalized bivariate Fibonacci and Lucas matrix polynomials and have a major chance to crosscheck new properties on these matrix polynomials. Hence, we enlarge the recent studies in the literature. That is,

- By giving $p(x, y) = s, q(x, y) = t$ in $H_n(x, y)$ and $K_n(x, y)$ of the results in Sections 2 and 3, we obtain the (s, t) -Fibonacci and (s, t) -Lucas matrix sequences which these results may be found in [4,5].

- By giving $p(x, y) = x, q(x, y) = y$ in $H_n(x, y)$ and $K_n(x, y)$ of the results in Sections 2 and 3, we obtain the bivariate Fibonacci and bivariate Lucas matrix polynomials.

- By giving $p(x, y) = 2s, q(x, y) = t$ in $H_n(x, y)$ and $K_n(x, y)$ of the results in Sections 2 and 3, we obtain the (s, t) -Pell and (s, t) -Pell-Lucas matrix sequences which these results may be found in [9].

- By giving $p(x, y) = 2x, q(x, y) = y$ in $H_n(x, y)$ and $K_n(x, y)$ of the results in Sections 2 and 3, we obtain the bivariate Pell and bivariate Pell-Lucas matrix polynomials.

- By giving $p(x, y) = s, q(x, y) = 2t$ in $H_n(x, y)$ and $K_n(x, y)$ of the results in Sections 2 and 3, we obtain the (s, t) -Jacobsthal and (s, t) -Jacobsthal-Lucas matrix sequences which these results may be found in [22].

- By giving $p(x, y) = x, q(x, y) = 2y$ in $H_n(x, y)$ and $K_n(x, y)$ of the results in Sections 2 and 3, we obtain the bivariate Jacobsthal and bivariate Jacobsthal-Lucas matrix polynomials which these results may be found in [25].

REFERENCES

- [1] R. Andre-Jeannin, "A note on general class of polynomials", *Fibonacci Quarterly*, **32**, 445-454 (1994).
- [2] M. Catalani, "Some Formulae for Bivariate Fibonacci and Lucas Polynomials", *arXiv preprint*, arXiv:math.CO/0406323v1 (2004).
- [3] M. Catalani, "Generalized Bivariate Fibonacci Polynomials", *arXiv preprint*, arXiv:math/0211366v2 (2004).
- [4] H. Cıvcıv, R. Türkmen, "On the (s, t) -Fibonacci and Fibonacci matrix sequences", *Ars Combinatoria*, **87**, 161-173 (2008).
- [5] H. Cıvcıv, R. Turkmen, "Notes on the (s, t) -Lucas and Lucas matrix sequences", *Ars Combinatoria*, **89**, 271-285 (2008).
- [6] A. Coskun, N. Taskara, "A note on the bi-periodic Fibonacci and Lucas matrix sequences", *Applied Mathematics and Computation*, **320**, 400-406 (2018).
- [7] A. Coskun, N. Taskara, "The matrix sequence in terms of bi-periodic Fibonacci numbers", *Communications Faculty of Sciences University of Ankara Series A1 Mathematics and Statistics*, **68**(2), 1939-1949 (2016).
- [8] E.E. Duman, N. Tuglu, "Generating Functions for the Generalized Bivariate Fibonacci and Lucas Polynomials", *Journal of Computational Analysis & Applications*, **18**(5) (2015).

- [9] H.H. Gulec, N. Taskara, "On the (s,t) -Pell and (s,t) -Pell-Lucas sequences and their matrix representations", *Applied Mathematics Letter*, **25**, 1554-1559 (2012).
- [10] A. Ipek, K. Ari, R. Turkmen, "The generalized (s,t) -Fibonacci and Fibonacci matrix sequences", *Transylvanian Journal of Mathematics and Mechanics*, **7**(2), 137-148 (2015).
- [11] N. Karaaslan, T. Yagmur, " (s,t) -Modified Pell Sequence and Its Matrix Representation", *Erzincan Üniversitesi Fen Bilimleri Enstitüsü Dergisi*, **12**(2), 863-873 (2019).
- [12] K. Kaygisiz, A. Sahin, "Generalized bivariate Lucas p -polynomials and Hessenberg Matrices", *Journal of Integer Sequences*, **15**, Article 12.3.4 (2012).
- [13] E.G. Kocer, S. Tuncez, "Bivariate Fibonacci and Lucas Like Polynomials", *Gazi University Journal of Science*, **29**(1), 109-113 (2016).
- [14] T. Koshy, *Fibonacci and Lucas Numbers with Applications*, John Wiley and Sons Inc. NY (2001).
- [15] A. Nalli, P. Haukkanen, "On Generalizing Fibonacci and Lucas Polynomials", *Chaos, Solitons and Fractals*, **42**, 3179-3186 (2009).
- [16] E. Ozkan, A. Aydogdu, I. Altun, "Some Identities For A Family of Fibonacci And Lucas Numbers", *Journal of Mathematics and Statistical Science*, **3**, 295- 303 (2017).
- [17] Y. Soykan, E. Tasdemir, V. Irge, "A Study On Matrix Sequence of Adjusted Tribonacci-Lucas numbers", *J. Int. Math. Virtual Inst.*, **11**(1), 85-100 (2021).
- [18] M. Tastan, E. Ozkan, A.G. Shannon, "The generalized k -Fibonacci polynomials and generalized k -Lucas polynomials", *Notes on Number Theory and Discrete Mathematics*, **27**(2), 148-158 (2021).
- [19] N. Tuglu, E.G. Kocer, A. Stakhov, "Bivariate Fibonacci Like p -Polynomials", *Applied Mathematics and Computation*, **217**(24), 10239-10246 (2011).
- [20] S. Tuncez, "Generalized Bivariate Fibonacci and Lucas polynomials", *Ms Thesis, Necmettin Erbakan University, Konya, Turkey* 2011.
- [21] S. Ucar, "On some properties of generalized Fibonacci and Lucas polynomials", *An International Journal of Optimization and Control: Theories & Applications*, **7**(2), 216-224 (2017).
- [22] K. Uslu, S. Uygun, "The (s,t) -Jacobsthal and (s,t) -Jacobsthal-Lucas Matrix Sequences", *Ars Combinatoria*, **108**, 13-22 (2013).
- [23] S. Uygun, H. Eldogan, " k -Jacobsthal and k -Jacobsthal Lucas matrix sequences", *International Mathematical Forum*, **11**(3) (2016).
- [24] S. Uygun, K. Uslu, "The (s,t) -Generalized Jacobsthal Matrix Sequences", *Computational Analysis*, Springer, 325-336 (2016).
- [25] S. Uygun, A. Zorcelik, "Bivariate Jacobsthal and bivariate Jacobsthal-Lucas matrix polynomial sequences", *J. Math. Comput. Sci.*, **8**(3), 331-344 (2018).
- [26] C.J.P.R. Velasco, "On bivariate s -Fibopolynomials", *arXiv preprint arXiv:1203.6055* (2012).
- [27] A.A. Wani, P. Catarino, S. Halici, "On a Study of (s,t) -Generalized Pell Sequence and its Matrix Sequence", *Punjab University Journal of Mathematics*, **51**(9) (2020).
- [28] A.A. Wani, V.H. Badshah, G.P.S. Rathore, P. Catarino, "Generalized Fibonacci and k -Pell matrix sequences", *Punjab University Journal of Mathematics*, **51**(1) (2020).
- [29] A. Włoch, "Some identities for the generalized Fibonacci numbers and the generalized Lucas numbers", *Applied Mathematics and Computation*, **219**(10), 5564-5568 (2013).
- [30] Y. Yazlik, N. Taskara, K. Uslu, N. Yilmaz, "The Generalized (s,t) -Sequence and its Matrix Sequence", *American Institute of Physics (AIP) Conf. Proc.*, **1389**, 381-384 (2011).

- [31] N. Yilmaz, A. Aydogdu, E. Ozkan, “Some Properties of k -Generalized Fibonacci Numbers”, *Mathematica Montisnigri*, **50**, 73-79 (2021).
- [32] N. Yilmaz, N. Taskara, “Matrix sequences in terms of Padovan and Perrin numbers”, *Journal of Applied Mathematics*, (2013).
- [33] N. Yilmaz, N. Taskara, “On the Negatively Subscripted Padovan and Perrin Matrix Sequences”, *Communications in Mathematics and Applications*, **5**(2), 59–72 (2014).

Received, March 4, 2022

**CORRECT DEFINITION OF INTERNAL ENERGY
AT THE PHENOMENOLOGICAL CONSTRUCTION OF MODEL
OF MULTICOMPONENT CONTINUOUS MEDIUM
BY METHODS OF NONEQUILIBRIUM THERMODYNAMICS**

A.V. KOLESNICHENKO

¹Keldysh Institute of Applied Mathematics, Russian Academy of Science

*Corresponding author. E-mail: kolesn@keldysh.ru

DOI: 10.20948/mathmontis-2022-53-6

Summary. Taking into account the methods of thermodynamics of irreversible processes using the Onsager principle, a model of a multicomponent continuous medium is constructed, the internal energy of which is "free" of the kinetic energy of diffusion. The model is designed for an imperfect continuous medium with chemical reactions in the field of conservative external forces. Generalized Stefan–Maxwell relations are obtained, which represent a system of hydrodynamic equations of motion of a mixture with true inertial forces. The proposed thermodynamic technique made it possible to obtain a number of algebraic relations known from the kinetic theory of gases for the transfer coefficients, relating, in particular, the coefficients of multicomponent diffusion with binary diffusivities, thermal diffusion ratios with thermal diffusion coefficients and multicomponent diffusion coefficients, true (molecular) thermal conductivity coefficient for multicomponent mixture with partial thermal conductivity coefficient, which indicates their versatility. The results obtained are intended for modeling not only liquid imperfect solutions, but also gas-dust mixtures with a finely dispersed dust component.

1. INTRODUCTION

Currently, there is a need to revise the stable paradigm associated with the definition of the internal energy of a continuous medium at the phenomenological construction of multicomponent hydrodynamics. In whole number of classical monographs on the thermodynamics of non equilibrium processes, the authors, by analogy with the kinetic theory of multicomponent gases (see, for example, [1-7]), introduce into consideration the internal energy of a multicomponent medium, defining it as the difference between the total energy and mechanical energy, the latter being determined in the approximation of equal acceleration of all components of the mixture. The incorrectness of this definition is due to the fact that, with this approach, the internal energy of the mixture contains, in addition to the contributions from the thermal motion of molecules and short range molecular interactions, which is consistent with the usual understanding of internal energy, contains also and the kinetic energy of diffusion.

So, within the framework of the classical approach, at modeling physical and mechanical processes in a multicomponent medium, many authors (see, for example, [4-6, 8-18]) when deter-

2010 Mathematics Subject Classification: 80A20, 82B30, 94A24.

Key words and Phrases: Nonequilibrium thermodynamics, Stefan – Maxwell relation, Non-ideal multicomponent mixtures, Kinetic energy of diffusion.

mining the balance equation for the specific internal energy of a mixture usually proceed from the law of conservation of the total specific energy $u(\mathbf{x}, t)$

$$\frac{\partial}{\partial t}(\rho u) + \nabla \cdot \mathbf{J}_u = 0 \quad (1)$$

and the previously derived balance equation for the specific mechanical energy of the mixture, equal to the sum of the local kinetic energy of the center of mass and potential energy, $u_m^* \equiv \frac{1}{2} \mathbf{v}^2 + \varphi$. Here \mathbf{J}_u is the local flow of total energy; $\rho(\mathbf{x}, t)$ – total density, $\varphi(\mathbf{x}, t)$ – specific potential energy, $\mathbf{v}(\mathbf{x}, t)$ – velocity of the center of mass of a liquid element. These quantities are determined by the relations

$$\rho = \sum_{k=1}^N \rho_k, \quad \mathbf{v} = \rho^{-1} \sum_{k=1}^N \rho_k \mathbf{v}_k, \quad \varphi = \rho^{-1} \sum_{k=1}^N \rho_k \varphi_k, \quad (2)$$

where, $\rho_k(\mathbf{x}, t)$, $\mathbf{v}_k(\mathbf{x}, t)$ and $\varphi_k(\mathbf{x})$ are the density, velocity and potential energy of the mass unit of component k , respectively. In this case, the specific internal energy $\varepsilon^*(\mathbf{x}, t)$ of the mixture is determined by the ratio

$$\varepsilon^* \equiv u - u_m^* = u - \frac{1}{2} \mathbf{v}^2 - \varphi \quad (3)$$

However, the value of the internal energy $\varepsilon^*(\mathbf{x}, t)$, introduced in this way, as mentioned above, is not entirely correct, since the specific mechanical energy u_m^* contains only the macroscopic kinetic energy of the components of the mixture in the center of mass system.

At the same time, it is possible to determine another, more deserving of this name, internal energy $\varepsilon(\mathbf{x}, t)$ per unit mass of the mixture, which does not include the kinetic energy of diffusion, by subtracting the specific mechanical energy $u_m(\mathbf{x}, t)$ from the total energy $u(\mathbf{x}, t)$, equal to the sum of the specific potential energy $\varphi(\mathbf{x})$ and the kinetic energy $u_K(\mathbf{x}, t)$ of all components,

$u_m \equiv \varphi + u_K = \varphi + \frac{1}{2} \rho^{-1} \sum_{k=1}^N \rho_k \mathbf{v}_k^2$; as a result we will have

$$\begin{aligned} \varepsilon = u - u_m &= u - \varphi - \frac{1}{2} \rho^{-1} \sum_{k=1}^N \rho_k \mathbf{v}_k^2 = u - \varphi - \frac{1}{2} \mathbf{v}^2 - \frac{1}{2} \rho^{-1} \sum_{k=1}^N \rho_k (\mathbf{v}_k - \mathbf{v})^2 = \\ &= \varepsilon^* - \frac{1}{2} \rho^{-1} \sum_{k=1}^N \rho_k (\mathbf{v}_k - \mathbf{v})^2 = \varepsilon^* - \frac{1}{2} \sum_{k=1}^N c_k \mathbf{w}_k^2. \end{aligned} \quad (4)$$

Here, $\mathbf{w}_k(\mathbf{x}, t) \equiv (\mathbf{v}_k - \mathbf{v})$, $v(\mathbf{x}, t) \equiv 1/\rho$ and $c_k(\mathbf{x}, t) \equiv \rho_k/\rho$ are the diffusion rate, specific volume and concentration of the substance, respectively. It can be seen from relation (4) that the "internal" energy of the mixture $\varepsilon^*(\mathbf{x}, t)$ used in the literature is not quite correct, since it differs from the true internal energy $\varepsilon(\mathbf{x}, t)$ by an amount $\frac{1}{2} \sum_{k=1}^N c_k \mathbf{w}_k^2$, associated with the kinetic energy of diffusion (due to the diffusion velocities $\mathbf{w}_k(\mathbf{x}, t)$ of the components of the mixture relative

to the local center of mass). There is no doubt that in most cases the kinetic energy of diffusion can be neglected in comparison with the kinetic energy of the center of mass (the classical kinetic theory of multicomponent gas mixtures was just developed in this “diffusion approximation”), however, in a more general case, the difference between the quantities $\varepsilon(\mathbf{x}, t)$ and $\varepsilon^*(\mathbf{x}, t)$ should be taken into account (for example, in the phenomenological design of models of liquid multicomponent non ideal solutions, models of the movement of gas-dust mixtures, when the volume concentration of the dispersed phase is low, etc.).

It is important to keep this circumstance in mind also because classical multicomponent hydrodynamics is based on the fundamental Gibbs relation

$$TdS = d\varepsilon^* + pdv + \sum_{k=1}^N \mu_k dc_k, \quad (5)$$

written for a system in a state of "local" equilibrium (see [8]). In relation (5), the quantities $T(\mathbf{x}, t)$, $p(\mathbf{x}, t)$ and $\mu_k(\mathbf{x}, t)$ are, respectively, the equilibrium temperature, mixture pressure and specific chemical potential of the component k . However, this quasi-equilibrium relationship, which is, in essence, the relationship between the equilibrium entropy $S = S(\varepsilon^*, v, c_k)$ and local quantities $\varepsilon^*(\mathbf{x}, t)$, $v(\mathbf{x}, t)$ and $c_k(\mathbf{x}, t)$, it would be more correct to write it in a slightly different

form, namely $TdS = d\varepsilon + pdv + \sum_{k=1}^N \mu_k dc_k$, because at equilibrium the diffusion fluxes \mathbf{w}_k should

disappear. For this reason, the use of the fundamental Gibbs equation, which plays a central role in the theory of nonequilibrium processes, in the form (5) in the general case is not entirely correct (see, for example, [10], pp. 34-35; [14], p. 119).

In this work, an attempt is made to construct models of multicomponent media, free from the above disadvantage. The development of models was carried out by us for non-ideal continuous media with chemical reactions located in the field of conservative external forces. For simplicity of presentation, we did not take into account here the antisymmetric of the pressure tensor, which is possible for a medium of this type, associated with the presence of an “internal” angular momentum [14].

2. LAWS OF CONSERVATION

The stated goal of the work can be achieved only by applying Onsager's thermodynamic approach to simulate multicomponent and chemically reacting hydro-thermodynamic systems with consideration of the complete system of equations for conservation of mass, momentum, energy and entropy in both local and substantial form.

We write the local form of the balance equation for an arbitrary intense quantity \mathcal{A} in the form

$$\frac{\partial}{\partial t}(\rho a) + \nabla \cdot (\rho a \mathbf{v} + \mathbf{J}_a) = \sigma_a, \quad (6)$$

where $a(\mathbf{x}, t)$, $\mathbf{J}_a(\mathbf{x}, t)$, $\sigma_a(\mathbf{x}, t)$ – respectively the specific value, flux density and density of the source of the quantity (the parameter can be a scalar, vector, tensor of the second rank, etc.).

Usually, the source density $\sigma_a(\mathbf{x}, t)$ is divided into internal $\sigma_a^{(i)}(\mathbf{x}, t)$ and external $\sigma_a^{(e)}(\mathbf{x}, t)$ components in accordance with the ratio $\sigma_a = \sigma_a^{(i)} + \sigma_a^{(e)}$, and the value $\sigma_a^{(i)}$ is determined by inhomogeneities that exist locally inside the system, associated with the gradients of velocity, temperature, density, etc., and the value $\sigma_a^{(e)}$ arises from long-range nature of external forces affecting the inner part of the system under consideration. Using equation (6), we write down the basic laws of conservation of mass, momentum, energy, entropy, etc. for a multicomponent system, while identifying the quantities with the corresponding physical parameters, introducing the flux and source densities for them.

The mass balance equations for a reacting mixtures. To write the mass balance equation for a separate component, it is necessary to put in equation (6), $a \equiv c_k, \mathbf{J}_a \equiv \mathbf{J}_k, \sigma_a \equiv \Gamma_k$ where $\mathbf{J}_k(\mathbf{x}, t) = \rho_k \mathbf{w}_k$ is the diffusion flux of the mass of the k -th component relative to the center of mass, $\Gamma_k = \sum_{j=1}^r \nu_{kj} J_j$ is the mass of the k -component, that appears due to chemical reactions in a unit of volume per unit of time.

Then the continuity equation for the substance k has the form:

$$\frac{\partial \rho_k}{\partial t} + \nabla \cdot (\rho_k \mathbf{v} + \mathbf{J}_k) = \Gamma_k \equiv \sum_{j=1}^r \nu_{kj} J_j, \quad (k = 1, 2, \dots, N). \quad (7)$$

Note that the quantity $\nu_{kj} J_j$ is the rate of formation of the component k per unit volume in the j -th chemical reaction. The value ν_{kj} divided by the molecular mass m_k of the component k is proportional to the stoichiometric coefficient with which the substance k enters the equation of the j -th chemical reaction. The coefficients ν_{kj} are considered positive when the components k enter the right side, and negative when they enter the left side of the reaction equation. The scalar quantity $J_j(\mathbf{x}, t)$ is called the rate of the j -th chemical reaction. It has the dimension of mass per unit volume per unit of time.

Summing (7) over all k and taking into account the relations

$$\sum_{k=1}^N \mathbf{J}_k = 0, \quad \sum_{k=1}^N \Gamma_k = 0, \quad (8)$$

of which the latter expresses the law of conservation of mass as a result of all chemical reactions, we obtain the general continuity equation for the mixture in the divergent form usual for hydrodynamics

$$\frac{\partial \rho}{\partial t} + \nabla \cdot (\rho \mathbf{v}) = 0. \quad (9)$$

In what follows, we will make extensive use of the operator relation

$$\rho \frac{da}{dt} = \frac{\partial}{\partial t}(\rho a) + \nabla \cdot (\rho a \mathbf{v}), \quad \frac{d}{dt}(\cdot) \equiv \frac{\partial}{\partial t}(\cdot) + \mathbf{v} \cdot \nabla(\cdot), \quad (10)$$

giving a connection between substantial and local changes in characteristics and allowing to write the differential balance equation (6) in the following substantial form

$$\rho \frac{da}{dt} = -\nabla \cdot \mathbf{J}_a + \sigma_a. \quad (6^*)$$

Note that relation (10) is a consequence of the continuity equation (9) and the definition of the total time derivative $da/dt \equiv \partial a/\partial t + \mathbf{v} \cdot \nabla a$ of the value $a(\mathbf{x}, t)$ in the accompanying coordinate system associated with an element of the medium moving with velocity $\mathbf{v}(\mathbf{x}, t)$.

Applying this relation to equation (7), we obtain the equation of the substitution mass balance of the k -th component

$$\rho \frac{dc_k}{dt} = -\nabla \cdot \mathbf{J}_k + \Gamma_k, \quad (k = 1, 2, \dots, N-1); \quad \sum_{k=1}^N c_k = 1. \quad (11)$$

The equation of motion for a multicomponent mixture. Setting in equation (6) $a \equiv \mathbf{v}$, $\mathbf{J}_a \equiv \mathbf{T}$, $\sigma_a \equiv \rho \mathbf{f}$, we obtain the law of conservation of specific impulse for any fluid continuum

$$\frac{\partial}{\partial t}(\rho \mathbf{v}) + \nabla \cdot (\rho \mathbf{v} \mathbf{v} + \mathbf{T}) = \rho \mathbf{f} \quad (12)$$

where $\mathbf{T}(\mathbf{x}, t)$ is the symmetric tensor of pressures (or stresses) of the medium, caused by short-range interactions between the particles of the system; $\mathbf{f}(\mathbf{x}, t)$ – external force acting on a unit mass of the medium; $\mathbf{v} \mathbf{v}$ – dyadic product.

Using the operator relation (10), we can write the equation of motion (12) in the form

$$\rho \frac{d\mathbf{v}}{dt} = -\nabla \cdot \mathbf{T} + \rho \mathbf{f}. \quad (12^*)$$

Equation (12) is valid for any continuum, but the expressions for the pressure tensor and the density of external forces for different continua are not the same. We will further consider Eq. (12) as a balance equation for the continuum obtained by a superposition N of continuous continuous media, the equations of motion for which (similar in structure to Eq. (12)) have the form:

$$\frac{\partial}{\partial t}(\rho_k \mathbf{v}_k) + \nabla \cdot (\rho_k \mathbf{v}_k \mathbf{v}_k + \mathbf{T}_k) = \rho_k \mathbf{f}_k + \sum_{k \neq j=1}^N \mathbf{r}_{kj}, \quad (k = 1, 2, \dots, N). \quad (13)$$

Here $\mathbf{T}_k(\mathbf{x}, t)$ is the symmetric pressure tensor of the k -ith component, ($\mathbf{T}_k = \mathbf{T}_k^T$; this relationship is a mathematical expression of the second Cauchy law for a multicomponent mixture); $\mathbf{f}_k(\mathbf{x})$ - an external force acting on a unit mass of a substance k ; $\mathbf{r}_{kj}(\mathbf{x}, t)$ - a vector (intercomponent force) that determines the intensity of intercomponent exchange of momentum due to collisions and intercomponent transitions of an impulse as a result of chemical reactions, $\mathbf{r}_{kj} = -\mathbf{r}_{jk}$.

Next, an explicit vector expression \mathbf{r}_{kj} will be found.

Summing equation (13) over k and using the relation

$$\sum_{k=1}^N \rho_k \mathbf{v}_k \mathbf{v}_k = \rho \mathbf{v} \mathbf{v} + \sum_{k=1}^N \rho_k^{-1} \mathbf{J}_k \mathbf{J}_k, \quad (14)$$

we obtain the following equation for the momentum balance of the mixture [19]:

$$\frac{\partial}{\partial t}(\rho \mathbf{v}) + \nabla \cdot \left(\rho \mathbf{v} \mathbf{v} + \sum_{k=1}^N \rho_k^{-1} \mathbf{J}_k \mathbf{J}_k + \sum_{k=1}^N \mathbf{T}_k \right) = \sum_{k=1}^N \rho_k \mathbf{f}_k, \quad (15)$$

where $\sum_{k=1}^N \rho_k^{-1} \mathbf{J}_k \mathbf{J}_k$ is the stress arising from the relative motion of components of different kinds.

When writing equation (15), the equality $\sum_{k=1}^N \sum_{k \neq j=1}^N \mathbf{r}_{kj} = 0$ was taken into account, which is a

consequence of the fact that a change in the specific impulse $\mathbf{v}(\mathbf{x}, t)$ for a multicomponent continuum, occurring both as a result of collisions between particles of its individual continua (Newton's third postulate), and as a result of chemical reactions is equal to zero. Indeed, denoting through Γ_{kj} the mass of the component k , which is formed as a result of chemical reactions from the component j , we obtain the following expression for the corresponding change in the density

of the specific impulse $\mathbf{v}(\mathbf{x}, t)$ of the total continuum: $\sum_{k=1}^N \sum_{j=1}^N (\Gamma_{kj} \mathbf{v}_j - \Gamma_{jk} \mathbf{v}_k) = 0$.

Total energy conservation for a mixture. The total specific energy for the continuum modeling the mixture as a whole satisfies the local balance equation (1) without a source. We now obtain this equation by adding the equations for the transfer of the total specific energy for each component of the system

$$\frac{\partial}{\partial t}(\rho_k u_k) + \nabla \cdot \mathbf{J}_{u_k} = \sigma_{u_k}^{(i)}, \quad (k = 1, 2, \dots, N). \quad (16)$$

Here $u_k(\mathbf{x}, t)$ is the total specific (per unit mass) energy of the k -component; $\mathbf{J}_{u_k}(\mathbf{x}, t)$ – local

flow of total energy carried by matter k ; $\sigma_{u_k}^{(i)}(\mathbf{x}, t)$ – the density of the internal source of total energy of particles of a sort k , is equal, on the one hand, to the heat released in the gas of particles of a given sort due to collisions with particles of other kinds, and, on the other hand, to a change in the total energy of a component k , as a result of chemical reactions, given by the expression.

$\sum_{k=1}^N (\Gamma_{kj} u_j - \Gamma_{jk} u_k)$. The quantities $u_k(\mathbf{x}, t)$ and $\mathbf{J}_{u_k}(\mathbf{x}, t)$ satisfy the relations

$$u_k = \varepsilon_k + \frac{1}{2} \mathbf{v}_k^2 + \varphi_k, \quad (17)$$

$$\mathbf{J}_{u_k} = \rho_k u_k \mathbf{v}_k + \mathbf{T}_k \cdot \mathbf{v}_k + \mathbf{q}_k, \quad (18)$$

where $\varepsilon_k(\mathbf{x}, t)$ and $\varphi(\mathbf{x})$ – respectively, the internal and potential energy of the unit mass of the substance k ; $\mathbf{q}_k(\mathbf{x}, t)$ is the heat flux carried by the particles of the k -th component, determined precisely by the relation (18).

Recall that in our discussion, for simplicity, we limited ourselves to considering only conservative external fields, which can be characterized by a scalar potential $\varphi_k(\mathbf{x})$ per unit mass of a component k , i.e. the equations are assumed to be valid

$$\mathbf{f}_k = -\nabla\varphi_k, \quad \partial\varphi_k / \partial t = 0. \quad (19)$$

However, in the general case, forces \mathbf{f}_k can be of a different nature, in particular, associated with non-conservative electromagnetic external fields.

Now summing (16) over all k and using the natural equality $\sum_{k=1}^N \sigma_k^{(i)} = 0$, as well as the formulas

$$\frac{1}{2} \sum_{k=1}^N \rho_k \mathbf{v}_k^2 = \frac{1}{2} \rho \mathbf{v}^2 + \frac{1}{2} \sum_{k=1}^N \rho_k^{-1} \mathbf{J}_k^2, \quad (20)$$

$$\frac{1}{2} \sum_{k=1}^N \rho_k |\mathbf{v}_k|^2 \mathbf{v}_k = \frac{1}{2} \rho |\mathbf{v}|^2 \mathbf{v} + \frac{1}{2} \sum_{k=1}^N \rho_k^{-1} |\mathbf{J}_k|^2 \mathbf{v} + \frac{1}{2} \sum_{k=1}^N |\mathbf{v}_k|^2 \mathbf{J}_k, \quad (21)$$

$$\sum_{k=1}^N \mathbf{T}_k \cdot \mathbf{v}_k = p \mathbf{v} + \sum_{k=1}^N \rho_k^{-1} p_k \mathbf{J}_k - \sum_{k=1}^N \boldsymbol{\tau}_k \cdot \mathbf{v}_k, \quad (22)$$

$$\varepsilon = \sum_{k=1}^N c_k \varepsilon_k, \quad \varphi = \sum_{k=1}^N c_k \varphi_k, \quad \mathbf{q} = \sum_{k=1}^N \mathbf{q}_k, \quad (23)$$

$$u = \varepsilon + \frac{1}{2} \mathbf{v}^2 + \varphi + \frac{1}{2} \sum_{k=1}^N \frac{|\mathbf{J}_k|^2}{\rho \rho_k}, \quad \mathbf{J}_q = \mathbf{q} + \sum_{k=1}^N h_k \mathbf{J}_k \quad (24)$$

$$\mathbf{T}_k = p_k \mathbf{I} - \boldsymbol{\tau}_k, \quad p = \sum_{k=1}^N p_k, \quad h_k = \varepsilon_k + p_k \rho_k^{-1}, \quad (25)$$

we obtain the total energy conservation law for the total continuum

$$\frac{\partial}{\partial t} (\rho u) + \nabla \cdot \left\{ \rho u \mathbf{v} + p \mathbf{v} + \mathbf{J}_q + \sum_{k=1}^N \left(\varphi_k + \frac{1}{2} |\mathbf{v}_k|^2 \right) \mathbf{J}_k - \sum_{k=1}^N \boldsymbol{\tau}_k \cdot \mathbf{v}_k \right\} = 0. \quad (26)$$

Here $p_k(\mathbf{x}, t) = k T n_k$, $n_k(\mathbf{x}, t) = \rho_k / m_k$, m_k , $h_k(\mathbf{x}, t)$ and $\boldsymbol{\tau}_k(\mathbf{x}, t)$ – respectively, hydrostatic pressure, number density, molecular weight, tensor of viscous stresses of the substance k ; $T(\mathbf{x}, t)$, $\mathbf{J}_q(\mathbf{x}, t)$, $\mathbf{q}(\mathbf{x}, t)$ – respectively, the temperature, the density of the total heat flux and the

reduced heat flux in the total continuum; $p = \sum_{k=1}^N p_k$ – the hydrostatic pressure of the mixture at a

given temperature (Dalton's law); k is the Boltzmann constant. When using the operator relation (10), equation (26) can be given the form:

$$\rho \frac{du}{dt} = -\nabla \cdot \left\{ \mathbf{J}_q + p\mathbf{v} + \sum_{k=1}^N \mathbf{J}_k \left(\varphi_k + \frac{1}{2} |\mathbf{v}_k|^2 \right) - \sum_{k=1}^N \boldsymbol{\tau}_k \cdot \mathbf{v}_k \right\}. \quad (26^*)$$

Potential energy balance. Multiplying the non-discontinuity equation (7) for the substance k by φ_k , summing over k and using (19) and (23), we obtain the equation for the local balance of the potential energy φ of the mixture in the form

$$\frac{\partial}{\partial t} (\rho\varphi) + \nabla \cdot \left\{ \rho\varphi\mathbf{v} + \sum_{k=1}^N \varphi_k \mathbf{J}_k \right\} = - \sum_{k=1}^N \rho_k \mathbf{f}_k \cdot \mathbf{v}_k + \sum_{k=1}^N \varphi_k \Gamma_k. \quad (27)$$

If we turn to equation (6), then such a comparison allows us to conclude that the first term on the right-hand side of (27) should be considered as a term corresponding to “external” sources, and the second term should be considered a term corresponding to an “internal” source of potential energy. Note that the density of the internal source $\sigma_\varphi^{(i)} = \sum_{k=1}^N \varphi_k \Gamma_k$ vanishes in all those cases when, due to chemical reactions, the equality

$$\sum_{k=1}^N \varphi_k v_{kj} = 0, \quad (j = 1, 2, \dots, r). \quad (28)$$

The fulfillment of this equality for the gravitational field is ensured by the conservation of mass. Taking into account the condition $\sigma_\varphi^{(i)} = 0$, the substantial form of the balance equation for the potential energy of the mixture takes the form

$$\rho \frac{d\varphi}{dt} = -\nabla \cdot \left\{ \sum_{k=1}^N \varphi_k \mathbf{J}_k \right\} - \rho \mathbf{v} \cdot \mathbf{f} - \sum_{k=1}^N \mathbf{f}_k \cdot \mathbf{J}_k. \quad (27^*)$$

Equation of the balance of the kinetic energy of the mixture. The derivation of the equation for the balance of kinetic energy is carried out as follows. Let us preliminarily rewrite the equation of motion of a multicomponent medium (15) in the form

$$\sum_{k=1}^N \left\{ \frac{\partial}{\partial t} (\rho_k \mathbf{v}_k) + \nabla \cdot (\rho_k \mathbf{v}_k \mathbf{v}_k - \boldsymbol{\tau}_k) \right\} = -\nabla p + \sum_{k=1}^N \rho_k \mathbf{f}_k, \quad (29)$$

or in substantial form

$$\sum_{k=1}^N \left\{ \rho_k \frac{d^{(k)} \mathbf{v}_k}{dt} \right\} = -\nabla p + \nabla \cdot \boldsymbol{\tau} + \rho \mathbf{f} - \sum_{k=1}^N \Gamma_k \mathbf{v}_k. \quad (30)$$

Here $d^{(k)}/dt$ is the total time derivative (substantial differential operator) for the component k , which is determined by the relation

$$\rho_k \frac{d^{(k)}(..)}{dt} = \rho_k \left\{ \frac{\partial(..)}{\partial t} + \mathbf{v}_k \cdot \nabla(..) \right\} = \rho_k \frac{d(..)}{dt} + \mathbf{J}_k \cdot \nabla(..). \quad (31)$$

Note that in deriving (30) we used the identity

$$\begin{aligned} \nabla \cdot (\rho_k \mathbf{v}_k \mathbf{v}_k) &= \rho_k (\mathbf{v}_k \cdot \nabla \mathbf{v}_k) + \mathbf{v}_k \nabla \cdot (\rho_k \mathbf{v}_k) = \\ &= \rho_k (\mathbf{v}_k \cdot \nabla \mathbf{v}_k) + \mathbf{v}_k (\partial \rho_k / \partial t - \Gamma_k) \end{aligned} \quad (32)$$

Now multiplying equation (30) scalarly by $\mathbf{v} = \mathbf{v}_k - \rho_k^{-1} \mathbf{J}_k$ and taking into account definition (31), as a result we obtain

$$\sum_{k=1}^N \left\{ \rho_k \frac{d|\mathbf{v}_k|^2 / 2}{dt} \right\} = \sum_{k=1}^N \mathbf{J}_k \cdot \left\{ \frac{d^{(k)} \mathbf{v}_k}{dt} - \frac{1}{2} \nabla |\mathbf{v}_k|^2 \right\} + \mathbf{v} \cdot \left(-\nabla p + \nabla \cdot \boldsymbol{\tau} + \rho \mathbf{f} - \sum_{k=1}^N \Gamma_k \mathbf{v}_k \right). \quad (33)$$

Finally, for the final derivation of the equation for the balance of specific kinetic energy, we calculate the substantial derivative with respect to time du_K / dt , using equations (11) and (33) for this; as a result we will have

$$\begin{aligned} \rho \frac{du_K}{dt} &= \sum_{k=1}^N \rho_k \frac{d}{dt} \left(\frac{|\mathbf{v}_k|^2}{2} \right) + \sum_{k=1}^N \frac{|\mathbf{v}_k|^2}{2} (\Gamma_k - \nabla \cdot \mathbf{J}_k) = \\ &= -\nabla \cdot \left(\frac{1}{2} \sum_{k=1}^N \mathbf{J}_k |\mathbf{v}_k|^2 \right) + \sum_{k=1}^N \mathbf{J}_k \cdot \left\{ \frac{d^{(k)} \mathbf{v}_k}{dt} + \frac{\Gamma_k}{2\rho_k^2} \mathbf{J}_k \right\} + \mathbf{v} \cdot (-\nabla p + \nabla \cdot \boldsymbol{\tau} + \rho \mathbf{f}). \end{aligned} \quad (34)$$

Mechanical energy balance for a mixture. Let us define the total mechanical energy per unit mass of the mixture as the sum of kinetic energy $u_K(\mathbf{x}, t)$ and potential energy $\varphi(\mathbf{x}, t)$. Adding (27*) and (34), we obtain the following equation of the substantial balance of the quantity $u_m(\mathbf{x}, t)$

$$\begin{aligned} \rho \frac{du_m}{dt} &= -\nabla \cdot \left\{ \sum_{k=1}^N \mathbf{J}_k \left(\frac{1}{2} |\mathbf{v}_k|^2 + \varphi_k \right) \right\} + \\ &+ \sum_{k=1}^N \mathbf{J}_k \cdot \left\{ \frac{d^{(k)} \mathbf{v}_k}{dt} - \mathbf{f}_k + \frac{1}{2} \rho_k^{-1} \sum_{j=1}^N (\Gamma_{kj} - \Gamma_{jk}) (\mathbf{v}_k - \mathbf{v}_j) \right\} - \mathbf{v} \cdot \nabla p + \mathbf{v} \cdot (\nabla \cdot \boldsymbol{\tau}). \end{aligned} \quad (35)$$

When writing this equation, the transformation was used

$$\begin{aligned} \frac{1}{2} \sum_{k=1}^N \rho_k^{-2} \Gamma_k |\mathbf{J}_k|^2 &= \frac{1}{2} \sum_{k=1}^N \mathbf{J}_k \cdot \left\{ \sum_{j=1}^N \rho_k^{-2} \mathbf{J}_k (\Gamma_{kj} - \Gamma_{jk}) \right\} = \\ &= \frac{1}{2} \sum_{k=1}^N \mathbf{J}_k \cdot \left\{ \sum_{j=1}^N \rho_k^{-1} (\Gamma_{kj} - \Gamma_{jk}) \left(\frac{\mathbf{J}_k}{\rho_k} - \frac{\mathbf{J}_j}{\rho_j} \right) + \sum_{j=1}^N \mathbf{J}_j \rho_k^{-1} \rho_j^{-1} (\Gamma_{kj} - \Gamma_{jk}) \right\} = \end{aligned}$$

$$= \frac{1}{2} \sum_{k=1}^N \mathbf{J}_k \cdot \left\{ \rho_k^{-1} \sum_{j=1}^N (\Gamma_{kj} - \Gamma_{jk}) (\mathbf{v}_k - \mathbf{v}_j) \right\}. \quad (36)$$

The internal energy balance equation for a medium. Subtracting equation (35) from equation (26 *), we find the internal energy $\varepsilon(\mathbf{x}, t)$ balance equation in the following form:

$$\rho \frac{d\varepsilon}{dt} = -\nabla \cdot \mathbf{J}_q - \sum_{k=1}^N \mathbf{J}_k \cdot \left\{ \frac{d^{(k)} \mathbf{v}_k}{dt} - \mathbf{f}_k - \rho_k^{-1} \nabla \cdot \boldsymbol{\tau}_k + \rho_k^{-1} \sum_{j=1}^N \frac{\Gamma_{kj} - \Gamma_{jk}}{2} (\mathbf{v}_k - \mathbf{v}_j) \right\} -$$

$$-p \nabla \cdot \mathbf{v} - \sum_{k=1}^N \boldsymbol{\tau}_k : \nabla \mathbf{v}_k. \quad (37)$$

By the way, we note that the above phenomenological derivation of the balance equation for the specific internal energy of the mixture (when taken into account in the kinetic energy of diffusion) was not previously known (see the remark on p. 119 in the cited monograph I. Gyarmati[14]).

3. THE PRODUCTION OF ENTROPY IN REACTING MIXTURES AND LINEAR KINEMATIC CONSTITUTIVE EQUATIONS

If we put in the general balance equation (6) $a \equiv S$, $\mathbf{J}_a \equiv \mathbf{J}_S$ and, $\sigma_a \equiv \sigma_S$ then we obtain the local equation of the balance of the entropy of the mixture, the substantial form of which will have the form:

$$\rho \frac{dS}{dt} + \nabla \cdot \mathbf{J}_S = \sigma_S \geq 0, \quad (38)$$

where $\sigma_S(\mathbf{x}, t)$ and $\mathbf{J}_S(\mathbf{x}, t)$ are the intensity of the "source" and the flux of entropy, respectively. To find an explicit form for these two quantities, we substitute in the fundamental Gibbs equation (5), previously written along the trajectory of the center of mass of the physical elementary volume and taking the form

$$T \frac{dS}{dt} = \frac{d\varepsilon}{dt} + p \frac{dv}{dt} - \sum_{k=1}^N \mu_k \frac{dc_k}{dt}, \quad (39)$$

derivatives $d\varepsilon/dt$, dv/dt and dc_k/dt , taken from equations (37), (10) and (11), respectively. As a result, we get

$$\rho \frac{dS}{dt} + \nabla \cdot \left\{ \left(\mathbf{J}_q - \sum_{k=1}^N \mu_k \mathbf{J}_k \right) / T \right\} =$$

$$= \frac{1}{T} \left\{ \sum_{k=1}^N \mathbf{J}_k \cdot \left(\boldsymbol{\Lambda}_k - T \nabla \frac{\mu_k}{T} \right) - \mathbf{J}_q \cdot \frac{\nabla T}{T} + \sum_{k=1}^N \boldsymbol{\tau}_k : \nabla \mathbf{v}_k - \sum_{j=1}^r J_j A_j \right\} \equiv \sigma_S. \quad (40)$$

Here the so-called chemical affinity for the j -th reaction is introduced, defined as follows:

$$A_j(\mathbf{x}, t) = \sum_{k=1}^N v_k \mu_k \quad (j = 1, \dots, r), \quad (41)$$

and thermodynamic forces

$$\Lambda_k(\mathbf{x}, t) \equiv \mathbf{f}_k - \frac{d^{(k)} \mathbf{v}_k}{dt} + \rho_k^{-1} \nabla \cdot \boldsymbol{\tau}_k - 1/2 \rho_k^{-1} \sum_{j=1}^N (\Gamma_{kj} - \Gamma_{jk}) (\mathbf{v}_k - \mathbf{v}_j). \quad (41^*)$$

It should be noted that in the general case, energy dissipation $T\sigma_S(\mathbf{x}, t) \geq 0$, which is a bilinear positive definite quantity, is determined by a set of generalized thermodynamic flows $\mathcal{Y}(\mathbf{x}, t)$ and the corresponding generalized thermodynamic forces $\mathcal{X}(\mathbf{x}, t)$

$$T\sigma_S(\mathcal{Y}, \mathcal{X}) = \sum_{j=1}^f \mathcal{Y}_j \mathcal{X}_j, \quad (42)$$

where f is the number of independent scalar flows $\mathcal{Y}_j(\mathbf{x}, t)$ and forces $\mathcal{X}_j(\mathbf{x}, t)$ [10]. In this case, thermodynamic flows and forces can be defined, generally speaking, in different ways. It is only necessary that they be coupled to each other by relation (42). The choice of their type in each specific case depends on the convenience of considering the problem. A consequence of the absence of interference of flows and thermodynamic forces of different tensor dimensions in an isotropic system (Curie principle) is the fact that vector phenomena of diffusion and heat conduction can be considered independently of scalar or tensor phenomena. In this work, we will focus on the derivation of the constitutive relations only for vector phenomena.

For energy dissipation due to diffusion and thermal conductivity, we have the following expression

$$T\sigma_S(\mathbf{x}, t) = -\mathbf{J}_q \cdot \mathbf{X}_q + \sum_{k=1}^N \mathbf{J}_k \cdot \mathbf{X}_k^*, \quad (43)$$

where

$$\mathbf{X}_q(\mathbf{x}, t) \equiv -\frac{1}{T} \nabla T, \quad \mathbf{X}_k^*(\mathbf{x}, t) \equiv \Lambda_k - T \nabla \frac{\mu_k}{T}, \quad (k = 1, 2, \dots, N). \quad (44)$$

In order to be able to compare the constitutive relations (derived further by methods of nonequilibrium thermodynamics) for the thermodynamic flows of diffusion $\mathbf{J}_k(\mathbf{x}, t)$ and heat $\mathbf{J}_q(\mathbf{x}, t)$ with analogous relations obtained by gas-kinetic methods (see, for example, [2,3]), we express gradients of chemical potentials $\mu_k(\mathbf{x}, t)$ through gradients of thermo-hydrodynamic parameters. Considering further the multicomponent medium as a non-ideal system, we write down the chemical potential $\mu_k(\mathbf{x}, t)$ per unit mass of the component k in the form [20].

$$\mu_k(T, p, x_k) = \mu_k^\ominus(T, p) + \frac{kT}{m_k} \ln a_k, \quad (k = 1, 2, \dots, N), \quad (45)$$

where $\mu_k^\circ(T, p)$ is the chemical potential of the pure component k at a given temperature T and pressure p ; $a_k = x_k \gamma_k$, $\gamma_k(T, p, x_k)$, n_k , $x_k = n_k / n$ – activity, activity coefficient, number density and molar concentration of the k -th component, respectively; $n = \sum_{k=1}^N n_k$ is the total numerical density of the system. For imperfect mixtures, activity $a_k = a_k(p, T, x_k)$ is determined from theory or experiment in the same way as function $\mu_k^\circ(T, p)$.

If we now use the well-known thermodynamic relations [20]

$$\left(\frac{\partial \mu_k}{\partial T} \right)_p = -\frac{h_k}{T^2}, \quad \left(\frac{\partial \mu_k}{\partial p} \right)_T = \frac{v_k^*}{m_k}, \quad (k=1, 2, \dots, N), \quad (46)$$

we get

$$T \nabla \left(\frac{\mu_k}{T} \right) = \frac{kT}{m_k} \frac{(\nabla a_k)_{p,T}}{a_k} + \frac{v_k^*}{m_k} \nabla p - \frac{h_k}{T} \nabla T, \quad (k=1, 2, \dots, N). \quad (47)$$

Here, $v_k^*(\mathbf{x}, t)$ and h_k are respectively the partial specific volume and specific enthalpy of the k -th component. Substituting (47) into (44) and (43), we find

$$T \sigma_S(\mathbf{x}, t) = \mathbf{q} \cdot \mathbf{X}_q - \sum_{k=1}^N \mathbf{J}_k \cdot \mathbf{X}_k, \quad (48)$$

where

$$\mathbf{X}_k(\mathbf{x}, t) \equiv \frac{h_k}{T} \nabla T - \mathbf{X}_k^*(\mathbf{x}, t) = \frac{kT}{m_k} (\nabla \ln a_k)_{p,T} + \frac{v_k^*}{m_k} \nabla p - \mathbf{\Lambda}_k \quad (k=1, 2, \dots, N). \quad (49)$$

Phenomenological relations for flows through forces for a multicomponent medium. In states close to equilibrium, flows can be represented as linear functions of forces (the main postulate of thermodynamics of irreversible processes):

$$q^\alpha(\mathbf{x}, t) = \mathcal{L}_{00}^{\alpha\beta} X_{q\beta} - \sum_{j=1}^N \mathcal{L}_{0j}^{\alpha\beta} X_{j\beta}, \quad (50)$$

$$J_k^\alpha(\mathbf{x}, t) = \mathcal{L}_{k0}^{\alpha\beta} X_{q\beta} - \sum_{j=1}^N \mathcal{L}_{kj}^{\alpha\beta} X_{j\beta}, \quad (k=1, 2, \dots, N). \quad (51)$$

The indices here $\alpha, \beta = 1, 2, 3$ refer to a rectangular coordinate system. Kinetic coefficients $\mathcal{L}_{kj}^{\alpha\beta}$ ($k, j = 1, 2, \dots, N$) are tensors that depend on the defining parameters characterizing the geometric symmetry of the medium. In what follows, we will consider isotropic media with respect to the full group of orthogonal coordinate transformations. According to the general theory of ten-

sors [12], the symmetry properties of isotropic media are fully characterized by the metric tensor $\mathbf{g}^{\alpha\beta}$; all tensors will be tensor functions of the metric tensor only:

$$\mathcal{L}_{kj}^{\alpha\beta} = \alpha_{kj} \mathbf{g}^{\alpha\beta}, \quad (k, j = 0, 1, 2, \dots, N).$$

For an isotropic medium in a rectangular coordinate system

$$\mathbf{g}^{\alpha\beta} = \delta^{\alpha\beta} = \begin{cases} 1, & \alpha = \beta; \\ 0, & \alpha \neq \beta \end{cases}$$

and the phenomenological equations connecting thermodynamic flows and forces take the form

$$\mathbf{q}(\mathbf{x}, t) = \alpha_{00} \mathbf{X}_0 - \sum_{j=1}^N \alpha_{0j} \mathbf{X}_j, \quad (52)$$

$$\mathbf{J}_k(\mathbf{x}, t) = \alpha_{k0} \mathbf{X}_0 - \sum_{j=1}^N \alpha_{kj} \mathbf{X}_j, \quad (k = 1, 2, \dots, N). \quad (53)$$

Once linear relations (52) and (53) are postulated, Onsager's theorem gives

$$\alpha_{kj} = \alpha_{jk}, \quad (k, j = 0, 1, 2, \dots, N). \quad (54)$$

A number of additional relationships follow from the fact of the independence of forces [10]

$$\sum_{j=1}^N \alpha_{kj} = 0, \quad (k = 0, 1, 2, \dots, N). \quad (55)$$

Thus, $(N+1)^2$ of the coefficients, there are $\frac{1}{2}N(N-1)$ independent phenomenological coefficients α_{ij} ($i, j = 0, 1, 2, \dots, N$).

Diffusive thermodynamic forces. For further purposes, it is convenient to material relations (52) and (53) for thermodynamic flows $\mathbf{q}(\mathbf{x}, t)$ and $\mathbf{J}_k(\mathbf{x}, t)$ can be written using some other linearly dependent vectors $\mathbf{d}_k^{(a)}(\mathbf{x}, t)$, closely related to $\mathbf{X}_k(\mathbf{x}, t)$. This can be done, for example, as follows: put $\mathbf{d}_k^{(a)}(\mathbf{x}, t) \equiv \rho_k \mathbf{X}_k / p - \rho_k \mathbf{K} / p$ and define a vector \mathbf{K} common for all components k from the condition

$$\sum_{k=1}^N \mathbf{d}_k^{(a)}(\mathbf{x}, t) = 0; \quad (56)$$

then, taking into account (49), we obtain

$$\mathbf{K} = \sum_{k=1}^N c_k \mathbf{X}_k = \sum_{k=1}^N c_k \left(\frac{kT}{m_k} (\nabla \ln a_k)_{p,T} + \frac{v_k^*}{m_k} \nabla p - \mathbf{\Lambda}_k \right) = \frac{1}{\rho} \nabla p - \sum_{k=1}^N c_k \mathbf{\Lambda}_k. \quad (57)$$

When writing (57), the Gibbs–Duhem relation was taken into account for the case of constant pressure and temperature

$$0 = \sum_{k=1}^N \rho_k (\nabla \mu_k)_{p,T} = kT \sum_{k=1}^N \rho_k \frac{(\nabla \ln a_k)_{p,T}}{m_k} = p \sum_{k=1}^N x_j (\nabla \ln a_k)_{p,T}$$

and the property $\sum_{k=1}^N n_k v_k^* = 1$ for partial specific volumes v_k^* (see [10]; p. 225).

Using (49) and (57), vectors $\mathbf{d}_j^{(a)}(\mathbf{x}, t)$ can be given the form:

$$\mathbf{d}_j^{(a)}(\mathbf{x}, t) = x_j (\nabla \ln a_j)_{p,T} + n_j v_j^* \nabla \ln p - \frac{c_j}{p} \rho \mathbf{\Lambda}_j - \frac{c_j}{p} \sum_{k=1}^N \rho_k \mathbf{X}_k .$$

If we now exclude vectors $\mathbf{X}_k(\mathbf{x}, t)$ from this formula using expression (49), then as a result we will have

$$\mathbf{d}_j^{(a)}(\mathbf{x}, t) = x_j (\nabla \ln a_j)_{p,T} + \frac{n_j v_j^* - c_j}{p} \nabla p - \frac{c_j}{p} \left(\rho \mathbf{\Lambda}_j - \sum_{k=1}^N \rho_k \mathbf{\Lambda}_k \right), \quad (j = 1, 2, \dots, N). \quad (58)$$

These vectors are usually called the diffusive thermodynamic forces of the component (see, for example, [3,6]).

Finally, the vectors $\mathbf{d}_k^{(a)}(\mathbf{x}, t)$ written taking into account expressions (42) take the following final form

$$\begin{aligned} \mathbf{d}_k^{(a)}(\mathbf{x}, t) \equiv \frac{1}{p} \left\{ \rho_k \frac{d^{(k)} \mathbf{v}_k}{dt} - \nabla \cdot \boldsymbol{\tau}_k - \rho_k \mathbf{f}_k + \sum_{j=1}^N \frac{(\Gamma_{kj} - \Gamma_{jk})}{2} (\mathbf{v}_k - \mathbf{v}_j) + \right. \\ \left. + p x_k \frac{(\nabla a_k)_{p,T}}{a_k} + n_k v_k^* \nabla p \right\} \end{aligned} \quad (59)$$

When writing this expression, we used, following from (30) and (42), the transformation

$$\begin{aligned} \sum_{k=1}^N \rho_k \mathbf{\Lambda}_k &= \sum_{k=1}^N \left\{ \rho_k \mathbf{f}_k - \rho_k \frac{d^{(k)} \mathbf{v}_k}{dt} + \nabla \cdot \boldsymbol{\tau}_k - \sum_{j=1}^N \frac{(\Gamma_{kj} - \Gamma_{jk})}{2} (\mathbf{v}_k - \mathbf{v}_j) \right\} = \nabla p + \\ &+ \sum_{k=1}^N \mathbf{v}_k \Gamma_k - \sum_{k=1}^N \sum_{j=1}^N \frac{(\Gamma_{kj} - \Gamma_{jk})}{2} (\mathbf{v}_k - \mathbf{v}_j) = \nabla p + \sum_{k=1}^N \sum_{j=1}^N \frac{(\Gamma_{kj} - \Gamma_{jk})}{2} (\mathbf{v}_k + \mathbf{v}_j) = \nabla p . \end{aligned}$$

Regarding expression (58) for vectors $\mathbf{d}_k^{(a)}$, it is important to note the following. In the case when the contribution of the kinetic energy of diffusion to the mechanical energy of the mixture (in this case $\mathbf{\Lambda}_k \equiv \mathbf{f}_k$) is not taken into account, and the multicomponent medium is a mixture of

ideal gases (for which $a_k = x_k$, $p = kTn$ the partial molar volume is also $v_k^* = 1/n$), this expression is reduced to the form

$$\mathbf{d}_k = \nabla x_k + \frac{x_k - c_k}{p} \nabla p - \frac{c_k}{p} \left(\rho \mathbf{f}_k - \sum_{j=1}^N \rho_j \mathbf{f}_j \right)$$

widely used in the kinetic theory of multicomponent gases [2,3].

Further, for brevity, in expression (59), we will further use the notation

$$\nabla_a p_k \equiv p_k \frac{(\nabla a_k)_{p,T}}{a_k} + n_k v_k^* \nabla p. \quad (60)$$

Substituting now vectors $\mathbf{X}_k = p \mathbf{d}_k^{(a)} / \rho_k + \mathbf{K}$ into equations (52) and (53) and taking into account relations (55), we obtain the transport equations in the form:

$$\mathbf{q}(\mathbf{x}, t) = \alpha_{00} \mathbf{X}_q - p \sum_{k=1}^N \frac{\alpha_{0k}}{\rho_k} \mathbf{d}_k^{(a)}, \quad (61)$$

$$\mathbf{J}_j(\mathbf{x}, t) = \alpha_{j0} \mathbf{X}_q - p \sum_{k=1}^N \frac{\alpha_{jk}}{\rho_k} \mathbf{d}_k^{(a)}, \quad (j = 1, 2, \dots, N). \quad (62)$$

We now use property (56) for vectors $\mathbf{d}_k^{(a)}$ and relations (54) and (55), introduce (by analogy with the kinetic theory of gases) generalized diffusion coefficients D_{ik} , generalized thermal diffusion coefficients D_i^T and a coefficient through which the thermal conductivity coefficient λ' will be further expressed λ . Then

$$\mathbf{q}(\mathbf{x}, t) = -\lambda' \nabla T - p \sum_{k=1}^N D_{Tk} \mathbf{d}_k^{(a)}, \quad (63)$$

$$\mathbf{J}_i(\mathbf{x}, t) = -\rho_i D_{Ti}^T \nabla \ln T - \rho_i \sum_{k=1}^N D_{ik} \mathbf{d}_k^{(a)}, \quad (j = 1, 2, \dots, N), \quad (64)$$

where, by definition, it is assumed

$$\lambda' \equiv \alpha_{00} / T, \quad D_{Tk} \equiv \alpha_{0k} / \rho_k = \alpha_{k0} / \rho_k, \quad (k = 1, 2, \dots, N), \quad (65)$$

$$D_{ik} = D_{ki} \equiv p \alpha_{ik} / \rho_i \rho_k, \quad (i, k = 1, 2, \dots, N). \quad (66)$$

According to relations (55) connecting the kinetic coefficients α_{0k} and α_{ik} , the generalized diffusion and thermal diffusion coefficients introduced by us are linearly dependent:

$$\sum_{k=1}^N \rho_k D_{Tk} = 0, \quad (1) \quad \sum_{k=1}^N \rho_k D_{ki} = 0, \quad (2) \quad (k = 1, 2, \dots, N). \quad (67)$$

Thus, we have $\frac{1}{2}N(N-1)$ independent multicomponent diffusion coefficients D_{ij} , which, together with independent thermal diffusion coefficients and the coefficient, will give independent transport coefficients in accordance with the general Onsager theory (see (52)-(55)). Expressions (63) and (64) in the particular case of ideal mixtures identically coincide with similar relations obtained phenomenologically, for example, in the monograph [13].

Thermal diffusion relations. It is known that thermal diffusion is an effect of the second order of smallness, important only in those cases when there is a large difference in the masses involved in the transfer of components. For further purposes, it is convenient to introduce new transfer coefficients to describe the effects of thermal diffusion – the so-called thermal diffusion ratios $k_{T\alpha}(\mathbf{x}, t)$:

$$\sum_{k=1}^N D_{ki} k_{Tk} = D_{Ti}, \quad (j = 1, 2, \dots, N), \quad (68)$$

$$\sum_{k=1}^N k_{Tk}(\mathbf{x}, t) = 0. \quad (69)$$

Thermal diffusion ratio $k_{Tk}(\mathbf{x}, t)$ characterizes a measure of the relative importance of thermal diffusion in relation to ordinary diffusion. Due to the correlation (67⁽²⁾), the determinant of the coefficients of the system of equations (68) vanishes. The only solution to the system of homogeneous equations corresponding to equations (68) is the N -component vector of mass concentrations $c_\alpha \equiv \rho_\alpha/\rho$, but, according to (67⁽¹⁾), this vector is orthogonal to the N -component vector of thermal diffusion coefficients. Thus, equations (68) have a solution in the form of a certain vector \mathbf{k}_T with components $k_{Tj}(\mathbf{x}, t)$ ($j = 1, 2, \dots, N$) determined up to some arbitrary constant multiplied by ρ_k ; condition (69) ensures the uniqueness of the vector \mathbf{k}_T .

When using coefficients k_{Tj} , expression (64) for the diffusion flux $\mathbf{J}_i(\mathbf{x}, t)$ can be written in the form of the following generalized Fick's law:

$$\mathbf{J}_i(\mathbf{x}, t) = -\rho_i \sum_{k=1}^N D_{ik} (\mathbf{d}_k + k_{Tk} \nabla \ln T), \quad (i = 1, 2, \dots, N). \quad (70)$$

We now make the following important remark regarding relation (63) for the heat flux $\mathbf{q}(\mathbf{x}, t)$. The coefficient λ' cannot be determined as a result of direct experimental measurement, since the temperature gradient in the gas mixture causes thermal diffusion and, therefore, leads to concentration gradients. Therefore, even in stationary processes, the vectors $\mathbf{d}_k^{(a)}$ are not equal to zero, which means that the heat flux due to the temperature gradient is always accompanied by

the heat flux due to the concentration gradients. Using relations (64), (66), and (70), it is possible to express vectors $\mathbf{d}_k^{(a)}$ in terms of diffusion fluxes and temperature gradient:

$$\sum_{k=1}^N D_{Tk} \mathbf{d}_k^{(a)} = \sum_{k=1}^N \sum_{j=1}^N D_{kj} k_{Tj} \mathbf{d}_k^{(a)} = - \sum_{j=1}^N k_{Tj} \left(\frac{1}{\rho_j} \mathbf{J}_j + D_{Tj} \nabla \ln T \right). \quad (71)$$

Substituting this expression in (63), we obtain the defining relation for the vector of the reduced heat flux in the form

$$\mathbf{q}(\mathbf{x}, t) = -\lambda \nabla T + p \sum_{k=1}^N \frac{k_{Tk}}{\rho_k} \mathbf{J}_k, \quad (72)$$

where $\lambda(\mathbf{x}, t)$ is the true (molecular) thermal conductivity coefficient of the multicomponent mixture,

$$\lambda(\mathbf{x}, t) \equiv \lambda' - k n \sum_{j=1}^N k_{Tj} D_{Tj}. \quad (73)$$

It is this coefficient that can be directly measured experimentally in a stationary system, since in the stationary case all diffusion fluxes $\mathbf{J}_j(\mathbf{x}, t)$ are equal to zero when the gas as a whole is at rest.

Finally, it follows from (70) and (72) that the contribution of the effects of heat conduction and diffusion to expression (43) for the rate of entropy appearance is

$$\overset{(vektor)}{\sigma_{(S)}} = \lambda |\nabla \ln T|^2 + p \sum_{k=1}^N \sum_{j=1}^N D_{kj} \left(\mathbf{d}_k^{(a)} + k_{Tk} \nabla \ln T \right) \cdot \left(\mathbf{d}_j^{(a)} + k_{Tj} \nabla \ln T \right) \geq 0. \quad (74)$$

From the condition that one of the terms can be equal to zero, while the others are not equal to zero, it follows that the coefficient of thermal conductivity $\lambda > 0$, and for the coefficients of multicomponent diffusion, the inequality

$$\sum_{k=1}^N \sum_{j=1}^N D_{kj} \mathbf{y}_k \mathbf{y}_j \geq 0 \quad (75)$$

for any vectors \mathbf{y}_j satisfying the condition $\sum_j \mathbf{y}_j = 0$. From the properties of a nonnegative definite

matrix of coefficients D_{kj} , one can indicate the following Sylvester conditions: $D_{kk} \geq 0$ – non negativity of all elements of the matrix D_{kj} on the main diagonal $D_{kj} D_{jk} \leq D_{kk} D_{jj}$; (each minor of a nonnegative definite matrix D_{kj} containing elements of its main diagonal as its own main diagonal must also be nonnegative), etc. Within the limits of these limitations, the diffusion

coefficients D_{kj} vary in a very wide range of values in accordance with the degree of connection between the processes of heat and mass transfer.

4. STEFAN-MAXWELL RELATIONS AND HEAT FLUX FOR MULTICOMPONENT NON-IDEAL MEDIUM

The use of constitutive relations (64) for diffusion fluxes $\mathbf{J}_k(\mathbf{x}, t)$ in the general multicomponent case is extremely difficult, since in the literature, with rare exceptions, there is no practical information on the generalized coefficients of multicomponent diffusion $D_{kj}(\mathbf{x}, t)$, and the existing experimental data refer mainly to diffusion coefficients in binary gas mixtures $\mathcal{D}_{kj}(\mathbf{x}, t)$. At the same time, the gas-kinetic theory of mixtures gives extremely cumbersome formulas connecting the diffusion coefficients $D_{kj}(\mathbf{x}, t)$ with binary coefficients $\mathcal{D}_{kj}(\mathbf{x}, t)$ for various pairs of mixture components. These formulas are usually difficult to use when solving specific problems. In addition, the system of diffusion equations obtained after substitution $\mathbf{J}_k(\mathbf{x}, t)$ from (64) into balance equations (11) turns out to be unresolved with respect to the higher derivatives. As is known, the numerical implementation of such systems is fraught with certain difficulties. Therefore, when analyzing diffusion processes in multicomponent gas mixtures, a different formulation of the problem is often advantageous, when constitutive relations (64) for diffusion flows $\mathbf{J}_k(\mathbf{x}, t)$ are used in a form that is resolved with respect to diffusion thermodynamic forces $\mathbf{d}_k(\mathbf{x}, t)$ through flows $\mathbf{J}_k(\mathbf{x}, t)$. Such an inverse transformation can be written in the form of the so-called generalized Stefan–Maxwell relations, which, instead of generalized coefficients of multicomponent diffusion $D_{kj}(\mathbf{x}, t)$, include molecular diffusion coefficients in binary gas mixtures $\mathcal{D}_{kj}(\mathbf{x}, t)$.

Generalized Stefan–Maxwell relations. For the phenomenological derivation of the Stefan–Maxwell relations, let us solve equations (61) and (62) with respect to generalized thermodynamic forces

$$\mathcal{X}_0 \equiv \mathcal{X}_q = -\frac{\nabla T}{T}, \quad \mathcal{X}_i = \mathcal{X}_i \equiv -p \frac{\mathbf{d}_i^{(a)}}{\rho_i}, \quad (i = 1, 2, \dots, N) \quad (76)$$

through flows $\mathbf{q}(\mathbf{x}, t)$ and $\mathbf{J}_k(\mathbf{x}, t)$ ($1, 2, \dots, N$). In relations (61) and (62), only N independent equations, since

$$\sum_{k=1}^N \mathbf{J}_k = 0, \quad (77)$$

$$\sum_{k=1}^N \alpha_{k0} = 0, \quad \sum_{k=1}^N \alpha_{kj} = 0, \quad (k = 1, 2, \dots, N). \quad (78)$$

Therefore, we omit the last equation from system (62) and write relations (61) and (62) in the form

$$\mathbf{q} - \alpha_{00}\boldsymbol{\mathcal{X}}_q = \sum_{k=1}^{N-1} \alpha_{0k}(\boldsymbol{\mathcal{X}}_k - \boldsymbol{\mathcal{X}}_N), \quad (79)$$

$$\mathbf{J}_j - \alpha_{j0}\boldsymbol{\mathcal{X}}_q = \sum_{k=1}^{N-1} \alpha_{jk}(\boldsymbol{\mathcal{X}}_k - \boldsymbol{\mathcal{X}}_N), \quad (j=1,2,\dots,N-1). \quad (80)$$

Solving system (80) with respect to $(\boldsymbol{\mathcal{X}}_k - \boldsymbol{\mathcal{X}}_N)$ ($j=1,2,\dots,N-1$), we find

$$\boldsymbol{\mathcal{X}}_j - \boldsymbol{\mathcal{X}}_N = \sum_{k=1}^{N-1} \beta_{jk}(\mathbf{J}_k - \alpha_{k0}\boldsymbol{\mathcal{X}}_0), \quad (j=1,2,\dots,N-1), \quad (81)$$

where the elements of the inverse matrix β_{jk} satisfy the relations

$$\sum_{k=1}^{N-1} \beta_{ik}\alpha_{kj} = \delta^{ij} = \begin{cases} 1, & i=j, \\ 0, & i \neq j. \end{cases} \quad (82)$$

The symmetry of the coefficients α_{ij} implies the symmetry of the coefficients β_{ij} :

$$\beta_{ij} = \beta_{ji}, \quad (i,j=1,2,\dots,N-1). \quad (83)$$

From relation (79), using (81), we find

$$\mathbf{q} = \left[\alpha_{00} - \sum_{k=1}^{N-1} \sum_{j=1}^{N-1} \alpha_{0k}\beta_{kj}\alpha_{j0} \right] \boldsymbol{\mathcal{X}}_0 + \sum_{j=1}^{N-1} \left[\sum_{k=1}^{N-1} \alpha_{0k}\beta_{kj} \right] \mathbf{J}_j. \quad (84)$$

Multiplying each of the equations (81) by c_j and summing them from 1 to $(N-1)$, we find

$$\boldsymbol{\mathcal{X}}_N = \boldsymbol{\mathcal{X}}_0 \sum_{k=1}^{N-1} \sum_{j=1}^{N-1} c_j \beta_{jk} \alpha_{k0} - \sum_{k=1}^{N-1} \mathbf{J}_k \left(\sum_{j=1}^{N-1} c_j \beta_{jk} \right), \quad (85)$$

$$\boldsymbol{\mathcal{X}}_i = \boldsymbol{\mathcal{X}}_0 \sum_{k=1}^{N-1} \left(\sum_{j=1}^{N-1} c_j \beta_{jk} - \beta_{ik} \right) \alpha_{k0} - \sum_{k=1}^{N-1} \left(\sum_{j=1}^{N-1} c_j \beta_{jk} - \beta_{ik} \right) \mathbf{J}_k, \quad (i=1,2,\dots,N). \quad (86)$$

The force can be found from expression (84). Equations (85) and (86) represent the sought inversion of relations (62).

In order to write these equations in the form of generalized Stefan - Maxwell relations with symmetric coefficients, we add to equations (84), (85), and (86) equation (77), respectively multiplied by the constants a_0, a_N and a_i ($i=1,2,\dots,N-1$), and determine the free parameters a_0 and a_i from symmetry conditions for the coefficients $\mathcal{A}_{ik} = \mathcal{A}_{ki}$. For this, it is necessary to put

$$a_0 = - \sum_{k=1}^{N-1} \sum_{j=1}^{N-1} c_j \beta_{jk} \alpha_{k0}, \quad (87)$$

$$a_i = a_N - \sum_{k=1}^{N-1} c_k \beta_{ki}, \quad (i = 1, 2, \dots, N-1). \quad (88)$$

Then we get

$$\mathbf{q} = \mathcal{A}_{00} \boldsymbol{\chi}_0 + \sum_{k=1}^N \mathcal{A}_{0k} \mathbf{J}_k, \quad (89)$$

$$-\boldsymbol{\chi}_i = \mathcal{A}_{i0} \boldsymbol{\chi}_0 + \sum_{k=1}^N \mathcal{A}_{ik} \mathbf{J}_k, \quad (i = 1, 2, \dots, N), \quad (90)$$

where the coefficients \mathcal{A}_{ik} are

$$\mathcal{A}_{00} = \alpha_{00} - \sum_{k=1}^{N-1} \sum_{j=1}^{N-1} \alpha_{0k} \beta_{kj} \alpha_{j0}, \quad (91)$$

$$\mathcal{A}_{0N} = \mathcal{A}_{N0} = a_0 = - \sum_{k=1}^{N-1} \sum_{j=1}^{N-1} c_j \beta_{jk} \alpha_{k0}, \quad (92)$$

$$\mathcal{A}_{0i} = \mathcal{A}_{i0} = a_0 + \sum_{k=1}^{N-1} \alpha_{0k} \beta_{ki} = \sum_{k=1}^{N-1} \alpha_{0k} \left(\beta_{ki} - \sum_{j=1}^{N-1} c_j \beta_{jk} \right), \quad (i = 1, 2, \dots, N-1), \quad (93)$$

$$\mathcal{A}_{ik} = \mathcal{A}_{ki} = a_N + \sum_{j=1}^{N-1} c_j (\beta_{ji} + \beta_{jk}) - \beta_{ik}, \quad (i = 1, 2, \dots, N-1), \quad (94)$$

$$\mathcal{A}_{Ni} = \mathcal{A}_{iN} = a_N + \sum_{k=1}^{N-1} c_k \beta_{ki}, \quad (95)$$

$$\mathcal{A}_{NN} = -a_N, \quad (96)$$

and the identity

$$\sum_{\alpha=1}^N c_\alpha \mathcal{A}_{\alpha 0} = 0. \quad (97)$$

Thus, the coefficients \mathcal{A}_{ik} ($i, k = 0, 1, \dots, N$) are determined to within a constant a_N , which, generally speaking, can be chosen arbitrarily. Here we define it, assuming the flows $\mathbf{J}_i(\mathbf{x}, t)$ ($i = 1, 2, \dots, N$) are arbitrary.

Let us rewrite relations (89), (90) in the form

$$\boldsymbol{\chi}_0 = \frac{1}{\mathcal{A}_{00}} \mathbf{q} - \sum_{k=1}^N \frac{\mathcal{A}_{0k}}{\mathcal{A}_{00}} \mathbf{J}_k, \quad (98)$$

$$\boldsymbol{\chi}_i = -\frac{\mathcal{A}_{i0}}{\mathcal{A}_{00}} \mathbf{q} + \sum_{k=1}^N \left(\frac{\mathcal{A}_{i0} \mathcal{A}_{0k}}{\mathcal{A}_{00}} - \mathcal{A}_{ik} \right) \mathbf{J}_k, \quad (i = 1, 2, \dots, N). \quad (99)$$

Using identity (56), notation (76), and the arbitrariness of vectors $\mathbf{J}_k(\mathbf{x}, t)$, taking into account (97)–(99), we obtain

$$\sum_{k=1}^N c_k \mathcal{A}_{ki} = 0, \quad (i = 1, 2, \dots, N). \quad (100)$$

Substituting the coefficients (94) and (95) into these relations, we find a_N :

$$a_N = - \sum_{k=1}^{N-1} \sum_{j=1}^{N-1} c_k c_j \beta_{kj}. \quad (101)$$

Thus, the constants in (94)–(96) are completely defined in terms of the elements of the symmetric matrix of phenomenological coefficients α_{ij} and the elements of the symmetric matrix β_{ij} inverse to it (see (83)).

Let us now bring expressions (90) to the form of the so-called generalized Stefan–Maxwell relations for multicomponent diffusion. For this we read from (90) the corresponding equality (100) multiplied by \mathbf{J}_i/c_i , then we find

$$-\mathbf{x}_i = \mathcal{A}_{i0} \mathbf{x}_0 + \sum_{k=1}^N \rho_k \mathcal{A}_{ik} (\mathbf{w}_k - \mathbf{w}_i), \quad (i = 1, 2, \dots, N), \quad (102)$$

or in more familiar notation

$$\mathbf{d}_i^{(a)} = \sum_{k=1}^N \frac{\rho_i \rho_k}{p} \mathcal{A}_{ik} (\mathbf{w}_k - \mathbf{w}_i) - \frac{\rho_i \mathcal{A}_{i0}}{p} \frac{\nabla T}{T}, \quad (i = 1, 2, \dots, N). \quad (103)$$

It remains to show that

$$\mathcal{A}_{i0} = - \sum_{k=1}^N \rho_k \mathcal{A}_{ik} \left(\frac{\alpha_{0k}}{\rho_k} - \frac{\alpha_{0i}}{\rho_i} \right), \quad (i = 1, 2, \dots, N). \quad (104)$$

Using (92)–(97) and identities (101) for this, we find

$$\begin{aligned} \sum_{k=1}^N \rho_k \mathcal{A}_{ik} \left(\frac{\alpha_{0k}}{\rho_k} - \frac{\alpha_{0i}}{\rho_i} \right) &= \sum_{k=1}^{N-1} \rho_k \left(\frac{\alpha_{0k}}{\rho_k} - \frac{\alpha_{0i}}{\rho_i} \right) \left[\alpha_N + \sum_{j=1}^{N-1} c_j (\beta_{ji} + \beta_{jk}) - \beta_{ik} \right] + \\ &+ \rho_N \left(\frac{\alpha_{0N}}{\rho_N} - \frac{\alpha_{0i}}{\rho_i} \right) \left(a_N + \sum_{k=1}^{N-1} c_k \beta_{ki} \right) = \sum_{k=1}^{N-1} \alpha_{0k} \left(\sum_{j=1}^{N-1} c_j \beta_{jk} - \beta_{ik} \right) - \\ &\frac{\alpha_{0i}}{c_i} \left(a_N + \sum_{k=1}^{N-1} c_k \beta_{ki} \right) - \sum_{k=1}^{N-1} \frac{c_k}{c_i} \alpha_{0i} \left(\sum_{j=1}^{N-1} c_j \beta_{jk} - \beta_{ik} \right) = \end{aligned}$$

$$= \sum_{k=1}^{N-1} \alpha_{0k} \left(\sum_{j=1}^{N-1} c_j \beta_{jk} - \beta_{ik} \right) = -\mathcal{A}_{i0}. \quad (105)$$

Substituting (104) into (103) and using notation (65) for the thermal diffusion coefficients, we finally find

$$\mathbf{d}_i^{(a)} = \sum_{k=1}^N \frac{\rho_k \rho_i \mathcal{A}_{ik}}{p} (\mathbf{w}_k - \mathbf{w}_j) + \frac{\nabla T}{T} \sum_{k=1}^N \frac{\rho_k \rho_i \mathcal{A}_{ik}}{p} (D_{Tk} - D_{Ti}), \quad (i = 1, 2, \dots, N), \quad (106)$$

which completely coincides for the case of ideal mixtures with the classical Stefan–Maxwell relations [6].

$$\mathbf{d}_i = \sum_{k=1}^N \frac{n_k n_i}{n^2 \mathcal{D}_{ik}} (\mathbf{w}_k - \mathbf{w}_j) + \nabla \ln T \sum_{k=1}^N \frac{n_k n_i}{n^2 \mathcal{D}_{ik}} (D_{Tk} - D_{Ti}), \quad (107)$$

if we identify the binary diffusion coefficients \mathcal{D}_{ik} of the kinetic theory with the expression

$$\mathcal{D}_{ik} = kT / m_i m_k n \mathcal{A}_{ik}. \quad (108)$$

Note that these coefficients are considered independent concentration x_k and there is no need to calculate them from the properties of molecules. You can use the experimental values measured on binary mixtures [7].

As noted above, very convenient parameters of thermodiffusion processes are thermal diffusion ratios k_{Tk} , which we define here through the phenomenological coefficients \mathcal{A}_{k0} by the formula

$$k_{Tk} = \rho_k \mathcal{A}_{k0} / p. \quad (109)$$

Then, by virtue of (97), equality (69) holds. In addition, using transformation (105), as well as definitions (108) and (109), it is easy to obtain the following system of equations

$$\sum_{k=1}^N \frac{n_i n_k}{\mathcal{D}_{ik} n^2} (D_{Ti} - D_{Tk}) = k_{Ti}(\mathbf{x}, t), \quad (i = 1, 2, \dots, N-1), \quad (110)$$

for finding thermal diffusion ratios k_{Ti} through binary diffusion coefficients \mathcal{D}_{ki} and thermal diffusion coefficients D_{Ti} . Thus, the thermal diffusion ratios k_{Tk} introduced earlier by formulas (68) and (69) completely coincide with the coefficients (109).

Finally, using formulas (108) and (110), we rewrite the generalized Stefan–Maxwell relations (103) for non ideal mixtures in the following final form:

$$\sum_{i=1}^N \frac{n_i n_k}{n^2 \mathcal{D}_{ik}} (\mathbf{v}_i - \mathbf{v}_k) - k_{Tk} \nabla \ln T = \mathbf{d}_k^{(a)}, \quad (k = 1, 2, \dots, N), \quad (111)$$

where

$$\mathbf{d}_k^{(a)} \equiv \frac{1}{p} \left\{ \rho_k \frac{d^{(k)} \mathbf{v}_k}{dt} - \nabla \cdot \boldsymbol{\tau}_k - \rho_k \mathbf{f}_k - \frac{1}{2} \sum_{i=1}^N (\Gamma_{ki} - \Gamma_{ik}) (\mathbf{v}_i - \mathbf{v}_k) + \nabla_a p_k \right\}. \quad (112)$$

This form of the Stefan–Maxwell relations, intended for finding the rates of relative diffusion, is most convenient for solving hydrodynamic problems, since the transfer coefficients $\mathcal{D}_{ki}(\mathbf{x}, t)$ and $\mathbf{k}_{Tk}(\mathbf{x}, t)$ have much simpler expressions for practical calculation than the multicomponent diffusion coefficients $D_{ik}(\mathbf{x}, t)$ and thermal diffusion coefficients $D_{Tk}(\mathbf{x}, t)$.

There is an interesting interpretation of the Stefan–Maxwell relation (111) as an equation of motion for a separate component of a non ideal mixture (see, for example, "Note I" in the monograph by Chapman and Cowling [1]). In this case, collisions between the molecules of the k -ith and i -th components lead to a force acting on each substance and tending to eliminate the relative velocity $(\mathbf{v}_i - \mathbf{v}_k)$. Substituting (112) into (111), we obtain

$$\begin{aligned} \rho_k \frac{d^{(k)}\mathbf{v}_k}{dt} = & -\nabla_a p_k + \nabla \cdot \boldsymbol{\tau}_k + \rho_k \mathbf{f}_k + \sum_{i=1}^N \theta_{ik} n_i n_k (\mathbf{v}_i - \mathbf{v}_k) + \\ & + \frac{1}{2} \sum_{i=1}^N (\Gamma_{ki} - \Gamma_{ik}) (\mathbf{v}_i - \mathbf{v}_k) + \mathbf{k} n \mathbf{k}_{Ti} \nabla T, \end{aligned} \quad (113)$$

where $\theta_{ki} = kT / n\mathcal{D}_{ki}$, and the parameter $\theta_{ki}(\mathbf{x}, t)$ (at least roughly) does not depend on the proportions of the mixture [1]; the penultimate term describes the change in the momentum of a component k during chemical reactions.

It should be noted that, in contrast to the analogous equation of motion obtained in the approximation of equal acceleration (when $d^{(k)}\mathbf{v}_k / dt \equiv d\mathbf{v} / dt$) by the methods of kinetic theory in the monograph cited above, system (113) is a system of hydrodynamic equations of a nonideal mixture with genuine inertial forces.

Full heat flux in ideal multi-component environments. From relation (89), taking into account (109), the expression for the reduced heat flux $\mathbf{q}(\mathbf{x}, t)$ follows

$$\mathbf{q} = \mathcal{A}_{00} \boldsymbol{\chi}_0 + \sum_{k=1}^N \mathcal{A}_{0k} \mathbf{J}_k = -\lambda \nabla T + p \sum_{k=1}^N \mathbf{k}_{Tk} \mathbf{w}_k, \quad (114)$$

where by the formula

$$\lambda = \mathcal{A}_{00} / T \quad (115)$$

the so-called true thermal conductivity coefficient was determined, which is related to the previously introduced coefficient by the ratio

$$\lambda = \lambda' - kT \sum_{k=1}^N \mathbf{k}_{Tk} D_{Tk} = \lambda' - kT \sum_{k=1}^N \sum_{j=1}^N \mathbf{k}_{Tk} D_{kj} \mathbf{k}_{Tj}. \quad (116)$$

Indeed, by virtue of (82), (91) and the transformation $\sum_{k=1}^N \alpha_{jk} \mathcal{A}_{k0} = \alpha_{0k}$ easily deduced using formulas (92) and (93), we will have

$$\begin{aligned} \mathcal{A}_{00} \equiv \alpha_{00} - \sum_{j=1}^{N-1} \sum_{k=1}^{N-1} \alpha_{0k} \beta_{kj} \alpha_{0j} &= \alpha_{00} - \sum_{j=1}^{N-1} \sum_{k=1}^{N-1} \alpha_{0k} \beta_{kj} \left[\alpha_{0N} \mathcal{A}_{N0} + \right. \\ &\left. + \sum_{i=1}^{N-1} \alpha_{ji} \mathcal{A}_{i0} \right] = \alpha_{00} - \sum_{k=1}^{N-1} \alpha_{0k} \mathcal{A}_{k0} - \mathcal{A}_{N0} \alpha_{0N} = \alpha_{00} - \sum_{k=1}^N \alpha_{0k} \mathcal{A}_{k0}. \end{aligned} \quad (117)$$

Hence, when using definitions (65), (109) and (115), expression (116) follows.

Thus, the total heat flux in multicomponent media can be written as

$$\mathbf{J}_q = -\lambda \nabla T + p \sum_{k=1}^N k_{Tk} \rho_k^{-1} \mathbf{J}_k + \sum_{k=1}^N h_k \mathbf{J}_k \quad (118)$$

in full agreement with the kinetic theory of gases [3].

Determination of multicomponent diffusion coefficients in terms of binary diffusion coefficients. We now obtain algebraic equations that allow calculating multicomponent diffusion coefficients through binary diffusion coefficients. It is easy to check that the relation

$$\sum_{k=1; k \neq j}^N \mathcal{A}_{kj} (\rho_k \alpha_{ij} - \rho_j \alpha_{ik}) = \rho_i (\delta^{ji} - c_j), \quad (j, i = 1, 2, \dots, N). \quad (119)$$

Indeed, by virtue of (65), (66), (94), and (97), we have

$$\begin{aligned} \sum_{k=1; k \neq j}^N \mathcal{A}_{kj} (\rho_k \alpha_{ij} - \rho_j \alpha_{ik}) &= \sum_{k=1}^N \mathcal{A}_{kj} (\rho_k \alpha_{ij} - \rho_j \alpha_{ik}) = -\rho_j \sum_{k=1}^N \mathcal{A}_{kj} \alpha_{ik} = \\ &= -\rho_j \left(\sum_{k=1}^{N-1} \mathcal{A}_{kj} \alpha_{ik} + \mathcal{A}_{kN} \alpha_{iN} \right) = -\rho_j \left[\sum_{l=1}^{N-1} c_l \left(\sum_{k=1}^{N-1} \beta_{lk} \alpha_{ki} \right) - \sum_{k=1}^{N-1} \beta_{kj} \alpha_{ik} \right] = \\ &= -\rho_j \left(\sum_{k=1}^{N-1} c_k \delta^{ki} - \delta^{ji} \right) = \rho_i (\delta^{ji} - c_j). \end{aligned} \quad (120)$$

When using the notation (66) and (108) for the quantities $\mathcal{A}_{ik} = p/m_i m_k n^2 \mathcal{D}_{ik}$ and $\alpha_{ik} = \rho_i \rho_k D_{ki} / p$, relations (120) can be rewritten in the form of the following equations

$$\sum_{k=1; k \neq j}^N \frac{n_k n_i}{n^2 \mathcal{D}_{ik}} (D_{ji} - D_{ki}) = \delta^{ji} - c_i, \quad (i, j = 1, 2, \dots, N), \quad (121)$$

suitable for determining the multicomponent diffusion coefficients of a mixture D_{ij} ($i, j = 1, 2, \dots, N$) through binary diffusion coefficients \mathcal{D}_{ik} ($i, k = 1, 2, \dots, N$). Equations (121) are linearly dependent (since their summation over leads to identity), therefore, one more equation should be added to them, namely (67⁽²⁾).

Then equations (121) and (67⁽²⁾) can be given the following form:

$$\sum_{\substack{k=1 \\ k \neq i}}^N \left(\frac{n_i n_k}{\mathcal{D}_{ik}} + \sum_{\substack{l=1 \\ l \neq i}}^N \frac{n_i n_l}{\mathcal{D}_{il}} \right) D_{jk} = n^2 (c_i - \delta^{ji}) \quad (i, j = 1, 2, \dots, N), \quad (122)$$

which is very convenient for practical calculations of multicomponent diffusion coefficients $D_{jk}(\mathbf{x}, t)$.

In the particular case of a mixture consisting of three components, equations. (122) allow one to find the following expressions for the coefficients of multicomponent diffusion

$$D_{11} = \frac{n^2}{\rho^2 n_1^2} \left(\frac{n_1 n_3 m_3^2 \mathcal{D}_{23} \mathcal{D}_{31} + n_1 n_2 m_2^2 \mathcal{D}_{12} \mathcal{D}_{23} + (\rho_2 + \rho_3)^2 \mathcal{D}_{12} \mathcal{D}_{31}}{n_1 \mathcal{D}_{23} + n_2 \mathcal{D}_{31} + n_3 \mathcal{D}_{12}} \right), \quad (123)$$

$$D_{12} = \frac{n^2}{\rho^2} \left(\frac{n_3 m_3^2 \mathcal{D}_{23} \mathcal{D}_{31} - m_2 (\rho_1 + \rho_2) \mathcal{D}_{12} \mathcal{D}_{23} - m_1 (\rho_2 + \rho_3) \mathcal{D}_{31} \mathcal{D}_{11}}{n_1 \mathcal{D}_{32} + n_2 \mathcal{D}_{31} + n_3 \mathcal{D}_{12}} \right). \quad (124)$$

Expressions for the remaining coefficients can be obtained from (123) and (124) using the appropriate permutation of the indices.

It should be noted that relations of the type (111), (119), and (121) were first obtained in the kinetic theory of gases of monatomic gases in the first approximation of the Chapman–Enskog method in the well-known work [21]. Here, their phenomenological conclusion is given, and thus the universal character of this kind of relations is established.

CONCLUSION

We have already noted that in the literature, when determining the internal energy balance equation, they usually proceed from the law of conservation of the total energy of the mixture. This is apparently due to the fact that the balance equations for mechanical energy are usually derived earlier; and thus, it is possible to derive the equation for the balance of internal energy, using only them. In other words, until recently, the literature was limited to mechanical balance equations for energy quantities containing only the kinetic energy of the center of mass $\frac{1}{2} \rho \mathbf{v}^2$ and not including the kinetic energy of diffusion.

At the same time, the balance equations for the total specific kinetic energy of the system $\frac{1}{2} \sum_k \rho_k |\mathbf{v}_k|^2$ can be written directly only when it can be derived from the balance equations for the total momentum of the system. However, such a direct conclusion was not known until recently. In this work, we managed to overcome this difficulty and, as a result, obtain the correct balance equation for the correct value of the local internal energy for multicomponent systems. Taking this equation into account, the generalized Stefan – Maxwell relations were thermodynamically derived, which are, in fact, a system of hydrodynamic equations of a mixture with genuine inertial forces. In addition, it was possible to obtain thermodynamically a number of algebraic relations for the transfer coefficients, connecting, in particular, the thermal diffusion relations with the coefficients of thermal diffusion and multicomponent diffusion, true and partial

coefficients of thermal conductivity, multicomponent and binary diffusion coefficients, which indicates their universal character. The results obtained are intended for modeling liquid multicomponent non-ideal media, as well as gas-dust mixtures with a finely dispersed dust component.

REFERENCES

- [1] S. Chapman, T.G. Cowling, *The Mathematical Theory of Non-Uniform Gases*. Cambridge (1939).
- [2] D. Hirschfelder, C. Curtiss and R. Bird, *Molecular Theory of Gases and Liquids*. John Wiley and Sons, New York and London (1954).
- [3] J. Ferziger, H. Kaper, *Mathematical Theory of Transport Processes in Gases*. North-Holland, Amsterdam (1972)
- [4] I. Prigogin, D. Kondepudi, *Modern Thermodynamics: From Heat Engines to Dissipative Structures*. Wiley Inter Science, New York (1998).
- [5] M.Ya. Marov, A.V. Kolesnichenko, *Turbulence and Self-Organization. Modeling Astrophysical Objects*. Springer, New York-Heidelberg-Dordrecht-London (2013).
- [6] A.V. Kolesnichenko. *Continuous models of natural and space environments. Problems of thermodynamic design*, Lenand, Moscow (2017) (in Russian).
- [7] D.A. Frank-Kamenetskii, *Diffusion and Heat Transfer in Chemical Kinetics*. Nauka, Moscow (1987) (in Russian).
- [8] S.R. de Groot, *Thermodynamics of Irreversible Processes*, Amsterdam (1951).
- [9] J. Meixner, H.G. Reik, *Thermodynamik der irreversiblen Prozesse. Handbuch der Physik, Bd. 3, T I. 2*, Berlin-Göttingen-Heidelberg (1959).
- [10] S.R. de Groot, P. Mazur, *Non-equilibrium Thermodynamics*. Amsterdam (1962). [11] E. Oran, J. Boris, *Numerical Simulation of Reactive Flow*. Cambridge University, Cambridge (2001).
- [12] L.I. Sedov, *Introduction to Continuum Mechanics*. Fizmatlit, Moscow (1962) (in Russian)
- [13] R. Haase, *Thermodynamik der irreversiblen Prozesse*, Darmstadt (1963).
- [14] I. Gyarmati, *Non-Equilibrium Thermodynamics. Field Theory and Variational Principles*, Springer-Verlag-Berlin-Heidelberg-New York (1970).
- [15] D.D. Pitts, *Nonequilibrium Thermodynamics*. New York - Toronto - London (1962).
- [16] A.V. Kolesnichenko, “Informational-thermodynamic conception of processes formation of self-organization in open systems under influence of external environment” *Math. Montis.*, **35**, 80-106, (2016).
- [17] P. Glansdorff and I. Prigogine, *Thermodynamic theory of structure, stability and fluctuations*. John Wiley & Sons, Ltd. London-New York-Sydney-Toronto (1971).
- [18] V.I. Mazhukin, A.V. Shapranov, V.E. Perezhigin, “Mathematical modeling of thermo-physical properties, heating and melting processes of metal with the molecular dynamics Method”, *Math. Montis.*, **24**, 47-66, (2012).

- [19] C. Truesdell, *Rational Thermodynamics*. Springer, New York. (1984).
- [20] I. Prigogine, R. Defay, *Chemical Thermodynamics*. Longmans Green and Co., London -New-York-Toronto (1954).
- [21] C.F. Curtiss, "Symmetric gaseous diffusion coefficients" *J. Chem. Phys.*, **49**, 2917-2919 (1968)

Received, December 8, 2021

MULTIGRID METHOD FOR NUMERICAL MODELLING OF HIGH TEMPERATURE SUPERCONDUCTORS

O.B. FEODORITOVA, M.M. KRASNOV, N.D. NOVIKOVA, V.T. ZHUKOV*

Keldysh Institute of Applied Mathematics, RAS. Moscow, Russia

*Corresponding author. E-mail: vic.zhukov@gmail.com

DOI: 10.20948/mathmontis-2022-53-7

Summary. An approach to numerical simulation of three-dimensional electrical and thermal fields in high-temperature superconductors is described. In such a semiconductor, the phenomena of superconductivity are observed at high temperatures above the temperature of liquid nitrogen. The absence of a generally accepted theory of superconductivity leads to the need to study physical processes in semiconductor structures using mathematical simulations. The main attention is paid to the calculation of temperature and electric current distributions in large-size mesas with a self-heating effect. An efficient algorithm for solving the equations describing these distributions is constructed. The basis of the algorithm is an adaptive multigrid method on structured Cartesian grids. The adaptability is based on the Chebyshev iterative method for constructing the smoothing procedures at each grid level and for solving the coarsest grid equations. The adaptive technique allows us to realistically simulate the anisotropic phenomena. The functionality of the algorithm is demonstrated along with an example of solving an anisotropic model problem with discontinuous coefficients.

1 INTRODUCTION

This paper is devoted to a problem of numerical simulation of three-dimensional electro-thermophysical processes in Bi-2212 semiconductors. In such a high-temperature semiconductor (HTS), the phenomena of superconductivity are observed at high temperatures above the temperature of liquid nitrogen, 77 K.

The absence of a generally accepted theory of superconductivity leads to the need to study physical processes in semiconductor structures using three-dimensional numerical simulations. In the Bi-2212 the superconducting and dielectric layers form anisotropic structure with Josephson mechanism of the electric current through non-conducting zones. The self-heating effect of the Bi-2212 is intensively studied; see for instance [1–5]. In the past decade, significant progress has been achieved by the high-temperature superconducting modelling community [6] to develop computational models for scientific investigations and for constructing of practical engineering devices [7–14].

As a result, numerical simulation has been recognized as a powerful instrument for investigating the electrical and thermal behavior of superconductors, and of HTS in particular.

For development of robust computational technique, we consider a mathematical model that takes into account the nonlinear electrical and thermal interactions. The electrical and thermal processes are modeled by a system of two coupled nonlinear differential equations for the temperature and the electric field potential. Physical fields in superconductors are anisotropic and of different scale nature. This is because the coefficients of thermal

2010 Mathematics Subject Classification: 35K05, 65M55, 82D55.

Key words and Phrases: Numerical simulation, High-temperature superconductor, Self-heating effect.

conductivity and the electrical resistivity are highly anisotropic. These coefficients depend on the temperature and the spatial coordinates. We take into account some typical formulas for these coefficients and their temperature dependences.

Due to nonlinearities some local features can be created by current-conducting hot channels. It is evident that efficient numerical models are needed to simulate these complex anisotropic phenomena accurately, and a coupling of the temperature and electrical current is critical. Calculations of such phenomena require the use of detailed three-dimensional grids with the large number of nodes, up to $\sim 10^9$ for complicated HTS devices.

The computational model introduced here is enabling us to model anisotropic phenomena realistically. We numerically compute temperature and electrical current distributions in mesas by solving jointly the non-linear heat conduction and potential equations with the adaptive multigrid method.

For spatial discrete approximation we use a conventional seven-point discretization on non-uniform Cartesian grids. As a result of discretization and linearization, the initial boundary-value problem is reduced to a multiple calculations of the systems of the discrete elliptic equations.

For solving these discrete equations we propose to apply the adaptive multigrid method. A detailed presentation of this algorithm, which is a version of R.P. Fedorenko classical method [15–17], can be found in [18–23]. The adaptive multigrid is based on the Chebyshev iterative method which is used for constructing smoothing procedures at each grid level and for solving the coarsest grid equations.

This adaptation procedure exploits the power method for an optimal Chebyshev polynomial. Convergence of such a power method is based on the property of Chebyshev polynomials to grow rapidly outside the segment of least deviation from zero. This approach provides an automatic adaptation during multigrid iterations.

Experimental and numerical researches of Josephson structures are carried out in Russian and foreign scientific centers. In the Keldysh Institute of Applied Mathematics such a study is being carried out on the initiative of Prof. V.M. Krasnov, an employee of the Laboratory of Experimental Physics of Condensed Matter, Stockholm University. He deeply involves in investigation of HTS structures, see [5, 9–13].

The paper is organized as follows. In Section 2 we introduce the mathematical model. In Section 3 the finite-volume discrete model is presented. In Section 4 we describe application of the adaptive multigrid method in relation to the considered problem. In Section 5 we demonstrate the efficiency of the adaptive multigrid method as standalone solver for the heat conduction equation with the constant highly anisotropic coefficients. The results of self-heating mesa computations are presented in Section 6. Some conclusions are given in the last section.

2 MATHEMATICAL MODEL

Inside a solid body, which is the parallelepiped $\Omega = \{(x^1, x^2, x^3) : l_\alpha^- \leq x^\alpha \leq l_\alpha^+, \alpha = 1, 2, 3\}$, for simplicity, consistent temperature and electric potential stationary distributions are searched. We denote a point (x^1, x^2, x^3) in three dimensional space \mathbb{R}^3 as x , and as well as (x, y, z) .

We use non-stationary formulation of the problem: in the parabolic cylinder $r = (t, x) \in G = [t_0; t_f] \times \Omega$, $\Omega \subset \mathbb{R}^3$: the unsteady system of the coupled equations to find steady-state distributions T, φ is considered

$$\begin{aligned} c(T) \frac{\partial T}{\partial t} &= \nabla \cdot k(T) \nabla T + \nabla \varphi \cdot \sigma(T) \nabla \varphi, \\ \frac{\partial \varphi}{\partial t} &= \nabla \cdot \sigma \nabla \varphi. \end{aligned} \quad (1)$$

Here $k(T)$ is the thermal conductivity tensor, $c(T)$ is the volumetric heat capacity and $\sigma(T)$ is the electrical conductivity tensor. Tensors $k(T)$ and $\sigma(T)$ are assumed to be diagonal with the elements $\kappa_{xx}, \kappa_{yy}, \kappa_{zz}$ and $\sigma_{xx}, \sigma_{yy}, \sigma_{zz}$ respectively. These elements are given functions of temperature and coordinates. We specify time interval as $[t_0; t_\infty]$, $t_0 = 0$, $t_\infty \rightarrow \infty$. In (1) the expression $\nabla \cdot \sigma \nabla \varphi$ reads as an inner product of vectors from \mathbb{R}^3 . For an inner product in the space of grid functions we use a notation (\cdot, \cdot) .

At any time $t > t_0$, the functions $T(r)$ and $\varphi(r)$ satisfy to a boundary condition (BC) on the boundary Γ of the parallelepiped (on six faces $x_\alpha = l_\alpha^\pm$, $\alpha = 1, 2, 3$). A conventional combination of BC types is possible.

For the temperature, either the Neumann condition $\partial T / \partial n = 0$ at all boundaries is set, or the Neumann condition is defined on the horizontal faces of the parallelepiped and the Dirichlet condition $T = T_B$ is set on the vertical faces. The Dirichlet condition simulates constant cooling at some given temperature T_B , for example, $T_B = 10 \text{ K}$.

For the potential φ , the Neumann condition $\partial \varphi / \partial n = 0$ at the vertical faces is set, and a constant potential is maintained at the horizontal faces, upper and lower ones, i.e., the Dirichlet conditions are specified.

$$\varphi(t, x^1, x^2, l_3^+) = +0.5U_0, \quad \varphi(t, x^1, x^2, l_3^-) = -0.5U_0 \quad (2)$$

with a given value U_0 . One can take $U_0 = 1 \text{ V}$, for example.

At $t = t_0$, the initial conditions $\varphi(t_0, x^1, x^2, x^3) = \varphi_0$, $T = T_0$, where φ_0, T_0 are the given functions or given constants, for example, $T_0 = T_B$, $\varphi_0 = 0$. One can take the linear distribution of the potential along the vertical coordinate z^3 :

$$\varphi_0 = \frac{U_0}{l_3^+ - l_3^-} (z^3 - l_3^+) + \frac{U_0}{2}$$

It is impossible to solve the equation for potential and for temperature independently, because the electrical conductivity $\sigma = \sigma(T)$ depends on the temperature significantly, and the intensity of heat release in a unit volume, i.e. the heat source $q = \nabla \varphi \cdot \sigma(T) \nabla \varphi$, is nonlinear function of T, φ . The function $q(T, \varphi)$ simulates the heating of a substance by an

electric current flowing in the sample. The presence of the time derivatives in the system (1) means that the stationary solution is computed by a time-stepping procedure.

For a model problem of HTS, the resistivity components ρ_{xx} , ρ_{yy} , ρ_{zz} , $Ohm \cdot m$, can be given in the form

$$\rho_{xx} = \rho_{yy} = \rho_0 \exp\left(\frac{300}{150+T}\right), \quad \rho_{zz} = a_\rho \rho_{xx}. \quad (3)$$

The diagonal elements of the electrical conductivity tensor σ_{xx} , σ_{yy} , σ_{zz} , $Ohm^{-1} \cdot m^{-1}$, have the form $\sigma_{xx} = 1/\rho_{xx}$, $\sigma_{yy} = 1/\rho_{yy}$, $\sigma_{zz} = 1/\rho_{zz}$. The components of the thermal conductivity tensor κ_{xx} , κ_{yy} , κ_{zz} , $W m^{-1} K^{-1}$, are set for the model case in the form $\kappa_{xx} = \kappa_{yy} = k_0 T$, $\kappa_{zz} = \kappa_{xx}/k_1$ with some empirical parameters k_0 , k_1 . The empirical formulas for the electrical and thermal conductivities are presented in Section 6.

The volumetric heat capacity $c(T)$, $J/(m^3 K)$, of a superconductor is set as a function of temperature T and density ρ : $c(T) = c_0 \cdot T^2 \rho$, $c_0 = 10^{-3}$. This function is determined by the specific heat c_m , $J/(kg \cdot K)$, and density ρ : $c(T) = c_m(T) \cdot \rho$ for the superconductor Bi-2212, one can take the density $\rho = 6 \cdot 10^3 kg/m^3$.

The dependencies (3) are of a model nature. In the vicinity of the critical temperature $T_{crit} \approx 85 K$ of the superconducting transition, the actual behavior of electrical conductivity, thermal conductivity and heat capacity is more complicated.

After finding the steady-state solutions T , φ we compute the electric field $E = -\nabla \varphi$ and the electrical current density vector

$$J = \sigma E = -\sigma \nabla \varphi. \quad (4)$$

There are semiconductor structures of different geometric complexity. A description of the realistic mesa-type Bi2212 can be found in [12].

In this paper, we focus on temperature and current distributions in mesas with a self-heating effect; see [1–7, 11]. It is difficult to experimentally obtain current and temperature distributions in mesas, therefore high performance computer simulation is required. For this purpose we develop an algorithm and computer code for numerical calculation of these distributions by solving the non-linear system (1).

In this paper we present the basic elements of our numerical model for the case of a rectangular parallelepiped. Below we briefly give a scheme of the adaptive multigrid algorithm on structured Cartesian grids, see [18–23].

3 DISCRETE MODEL

We consider a model mesa as a parallelepiped Ω of sizes $l_x \times l_y \times l_z$. Typical values are $l_x \approx 3$, $l_y \approx 1.5$, $l_z \approx 0.02$ and $l_x \approx 50$, $l_y \approx 50$, $l_z \approx 1$, μm , for small-size mesa and large-size mesa respectively. We map this parallelepiped into the unit cube $\Omega = [0; 1]^3$ with corresponding scale of the coefficients of the governing system.

In Ω we introduce a Cartesian grid $\Omega_h = \{x_n \in \Omega, 0 \leq n \leq N\}$ with the grid boundary Γ_h . The grid Ω_h is non-uniform in each coordinate direction with the number of cells N_x, N_y, N_z respectively and depends on a parameter h which characterizes the average cell size. The grid nodes are denoted as (x_i, y_j, z_k) , or (i, j, k) , where $i = 0, \dots, N_x, j = 0, \dots, N_y, k = 0, \dots, N_z$.

The grid functions T, φ , the coefficients of equations, residuals of the equations and etc. are determined at the grid nodes of Ω_h . We construct a node-based discrete scheme with finite-volume method. For this purpose we integrate the original equations over each dual volume $[x_{i-1/2}; x_{i+1/2}] \times [y_{j-1/2}; y_{j+1/2}] \times [z_{k-1/2}; z_{k+1/2}]$ associated with (i, j, k) -node excluding the Dirichlet type nodes. If a grid index goes beyond values $0, N_x, N_y, N_z$, then such an index takes the closest value from $i = 0, \dots, N_x, j = 0, \dots, N_y, k = 0, \dots, N_z$.

The areas of six faces of the dual cell (i, j, k) are denoted as $S_{i+1/2, j, k}, S_{i, j+1/2, k}, S_{i, j, k+1/2}$ and the cell volume is denoted as $V_{i, j, k}$. Evidently that $V_{i, j, k} = 0$ for the Dirichlet type nodes. The grid function space U_h is defined in the standard manner with the inner product

$$(u, w) = \sum_{i, j, k} u_{i, j, k} w_{i, j, k} V_{i, j, k},$$

and the corresponding grid L_2 - norm. Here, the sum is taken over all grid nodes.

On the space U_h we introduce the discrete operators L_h^T and L_h^φ which approximate the linear differential operators $L^T = -\nabla \cdot \kappa \nabla$ and $L^\varphi = -\nabla \cdot \sigma \nabla$ with the second order accuracy on smooth functions, taking into account the boundary conditions. Here, the coefficients κ, σ are known functions of the spatial coordinates and they are determined by the temperature from the lower time layer. In 3D space the operators L_h^T and L_h^φ are constructed using a finite-volume 7-point discretization. They are self-adjoint with non-negative eigenvalues. We suppose that some estimates for the bounds of the spectrum $\lambda_{min} \geq 0$ and λ_{max} of each operator are known; these estimates can be calculated in a few simple cases [24]. In general cases, an estimate for λ_{max} is obtained with Gershgorin's circle theorem for estimating the eigenvalues of a matrix [25].

We introduce the semi-discrete approximation of the initial-boundary value problem (1) in an operator form:

$$c \frac{\partial T}{\partial t} + L_h^T \cdot T = f, \tag{5}$$

$$\frac{\partial \varphi}{\partial t} + L_h^\varphi \cdot \varphi = g. \tag{6}$$

We assume that the boundary conditions are taken into account with the definition of the operators L_h^T, L_h^φ and the right-hand side functions f, g .

The values of a grid function u at the time layer t_m is denoted as u_m . The transition from the layer t_m to the layer $t_{m+1} = t_m + \tau$ can be implemented in different ways. We write the convenient first order implicit scheme for the system (5)–(6)

$$\frac{T_{m+1} - T_m}{\tau} + \frac{1}{c} L_h^T \cdot T_{m+1} = \frac{1}{c} f_m, \quad (7)$$

$$\frac{\varphi_{m+1} - \varphi_m}{\tau} + L_h^\varphi \cdot \varphi_{m+1} = g_m. \quad (8)$$

The right-hand sides in these equations are taking into account the Dirichlet boundary conditions in nodes adjacent to the Dirichlet type nodes. The grid function f_m includes the heat source

$$q_m = q(T_m, \varphi_m) = \nabla \varphi_m \cdot \sigma(T_m) \nabla \varphi_m, \quad (9)$$

which arises from Joule-heating effect.

This implicit linear scheme can be written as a system of two operator equations

$$\left(I + \tau \cdot C^{-1} L_h^T \right) T_{m+1} = T_m + \tau C^{-1} f_m,$$

$$\left(I + \tau \cdot L_h^\varphi \right) \varphi_{m+1} = \varphi_m + \tau g_m,$$

where I is the identity grid operator, $C = c(T_m)I$. We rewrite this system as two linear systems

$$A_h u_h = f_h, \quad (10)$$

$$B_h v_h = g_h. \quad (11)$$

The operators $A_h = \tau^{-1}I + C^{-1}L_h^T$ and $B_h = \tau^{-1}I + L_h^\varphi$ are $N \times N$ -matrices, u_h, v_h are the seeking functions, $f_h = \tau^{-1}T_m + C^{-1}f_m$, $g_h = \tau^{-1}\varphi_m + g_m$ are the given grid functions.

Each of the equations (10) and (11) can be solved separately at each time step. Recalculation of the source (9) at each time step, as well as the coefficients of thermal and electrical conductivities, couples these equations. For convenience of description, we rewrite each equation in a compact form

$$A u = f, \quad (12)$$

where A is a self-adjoint positive definite operator, corresponding to A_h or B_h .

We describe the spatial discretization of the governing equations using their representation in a more convenient form:

$$-\sum_{\alpha=1}^3 \frac{\partial}{\partial x^\alpha} \left(A_\alpha \frac{\partial u}{\partial x^\alpha} \right) + A_0 u = f. \quad (13)$$

Here A_0, A_1, A_2, A_3, f are the given non-negative functions of coordinates $(x^1, x^2, x^3) \equiv (x, y, z)$. In a discrete model the coefficients A_0, A_1, A_2, A_3 are calculated at grid points. To calculate the fluxes, the coefficients A_1, A_2, A_3 are additionally calculated on the faces of the dual cells $\{i + \frac{1}{2}, j, k\}$, $\{i, j + \frac{1}{2}, k\}$, $\{i, j, k + \frac{1}{2}\}$, i.e. on the faces passing through the centers of the geometric mesh cells $[x_i; x_{i+1}] \times [y_j; y_{j+1}] \times [z_k; z_{k+1}]$ and the middle of the edges; denote these coefficients as $A_1^{i+1/2, j, k}$, $A_2^{i, j+1/2, k}$, $A_3^{i, j, k+1/2}$, respectively. Each of these coefficients is calculated as the harmonic mean of the corresponding nodal values.

One considers the discretization of the heat source (9)

$$q = \nabla \varphi \cdot \sigma(T) \nabla \varphi = \frac{\partial \varphi}{\partial x} \cdot \sigma_1 \frac{\partial \varphi}{\partial x} + \frac{\partial \varphi}{\partial y} \cdot \sigma_2 \frac{\partial \varphi}{\partial y} + \frac{\partial \varphi}{\partial z} \cdot \sigma_3 \frac{\partial \varphi}{\partial z} \equiv q_x + q_y + q_z. \quad (14)$$

The grid approximation of the function q is calculated at all nodes, except the Dirichlet type node for the heat equation. In the considered case, the Dirichlet BC is given only at the faces $k=0$ and $k=N_z$. For $\partial \varphi / \partial x$ in each grid node (i, j, k) with the index $0 < i < N_x$ we have

$$\frac{\partial \varphi}{\partial x} \simeq \frac{\varphi(x_{i+1}, y_j, z_k) - \varphi(x_{i-1}, y_j, z_k)}{x_{i+1} - x_{i-1}}.$$

Therefore for such a (i, j, k) -node

$$q_x \simeq \sigma_1(x_i, y_j, z_k) \cdot \left(\frac{\varphi(x_{i+1}, y_j, z_k) - \varphi(x_{i-1}, y_j, z_k)}{x_{i+1} - x_{i-1}} \right)^2.$$

At the faces $i=0$ and $i=N_x$ we have prescribed the BC $\partial \varphi / \partial x = 0$, therefore $q_x = 0$ at these faces. At the nodes $(0, j, k)$ and (N_x, j, k) , the terms q_y and q_z are written in the same way. On the edges of the cube, which shares two faces with the Dirichlet and Neumann conditions, the Dirichlet condition has priority. The discretization of the terms q_y, q_z is the same in the interior nodes. At the faces $z=0$ and $z=N_z$ we have prescribed the Dirichlet BC (2) for the potential and the Neumann BC for the temperature. Therefore the source function (14) must be computed at these faces. To provide such a procedure we discretize $\partial \varphi / \partial z$ by the convenient three-point difference derivatives with second order of accuracy.

For linear equations the implicit scheme does not require any restriction on time step size. But in our nonlinear case the choice of the time step size τ is limited by an empirical rule: the growth of the heat source $q = q(T, \varphi)$ must be restricted. We require $\|q_{m+1}\| < q_{tol} \|q_m\|$ for transition from the layer t_m to the layer $t_{m+1} = t_m + \tau$ with a given tolerance q_{tol} .

4 GENERAL SCHEME OF THE ADAPTIVE MULTIGRID METHOD

This section briefly presents the results of the development of the classical multigrid method [15-18, 21] in relation to the described problem. We assume that the system (12) is the result of the grid approximation of the boundary value problem for the equation (13). Various iterative methods are usually used to solve such a system. Size of these systems $N = N_x \times N_y \times N_z$ effects on the efficiency of the methods, and a value N can be very large. Additional difficulties arise from anisotropy, which is also characteristic of the problem under consideration (1).

For elliptic differential equations the multigrid method [15-17] is theoretically optimal: the computational complexity of the method grows linearly with an increase of unknowns. Its real efficiency depends on the implementation of the algorithmic elements. The main elements are intergrid transfer operators, smoothing operators and procedures for solving the coarsest grid equations. In this paper, we summarize the main elements of the multigrid method and the principle of automatic adaptation during multigrid iterations. Detailed information can be found in [18-23].

Every multigrid iteration step consists of the transition from a fine grid level to the next grid level up to the coarsest grid and back (V – cycle). It is convenient to represent the multigrid method in a two-grid representation, describing the transition from a fine h –grid to a coarse H – grid. We rewrite the initial system of discrete equations at a fine grid level as $A_h u_h = f_h$.

On the coarse grid level, a correction system in the form $A_H w_H = g_H$ is constructed. We construct the operator A_H with discretization on the H –grid. The right-hand side g_H is the constraint of the residual $g_h = f_h - A_h u_h$ on the coarse grid, i.e. $g_H = R g_h$. Here P and R are the interpolation and projection operators, they are conjugate, $R = P^*$. The operator P can be constructed with the trilinear interpolation. Along with a trilinear interpolation, we use an approximate solution of the local discrete boundary value problem. Such operators P and R provide a problem-dependent intergrid transfer and they provide robustness of the multigrid method for discontinuous coefficient equations, see [18].

In the two-grid representation the error propagation operator can be write as

$$Q = S_p(I - P A_H^{-1} R A_h) S_p, \quad (15)$$

where I is the identity operator, S_p is the smoothing operator. The given two-grid algorithm is recursively generalized to an arbitrary of grid levels.

Smoother procedure S_p plays a key role in the multigrid efficiency. We propose to construct an explicit iterative Chebyshev smoother providing the ability to adapt during the multigrid iterations, see [21, 22]. This adaptive smoother can be explained together with the coarsest grid solver for the linear system $A_H \cdot y = g_H$ with $g_H = R \cdot (g_h - A_h u_h)$.

For generality we consider a linear system (12) with self-adjoint and positive definite matrix A . To solve this system, one can apply the explicit Chebyshev iterative method [24]

$$u_j = u_{j-1} + \omega_j(f - A \cdot u_{j-1}) \quad (16)$$

with an optimal set of parameters $\{\omega_j\}$ and an initial guess u_0 . Here $j=1, \dots, p$ is the iteration number, and p is a priori defined by the condition to reach a prescribed relative accuracy $\varepsilon: \|r_p\| < \varepsilon \|r_0\|$, where r_0 and $r_p = f - A \cdot u_p$ are the initial and final residuals. The number p depends on ε and the number $\eta = \lambda_{min}/\lambda_{max}$ according to the formula

$$p = p(\varepsilon, \eta) = \ln\left(\varepsilon^{-1} + \sqrt{\varepsilon^{-2} - 1}\right) / \ln\left(\frac{1 + \sqrt{\eta}}{1 - \sqrt{\eta}}\right), \quad (17)$$

where $0 < \lambda_{min}, \lambda_{max}$ are minimal and maximal eigenvalues of A . This well-known iteration procedure is defined by the Chebyshev polynomial F_p of degree p , that deviates least from zero on $[\lambda_{min}; \lambda_{max}]$ and is normalized by the condition $F_p(0) = 1$. The parameters ω_j , $j = 1, \dots, p$ are reordered for computational stability [24].

We use notations λ_{min} and λ_{max} for the exact eigenvalues, λ_{min}^* and λ_{max}^* for their approximate estimates. The values λ_{min} and λ_{max} are usually unknown.

After running the algorithm (16), we obtain the relation $r_p = F_p(A)r_0$ for the initial and final residuals. To start the algorithm it is necessary to set the bounds λ_{min}^* and λ_{max}^* of the spectrum of operator A . The desired bound $\lambda_{max}^* \geq \lambda_{max}$ is estimated with the Gershgorin theorem [25]. As an initial bound of eigenvalue λ_{min}^* the Rayleigh–Ritz ratio $\lambda_{min}^* = (Av, v)/(v, v)$ can be used, where v is the right-hand side of the linear system of equations. With adaptation any empirical upper estimate λ_{min}^* is appropriate.

The relations $0 < \lambda_{min} \leq \lambda_{min}^* \leq \lambda_{max} \leq \lambda_{max}^*$ are guaranteed the convergence of the method (16). The desired estimate is specified during the external iterative process (or adaptation cycle). Let λ_{min}^* be a current guess, and λ_{new}^* is its update. The adaptation algorithm has the following form. One needs to solve a linear system with a prescribed accuracy ε_{tot} , but firstly the lower accuracy value $\varepsilon_1 < \varepsilon_{tot}$ we set. For instance, $\varepsilon_{tot} = 10^{-10}$ and $\varepsilon_1 = 10^{-2}$. We implement one step of the Chebyshev algorithm with the given data $\lambda_{min}^*, \lambda_{max}^*, \varepsilon_1$ and obtain $\delta = \|r_p\|/\|r_0\|$ with $r_p = F_p(A)r_0$. Here $\delta \equiv \delta_k$ is an accuracy achieving in the current adaptation cycle with the number $k = 1, \dots$, and r_0, r_p are the initial and final residuals. Assume that $\delta > \varepsilon_1$. Then the new update is found as the unique root of the algebraic equation $F_p(\lambda) = \delta$, therefore $\lambda_{min}^* = \arg(F_p(\lambda) - \delta = 0)$. If the accuracy ε_{tot} is not achieved, we pass to a new adaptation cycle with $\lambda_{min}^*, \lambda_{max}^*, \varepsilon_1$ and with the Chebyshev polynomial degree calculated by formula (17).

An accuracy $\delta = \delta_k \leq \varepsilon_1$ can be achieved at an adaptation step k . In general this means that the estimate λ_{min}^* is sufficiently accurate. Therefore we can perform the next step with

the previous data λ_{min}^* , λ_{max}^* , ε_1 , or change the accuracy by setting $\varepsilon_1 = \varepsilon_{tot}/(\delta_1 \times \dots \times \delta_k)$. With this choice, the desired accuracy ε_{tot} is achieved in one adaptation step.

This adaptation procedure exploits the power method for the polynomial $F_p(A)$ which is an eigenvalue algorithm: for $F_p(A)$ this algorithm produces a number λ , which is the greatest (in absolute value) eigenvalue: $\lambda = \lambda_{max}^F$. Evidently that $\lambda_{max}^F = F_p(\lambda_{min}^*)$. Convergence of such a power method is based on the property of Chebyshev polynomials to grow rapidly outside the segment of least deviation from zero.

This adaptation algorithm can be easily integrated into the multigrid method. It provides the efficiency of solving the coarsest grid system by refining the estimate λ_{min}^* and it is well suited for constructing an adaptive smoother at each grid level, see [21, 22]. The adaptive Chebyshev smoother serves to reduce the initial residual on the high-frequency part of the spectrum $[\lambda_{min}^c; \lambda_{max}^*]$. The high-frequency spectrum bound λ_{min}^c is unknown in advance and is found in adaptation process. Adaptation is turned on automatically if a relation $\delta = \|r_p\| / \|r_0\| > \varepsilon_{smooth}$ is obtained on some grid level after the smoothing. This means that the given smoothing accuracy ε_{smooth} is not achieved. In this case, we refine the parameters of the smoothers using simple formulas, see [21, 22]. For example, for the Chebyshev smoother the parameters are updated according to the new boundary λ_{min}^c and the known upper boundary λ_{max}^* .

After updating λ_{min}^c at all grid levels, multigrid iterations are continued with new values, repeating if necessary adaptation (while $\varepsilon_{smooth} < \delta < 1$). As a rule, in calculations after several (2–3) multigrid iterations the parameters of smoothing are stabilized, the specified accuracy of smoothing s_{smooth} is achieved, and the asymptotic convergence rate of the multigrid iterations becomes equal to the expected value ε_{smooth}^2 .

The presented technique exploits the explicit iterations therefore this method is suitable for the efficient implementation on ultra-parallel computers with potential scalability on a large number of processors.

5 STANDALONE ADAPTIVE MULTIGRID SOLVER

The problem of calculating a HTS structure is characterized by a high difference in the geometric sizes of the domain, highly anisotropic parameters, and the grid anisotropy can deliver an additional difficulty.

Firstly we demonstrate the efficiency of the adaptive multigrid method as standalone solver for the equation (13) with constant highly anisotropic coefficients $A_1 = 10000$, $A_2 = 100$, $A_3 = 1$, $A_0 \equiv 0$ in the unit cube Ω with the Dirichlet boundary conditions and with uniform and non-uniform Cartesian grids. The convergence rates of the multigrid iterations are characterized by the relation $s = r_n / r_{n-1}$, where r_{n-1} , r_n are the grid norms of the residuals at two sequential multigrid iterations. The grid of cells $64 \times 64 \times 64$ is taken, the number of grid levels is 3, the grids of the next levels are $32 \times 32 \times 32$ and

$16 \times 16 \times 16$. In the experiments, grids are taken up to 2048^3 cells. We set the smoothing factor $\varepsilon_{smooth} = 0.5$. So, we try to achieve the condition $d = r_{before} / r_{after} < \varepsilon_{smooth}$ for the ratio of residual norms before and after smoothing at any stage of smoothing. This goal is achieved with the adaptive refining of the spectrum bounds. The coarsest grid equations are solved with relative accuracy $ctol = 10^{-3}$ using the Chebyshev adaptive method. Convergence of multigrid iterations is controlled by condition $r_m < \varepsilon_{tot} \cdot r_0$ with accuracy $\varepsilon_{tot} = 10^{-14}$.

We compute this problem for two cases: using uniform and a non-uniform grids. Figure 1 demonstrates on a logarithmic scale the evolution of the residual norm and the convergence rate $s = r_n / r_{n-1}$, with respect to the number n of the multigrid iterations for a non-uniform grid. We use the geometric progression of mesh sizes in the vertical direction, so that the cell sizes in the vertical direction are equal to 0.1 for the lower and 10^{-4} for upper boundary of the unit cube respectively. For the both cases such graphics are practically similar. Adaptation works equally well. The computational costs are different: for the non-uniform grid CPU time increases by 25%. In terms of the number of smoothing iterations, the costs are 1100 and 1620 iterations totally. The residual norm during multigrid iterations decreases from the initial value 10^7 down to $\sim 5 \cdot 10^{-8}$. Adaptation is turned on after the second multigrid iteration.

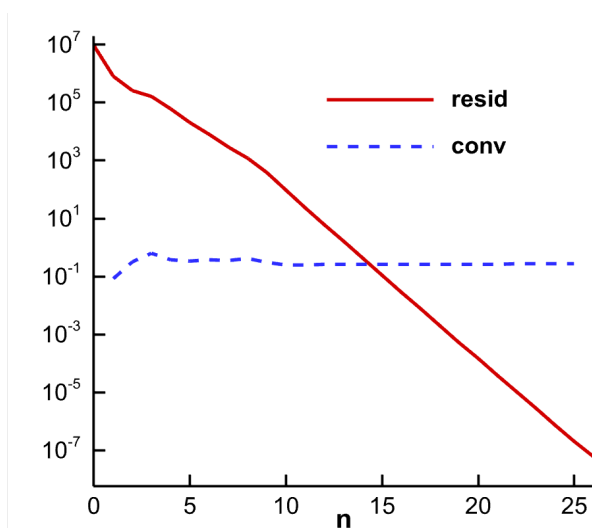


Fig. 1. Multigrid iterations: the residual norm (solid line) and the convergence rate (dashed line)

The convergence rate s (dashed lines in Figure 1) stabilizes during the first 5-7 iterations at $s = 0.27$. It indicates that the multigrid asymptotic convergence rate is practically achieved. This value is close to the theoretical value $s = \varepsilon_{smooth}^2 = 0.25$. If we take the relative accuracy of coarsest grid solver as $ctol = 10^{-9}$, the convergence rate s stabilizes at the theoretical value $s = \varepsilon_{smooth}^2 = 0.25$. The computational cost practically does not increase at the same time. For this case one can observe influence of adaptation: the computation time is reduced by 25%, and the total number of operations for calculating residuals also is reduced. For

parallel implementation, it is important to reduce the number of multigrid iterations, which leads to a reduction of global operations like calculating residual norms.

6 RESULTS OF SELF-HEATING MESA COMPUTATIONS

We are adjusting the statement of the considered initial boundary-value problem under the following assumptions. A computational domain is the unit cube. Since we are seeking for a steady-state distribution of electrical potential and temperature, we assume the volumetric heat capacity $c(T) \equiv 1$. All coefficients $\kappa(T)$, $\sigma(T)$ correspond to a conventional semiconductor microscale structure $l_x \times l_y \times l_z$. We map this parallelepiped into the unit cube and set the input data as

$$\begin{aligned} T_0 = T_b = 10, \quad U_0 = 1, \\ \kappa_{xx} = \kappa_{yy} = 0.1 \cdot T, \quad \kappa_{zz} = 50 \cdot \kappa_{xx}, \end{aligned} \quad (18)$$

$$\begin{aligned} \sigma_{xx} = \sigma_{yy} = 100 \cdot \exp(-300/(150 + T)), \\ \sigma_{zz} = \begin{cases} 5 \cdot 10^{-1} \sigma_{xx}, & x \notin [0.375; 0.625], \\ 4 \cdot 10^{-3} \sigma_{xx}, & x \in [0.375; 0.625]. \end{cases} \end{aligned} \quad (19)$$

We focus on discontinuity of the component σ_{zz} , see (19). This is an artificial introduction of a feature in order to demonstrate the capabilities of the method.

The boundary conditions (BCs) of the six faces of the cube can be written in the form:

$$\begin{aligned} x=0: \quad \partial\varphi/\partial n = 0, \quad T = T_b; \quad x=1: \quad \partial\varphi/\partial n = 0, \quad T = T_b, \\ y=0: \quad \partial\varphi/\partial n = 0, \quad \partial T/\partial n = 0; \quad y=1: \quad \partial\varphi/\partial n = 0, \quad \partial T/\partial n = 0, \\ z=0: \quad \varphi = -0.5U_0, \quad \partial T/\partial n = 0; \quad z=1: \quad \varphi = +0.5U_0, \quad \partial T/\partial n = 0. \end{aligned}$$

The initial data at $t = t_0$:

$$T = T_0(x, y, z) = T_b, \quad \varphi = \varphi_0(x, y, z) = U_0(z-1) + 0.5U_0.$$

We emphasize again this statement of the problem serves to demonstrate the methodological capabilities of our approach, and not to simulate a specific device. The 3D typical temperature distribution is shown on Figure 2.

If we take constant values for the heat and electrical conductivities, then a solution of the governing system has too simple an analytical representation: $T = 0.5\sigma_z x(1-x)$, $\varphi = U_0(z-1) + 0.5U_0$. Using the resistivity components in the form (3) doesn't make the solutions complicated. To simulate a genuine non-trivial two-dimensional solution, we take the input data (18), (19) and in additional define the BC for the potential φ like a "hat" function on the down and upper faces $z=0$ and $z=1$. These conditions define as

$$\varphi(t, x, y, 0) = -0.5 U_0 - b f, \quad \varphi(t, x, y, 1) = +0.5 U_0 + b f,$$

at the faces $z=0$ and $z=1$ respectively. Here the function $f(x)$ is given by the formula

$$f = \begin{cases} 0.5(\tanh(a(x - 0.25)) + 1), & x < 0.5, \\ 1 - 0.5(\tanh(a(x - 0.75)) + 1), & x \geq 0.5. \end{cases}$$

Here a, b are free parameters, for instance $a = 40, b = 0.1$. We have $\varphi_x(t, x, y, 0) = b f_x = ab \cdot \text{sech}^2(a(x - 0.25))$. Therefore $\max |\varphi_x(t, x, y, 1)| = ab$ and the solution becomes two-dimensional one. The plot of the function $\varphi(t, x, y, 1)$ with respect to x is shown on Figure 3. The function $\varphi(t, x, y, z)$ does not depend on y .

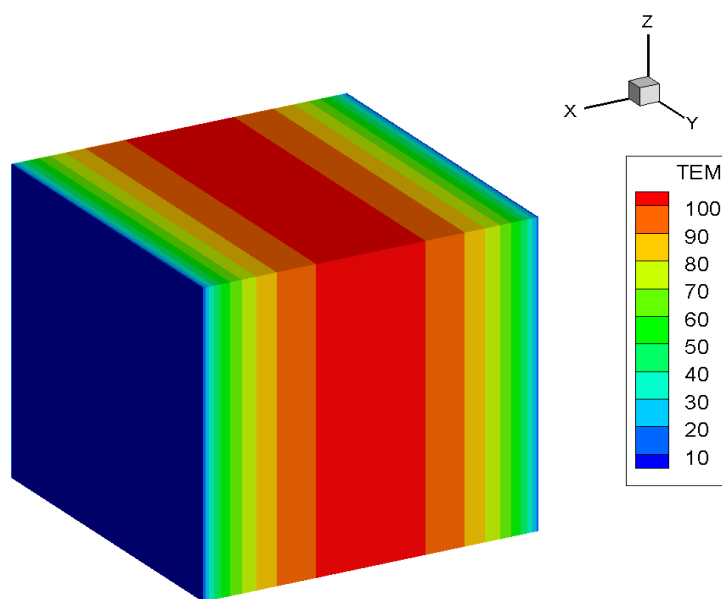


Fig. 2. A typical temperature distribution

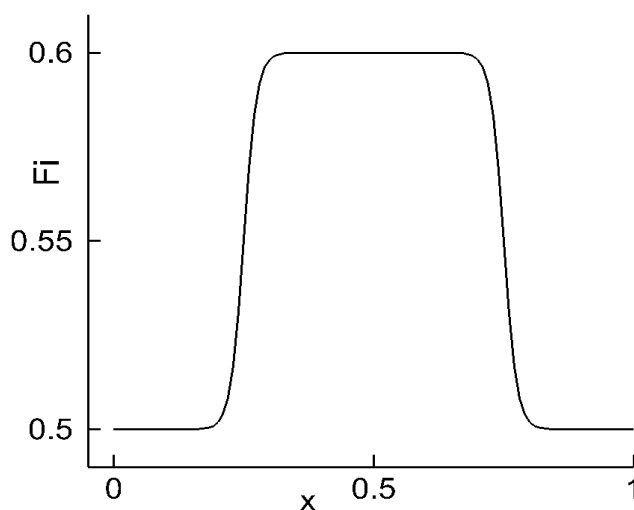


Fig. 3. The profile $\varphi(t, x, y, z)$ along Ox at the point $(z, y) = (1, 0.5)$

In computations we take a few grids with $N_x \times N_y \times N_z$ cells with $N_x = N_z = 128, 256, 512$. Since the sought solution does not depend on y we set $N_y = 3$.

A numerical solution which is obtained on the grid $512 \times 3 \times 512$ practically does not depend on the further grid refinement. Therefore we present the results on this most detailed grid. The parameters of the adaptive multigrid used to solve the implicit discrete system (7), (8) on each time level can be varied, but the results are given below for the following values: the four multigrid levels; the relative accuracy of the coarsest grid equations $ctol = 10^{-3}$; the smoothing factor $\varepsilon_{smooth} = 0.5$; the accuracy of the multigrid iterations $\varepsilon_{tot} = 10^{-6}$.

An initial time step size is $\tau_1 = 0.01$. In the time stepping we increase the time step size with $t_{m+1} = t_m + \tau_m$, $\tau_{m+1} = (m+1) \cdot \tau_m$, $m = 1, 2, \dots$. As a result, a steady-state solution is achieved when $m > 10$. We control the solution stabilization in time with calculation of the norm of the grid functions $\Delta T_m = T_{m+1} - T_m$, $\Delta \varphi_m = \varphi_{m+1} - \varphi_m$. The evolution of the norm of ΔT_m , $\Delta \varphi_m$ is shown on Figure 4. At $m = 11$ the absolute values $\max |\Delta T_m| \approx 0.1$, $\max |\Delta \varphi_m| \approx 3 \cdot 10^{-7}$, i.e. the relative error of the time stepping process is less than 0.01 for temperature and less than 10^{-6} for potential. The difference in the errors has clear explanation: in the heat conduction equation, the source is discontinuous in correspondence with (19).

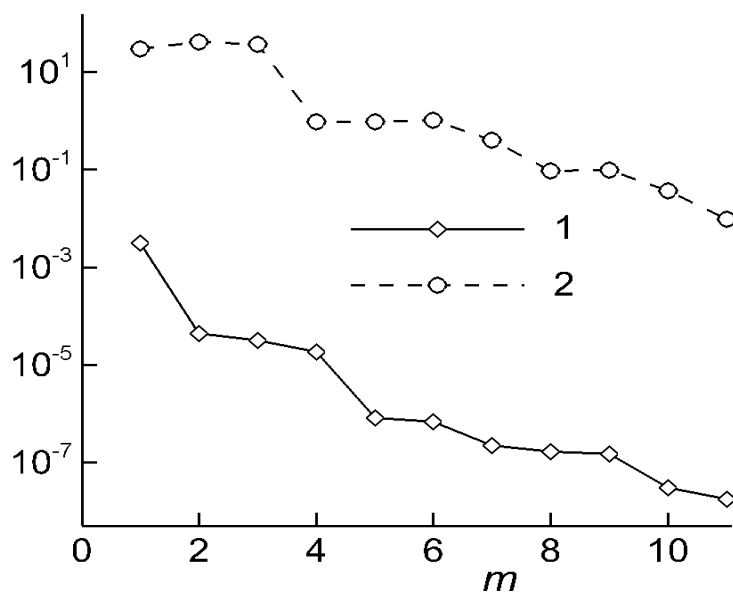


Fig. 4. The time evolution of the norm of $\Delta \varphi_m$ and ΔT_m : 1 and 2 respectively

The Oxz plane distribution of the potential is show on Figure 5. The profiles of the temperature and the vertical component J_z of the electrical current density vector (4) are given on Figure 6, 7 respectively. We show the profiles along Ox at the point $(z, y) = (0.5, 0.5)$. In the central part of the domain, in accordance with (19), there is no

Joule heating, the temperature of this zone achieves $T = 100\text{ K}$ by the heating of this zone due to thermal conductivity.

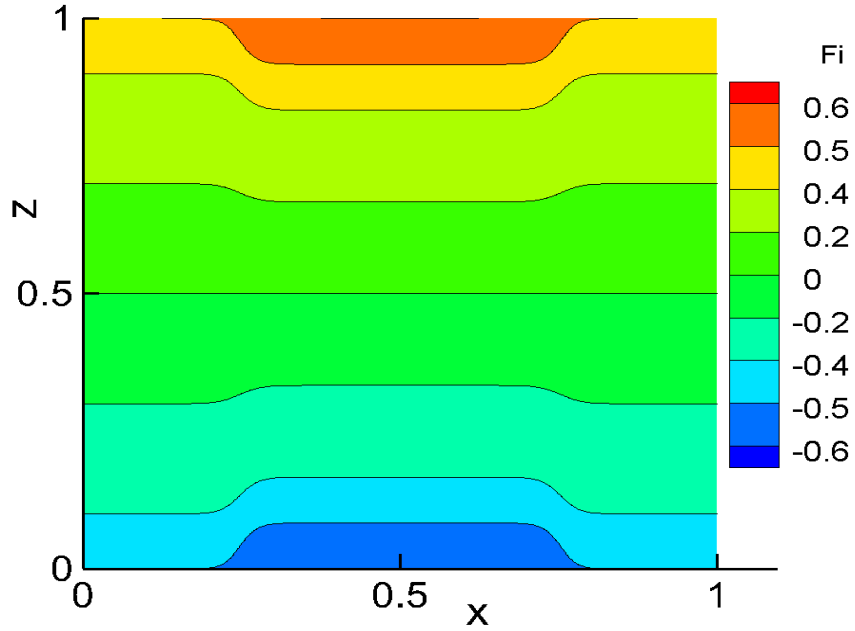


Fig. 5. Potential distribution in Oxz plane

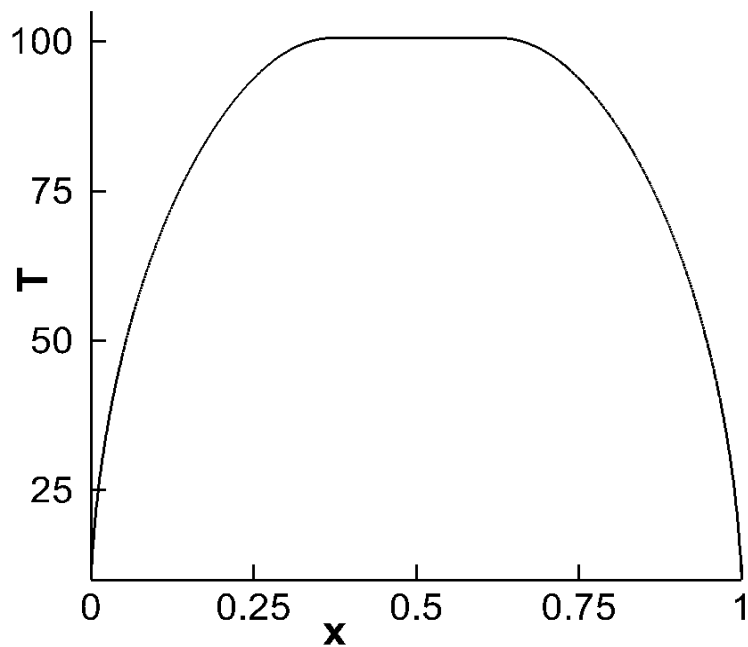


Fig. 6. Temperature: the profile along Ox at the point $(z, y) = (0.5, 0.5)$

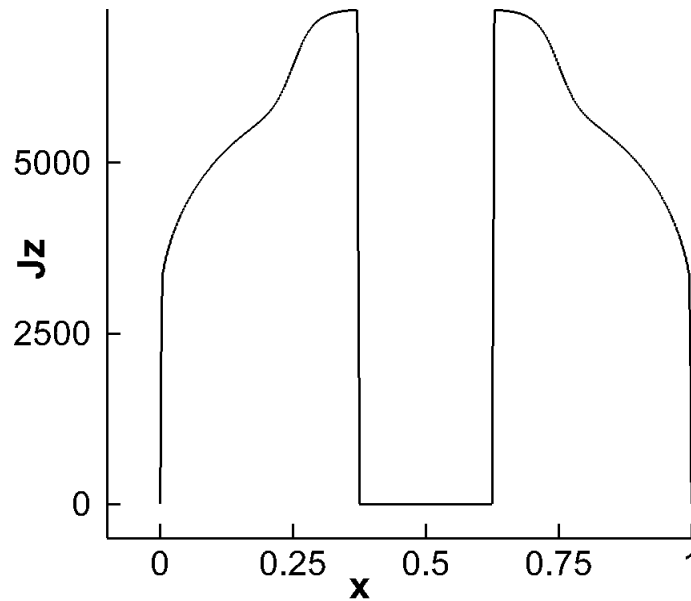


Fig. 7. The vertical component of the electrical current density vector: the profile along Ox at the point $(z, y) = (0.5, 0.5)$

The presented numerical results prove the efficiency of the proposed approach in solving problems with anisotropic discontinuous coefficients, which is typical for HTS problem.

7 CONCLUSION

In this work, an efficient approach to the numerical modelling of coupled electric and thermal fields in high-temperature superconductor (HTS) is developed. The absence of accurate knowledge of superconductivity leads to the need to study HTS structures using mathematical simulations. We have modeled heat transport and the resulting spatial temperature distribution in the presence of Joule self-heating due to electrical current in mesa material.

We have proposed a numerical technique to study temperature and current distributions in large-size mesas with a self-heating effect. The robust algorithm for solving the governing equations is constructed. The key element of the algorithm is an adaptive multigrid method on structured Cartesian grids. The adaptability allows us to realistically simulate the anisotropic phenomena that are typical for HTS problems. The numerical experiments show the robustness of the algorithm as standalone solver for highly anisotropic model problem as well as a solver for the system of two coupled nonlinear equations for the temperature and the electric field potential.

In the case of the usage of the multigrid algorithm as a standalone solver the adaptive approach allows us to achieve automatically the prescribed convergence rate. In the case of two coupled nonlinear equations the efficiency of the multigrid can be improved by analyzing and exploiting a convergence history in the solution process. For optimal incorporation of time-stepping information in the solution process further researches are needed.

The role of interconnections of thermal conductivity, electrical resistance and the device geometry are under investigations.

The adaptive method is suitable for the efficient implementation of the computer code on conformal block-structured grids with potential scalability on ultra-parallel computers with a large number of processors.

The proposed computational technique can be adopted for solving a similar problem, for instance a problem of thermal breakdown in solid dielectrics [26, 27].

Acknowledgements. The study was supported by Russian Foundation for Basic Research (project no. 19-01-00670 A).

REFERENCES

- [1] D.Oikawa, H. Mitarai, H. Tanaka, K. Tsuzuki, Y. Kumagai, T. Sugiura, H. Andoh, and T.Tsukamoto, “Numerical analysis of temperature and current distributions in large-size intrinsic Josephson junctions with self-heating”, *AIP Advances*, **10**, 085113 (2020). <https://doi.org/10.1063/5.0018989>.
- [2] A. Yurgens, “Temperature distribution in a large $\text{Bi}_2\text{Sr}_2\text{CaCu}_2\text{O}_{8+\delta}$ mesa”, *Phys.Rev. B*, **83**, 184501 (2011). <https://doi.org/10.1103/PhysRevB.83.184501>.
- [3] Oliver M. G. Ward, Edward McCann, “The heat equation for nanoconstrictions in 2D materials with Joule self-heating”, *J. Physics D: Applied Physics*, **54**(47), (2021). doi: 10.1088/1361-6463/ac21fe.
- [4] M. Ainsli., D. Hu, V. Zermeno, F. Grilli. “Numerical Simulation of the Performance of High-Temperature Superconducting Coils”, *J. Superconductivity and Novel Magnetism*, **30**, 1987-1992 (2017). <https://doi.org/10.1007/s10948-016-3842-2>.
- [5] V.M. Krasnov, M. Sandberg and I. Zogaj, “In situ Measurement of Self-Heating in Intrinsic Tunneling Spectroscopy”, *Phys. Rev. Lett.*, **94**, 077003 (2005).
- [6] HTS Modelling Workgroup. <http://www.htsmodelling.com>.
- [7] F. Rudau et al, “Three-Dimensional Simulations of the Electrothermal and Terahertz Emission Properties of $\text{Bi}_2\text{Sr}_2\text{CaCu}_2\text{O}_8$ Intrinsic Josephson Junction Stacks”, *Phys. Rev. Appl.*, **5**, 044017 (2016).
- [8] V. Krasnov, A. Yurgens, D. Winkler, P. Delsing, “Self-heating in small mesa structures”, *J. Appl. Phys.*, **89**, 5578-5580 (2001).
- [9] V.M. Krasnov, “Quantum Cascade Phenomenon in $\text{Bi}_2\text{Sr}_2\text{CaCu}_2\text{O}_{8+\delta}$ Single Crystals”, *Phys. Rev. Lett.*, **97**, 257003 (2006).
- [10] V.M. Krasnov, “Non-equilibrium spectroscopy of high-Tc superconductors”, *J. of Phys.: Conf. Ser.*, **150**, 052129 (2009).
- [11] V.M. Krasnov, “Temperature dependence of the bulk energy gap in underdoped $\text{Bi}_2\text{Sr}_2\text{CaCu}_2\text{O}_{8+\delta}$: Evidence for the mean-field superconducting transition”, *Phys. Rev. B.*, **79**(21). (2009).
- [12] M.M. Krasnov, N.D. Novikova, R. Cattaneo, A.A. Kalenyuk, V.M. Krasnov. “Design aspects of $\text{Bi}_2\text{Sr}_2\text{CaCu}_2\text{O}_{8+}$ THz sources: optimization of thermal and radiative properties”, *Beilstein J. Nanotechnol.*, **12**, 1392–1403 (2021). <https://doi.org/10.3762/bjnano.12.103>.
- [13] R. Cattaneo, E. A. Borodianskyi, A. A. Kalenyuk, V. M. Krasnov “Superconducting THz sources with 12% power efficiency”, *Phys. Rev. Appl.*, **16**, L061001 (2021). doi: 10.1103/PhysRevApplied.16.L061001, arXiv:2109.00976 [cond-mat.supr-con].

- [14] Dorbolo S., Ausloos M. “Influence of a low magnetic field on the thermal diffusivity of Bi-2212“, *Phys. rev. B, Condensed matter*, **65**(21) (2002).
- [15] R.P. Fedorenko, “A relaxation method for solving elliptic difference equations”, *Comput. Math. Math. Phys.*, **1** (4), 1092–1096 (1962).
- [16] R.P. Fedorenko, “Iterative methods for elliptic difference equations”, *Russ. Math. Surv.*, **28**(2), 129–195 (1973).
- [17] U. Trottenberg, C.W. Oosterlee, and A. Schuller, *Multigrid*, Academic, New York, (2001).
- [18] V.T. Zhukov, N. D. Novikova, O. B. Feodoritova, “Multigrid method for elliptic equations with anisotropic discontinuous coefficients”, *Comput. Math. Math. Phys.*, **55** (7), 1150–1163 (2015).
- [19] V.T. Zhukov, N.D. Novikova, O.B. Feodoritova, “On the Solution of Evolution Equations Based on Multigrid and Explicit Iterative Methods”, *Comput. Math. Math. Phys.*, **55** (8), 1276–1289 (2015).
- [20] V.T. Zhukov, N.D. Novikova, O.B. Feodoritova, “Parallel multigrid method for solving elliptic equations”, *Math. Models Comput. Simul.* **6**(4), 425–434 (2014).
- [21] V.T. Zhukov, N.D. Novikova, O.B. Feodoritova, “Multigrid method for anisotropic diffusion equations based on adaptive Chebyshev smoothers”, *Math. Montis.*, **36**, 14–26 (2016).
- [22] O.B. Feodoritova, M.M. Krasnov, V.T. Zhukov, “Adaptive technique for Chebyshev-based solvers for three-dimensional elliptic equations”, *J. Phys: Conf. Ser.*, 012012 (2018).
- [23] O.B. Feodoritova, V.T. Zhukov, “An adaptive multigrid on block-structured grids”, *J. Phys.:Conf.Ser.*, 1640012020 (2020). doi:10.1088/1742-6596/1640/1/012020.
- [24] A.A. Samarskii, E.S. Nikolaev, *Numerical Methods for Grid Equations, v.1 Direct Methods, v.2 Iterative Methods*. Birkhauser Verlag, Basel, Boston, Berlin. (1989).
- [25] F. R. Gantmacher, *The Theory of Matrices*. Chelsea, New York. (1959).
- [26] E. Zipunova, E. Savenkov, “Phase field model for electrically induced damage using microforce theory”, *Math. and Mechanics of Solids*, (2021). doi:10.1177/10812865211052078.
- [27] E. Zipunova, E. Savenkov, “On the Diffuse Interface Models for High Codimension Dispersed Inclusions”, *Mathematics*, **9**(18). 2206.(2021) <https://doi.org/10.3390/math9182206>.

Received, December 20, 2021

MOLECULAR DYNAMICS STUDY OF THERMAL HYSTERESIS DURING MELTING-CRYSTALLIZATION OF NOBLE METALS

V.I. MAZHUKIN, O.N. KOROLEVA*, A.V. SHAPRANOV,
A.A. ALEKSASHKINA, M.M. DEMIN

Keldysh Institute of Applied Mathematics of RAS
*Corresponding author. E-mail: koroleva.on@mail.ru

DOI: 10.20948/mathmontis-2022-53-8

Summary. By constructing the thermal hysteresis of the enthalpy and density of the noble metals of gold (Au) and copper (Cu), non-equilibrium processes are investigated during the melting – crystallization phase transformations, i.e. during the solid–liquid transition. Thermal hysteresis is obtained from the atomistic modeling. The limiting temperatures of superheating of the solid phase during melting and undercooling of the liquid phase during crystallization of gold and copper are obtained. The possibility of the formation of highly superheated-undercooled metastable states of solid and liquid phases with rapid heating-cooling of the studied metals has been confirmed. The results obtained are compared with the results of alternative calculations.

1 INTRODUCTION

The phenomenon of melting-crystallization of metals, which is a phase transformation of the first kind, plays an important role in materials science and engineering. In recent years, extensive experimental [1-10] and theoretical studies combined with modeling of melting-crystallization of solids [11-21] have significantly expanded the understanding of the nature of this phenomenon. The processes of melting-crystallization proceeding in a quasi-equilibrium way are the most studied [22,23,24]. The trajectory of melting-crystallization processes in phase space passes through the equilibrium states only in the extreme case of infinitely slow heating/cooling. In this case, the temperatures of the beginning and end of melting, as well as the beginning and end of crystallization, will coincide both with each other and with the equilibrium melting temperature. Changing the heating regimes of the target can lead to a non-equilibrium behavior of the melting – crystallization processes, manifested in the phenomenon of thermal hysteresis. Thermal hysteresis is characterized by a mismatch of melting and crystallization temperatures, as well as thermodynamic characteristics of the material (enthalpy, density) during heating and cooling. The study of thermal hysteresis has been carried out by many researchers both experimentally [1-4] and theoretically [17-21]. The studies were carried out mainly to analyze the dimensional effect and the influence of the interphase structure on the melting processes [2,4,5,7,17,21], to study the degree of overheating-undercooling of metals [1-3,18-20], the influence of thermal hysteresis on the properties of metals [2,17,18].

One of the regimes of thermal action, in which the phenomenon of thermal hysteresis of metals occurs, is the rapid action of powerful concentrated energy flows on the target. Under such influence, the melting-crystallization processes become non-equilibrium, and phase transitions are accompanied by the appearance of metastable superheated-undercooled states

2020 Mathematics Subject Classification: 82C26, 82M37, 00A69.

Key words and Phrases: Thermal hysteresis, Molecular dynamics, Phase transitions.

in the initial phase [20,25]. The magnitude of thermal hysteresis, being a characteristic of the degree of superheating-undercooling of the condensed phase, is related to the velocity of the phase front [12, 26]. The magnitude of energy costs during the destruction of long-range bonds during melting gives an idea of the degree of non-equilibrium of the melting process. Therefore, the hysteresis properties are of significant interest for the study of non-equilibrium melting-crystallization. The study of this phenomenon also contributes to solving such a fundamental problem as determining the limit values of superheating of a solid and undercooling of a liquid. The experimental approach to the study of thermal hysteresis of materials, which is traditional, has a number of limitations, primarily in the range of measurement conditions, especially in the melting region. It is known that experiments on the study of undercooling of metals [10] are well described in the literature, in contrast to studies of superheating. Because of this, it is relevant to use the theoretical approach [11-17, 19-21, 26, 27] in the study of melting-crystallization processes, the main tool of which is the method of molecular dynamics (MD).

This article discusses the features of non-equilibrium melting and crystallization of noble metals of gold and copper based on thermal hysteresis of enthalpy and density in the temperature range $0.60 \leq T \leq 2.00$ kK. Thermal hysteresis is obtained for the metals under study from the molecular dynamic modeling. The potentials from the “embedded atom method” (EAM) group developed and tested in [27] for gold and in [28] for copper were used as interparticle interaction potentials.

2 METHODS AND APPROACHES

In this paper, the thermal hysteresis of enthalpy and density for gold and copper is obtained based on an atomistic approach. The method of molecular dynamics (MD) has become widely used for the numerical solution of atomistic models. The atomistic approach is based on a model representation of a polyatomic molecular system in which all atoms are represented by material points whose motion is described by classical Newton equations. Atomistic models are a system of differential equations, for the integration of which initial conditions are set in the form of values of coordinates and velocities of all particles at the initial time $t = 0$. The resulting system of ODE is solved using the finite-difference Verlet scheme [29].

In MD modeling, the choice of the interaction potential between the particles plays an important role, since the reliability of the results obtained directly depends on it. To model the properties of the metals under consideration, the potentials from the EAM group were used, developed and tested for gold in [27], for copper in [28], allowing for a good description of both the crystalline and liquid phases of the metals under study.

For both metals, the simulation was carried out in the temperature range $0.60 \leq T \leq 2.00$ kK using the widespread LAMMPS package (large-scale atomic-molecular massively parallel simulator) [30]. It implements support for many paired and multiparticle short-range potentials, the ability to record atomic configurations in a text file, and also has built-in thermostats and barostats. The temperature and pressure for the ensemble of particles were regulated using a thermostat and a Berendsen’s barostat [31].

In this paper, the enthalpy and density of metals in an isobaric heating and cooling process involving phase transitions were determined from a series of molecular dynamic calculations within the framework of a single computational experiment. The computational experiments planned in a similar way were carried out for both metals. The calculated area was selected in

the form of a cube, with dimensions of $30 \times 30 \times 30$ elementary cells, containing a FCC crystal of 108,000 particles. Periodic boundary conditions were set in all directions. The particle velocities were set in accordance with the Maxwell distribution at a temperature of 0.60 kK. The relaxation procedure preceding the simulation was carried out at a temperature of 0.30 kK and zero pressure. Next, the sample was heated at a constant rate of approximately $V \sim 0.56 \times 10^{12}$ K/s. Heating continues to a temperature of 2.0 kK, at which the sample was completely melted, which made it possible to record the temperature dependences of density $\rho(T)$ and enthalpy $H(T)$ during heating. At the same time, the sample was prepared for cooling and subsequent registration of the dependences of density $\rho(T)$ and enthalpy $H(T)$ during cooling. Cooling, as well as heating, of the sample was carried out at the same constant speed V . The experiments were carried out at a constant zero pressure $P = 0$.

During modeling of the changes in a condensed medium, it is important to distinguish its aggregate state due to long-range and short-range bonds. The order parameter can be used as a criterion for this. In order to distinguish the type of ordering during the melting-crystallization phase transition, the order parameter of the heating and cooling was obtained for copper and gold. The approaches to determining the order parameter used in this paper are presented in [32].

3 MODELING RESULTS

The results of MD modeling are presented in Fig.1-4. Fig.1(a,b) shows the thermal hysteresis loops of the enthalpy of gold and copper, which are represented by the generally accepted values of the increment $\Delta H(T) = H(T) - H(0.298 \text{ kK})$. The hysteresis of the density of copper and gold is shown in Fig.2 (a,b). Figure 3.4 shows the order parameter for the heating and cooling of copper and gold. The vertical dotted lines in all figures indicate the equilibrium melting point, which for gold is $T_m = 1.332$ kK, for copper – $T_m = 1.33$ kK. These values of the equilibrium melting point of copper and gold are obtained from molecular dynamic calculations [33, 34] using the potentials [27,28]. The reference values [35] of the equilibrium melting point are for gold $T_m = 1337$ K and copper $T_m = 1356$ K. The difference between the reference values and the obtained values for gold was $\Delta T_m = 0.38\%$ and for copper $\Delta T_m = 1.96\%$. The error is quite acceptable for modeling.

Figures 1, 2 also show the temperature of the end of crystallization T_{cr} , the limit temperatures of superheating of the solid phase T^+ and supercooling of the liquid phase T^- , which are the temperatures of the beginning of melting and the beginning of crystallization, respectively. These temperatures determine the vertices of the hysteresis contour, which in Figures 1, 2 is indicated by the letters ABCDEF.

The thermal hysteresis loops (Fig. 1,2) are formed when the heating (red) and cooling (blue) curves are combined, taking into account the forward (melting) and reverse (crystallization) phase transitions. The directions of the heating and cooling processes are shown in Figures 1,2 with arrows. In the considered temperature range, the heating of copper and gold occurs with the absorption of heat (endoprocess), which is expressed in the superheating of the solid phase. The most important characteristic of the stability limit of the crystal lattice is the limit temperature of superheating of the solid phase T^+ . The maximum superheating temperatures of gold and copper, normalized by the corresponding equilibrium melting temperatures T_m , are shown in Table 1.

	Heating			Cooling			Ref. [20]				Ref. [37]
	T_m [kK]	T^+	θ^+	T_{cr} [kK]	T^-	θ^-	θ_{md}^+	θ_{ns}^+	θ_{md}^-	θ_{ns}^-	θ_{ns}^+
Au	1.332	$1.235T_m$	0.235	0.983	$0.589T_m$	0.354	0.3	0.2	0.44	0.25	0.184
Cu	1.33	$1.203T_m$	0.203	0.975	$0.603T_m$	0.357	0.21	0.19	0.3	0.24	0.174

Table 1. Heating-cooling properties of gold and copper.

As one can see, the value of superheating in gold is slightly higher than in copper. Upon reaching the temperature T^+ (point B in the hysteresis contour in Fig. 1, 2), a superheated metastable state of the solid phase begins to form, which is characterized by the beginning of the formation of stable nuclei of the liquid phase and intensive destruction of the crystal lattice. Therefore, the temperature of the ultimate overheating T^+ is the temperature of the beginning of melting. The formation of a metastable state in both gold and copper is accompanied by a further drop in the density of the solid phase (Fig. 2). During the melting process, in the temperature range $T_m < T < T^+$ (line BC of the hysteresis contour in Fig.1, 2), part of the kinetic energy of the chaotic motion of particles is spent on the destruction of the crystal lattice. The temperature of the end of melting (Fig. 1, Fig.2) in our calculation, at the heating rate $V \sim 0.56 \times 10^9$ kK/s, it practically coincides with the equilibrium melting point of each of the metals T_m . At a higher heating rate, the difference between these temperatures can be significant [36,37]. With further heating, the thermal expansion of the liquid occurs. Relative overheating of the solid phase $\theta^+ = (T^+ - T_m)/T_m$, which is observed in the enthalpy hysteresis (Fig.1) and the densities (Fig.2) of the metals under study are given in Table 1. For gold $\theta^+ \approx 0.235$, for copper – $\theta^+ \approx 0.203$. In [20], the values of relative overheating of gold $\theta_{md}^+ \approx 0.3$ (md index) and copper $\theta_{md}^+ \approx 0.21$ were obtained from MD calculations with a heating rate $V = 10^9$ kK/s and calculated using the classical theory of homogeneous nucleation (ns - nucleation in the solid phase) for gold $\theta_{ns}^+ \approx 0.2$, for copper $\theta_{ns}^+ \approx 0.19$. In [38], the values of the relative overheating of the solid phase of copper $\theta_{ns}^+ \approx 0.174$ and gold $\theta_{ns}^+ \approx 0.184$ were also obtained. Comparison of the obtained results with the results of alternative calculations [20, 38] shows a good correspondence. According to estimates [17, 20], metals can be superheated to the temperature of the beginning of a massive homogeneous transformation $T^+ \approx 1.3T_m$, which is also consistent with the results for the metals studied in this work.

The melting phase transition at a temperature of $\sim T_m$ for gold and copper (see Table 1) is clearly identified by a large difference in the enthalpies of the liquid and solid phases, representing the specific heat of melting L_m of the metals under study. According to the results of calculations, the specific heat of melting for gold is $L_m \approx 12.39$ kJ/mol, or 43.14%, for copper – $L_m \approx 12.05$ kJ/mol, or 41.46% (Fig.1). The increase in enthalpy is accompanied by a decrease in density, while the difference in density of the liquid and solid phases is for gold $\Delta\rho_{melt}(T_{sl}) \approx 6\%$, and for copper $\Delta\rho_{melt}(T_{sl}) \approx 4.8\%$ (Fig.2 (a,b)). The temperature dependences of the order parameter of copper and gold during heating are shown in Fig.3 (a, b). With increased heating, the order parameters of the solid phase decrease until the maximum temperature of superheating $T^+ > T_m$ is reached, resulting in the destruction of the crystal lattice and intensive nucleation of the liquid phase. At a temperature close to T_m , the order parameter decreases sharply to almost zero, confirming the transformation of a metal

crystal into a liquid. As one can see, during the phase transition of the 1st kind, the order parameter changes abruptly.

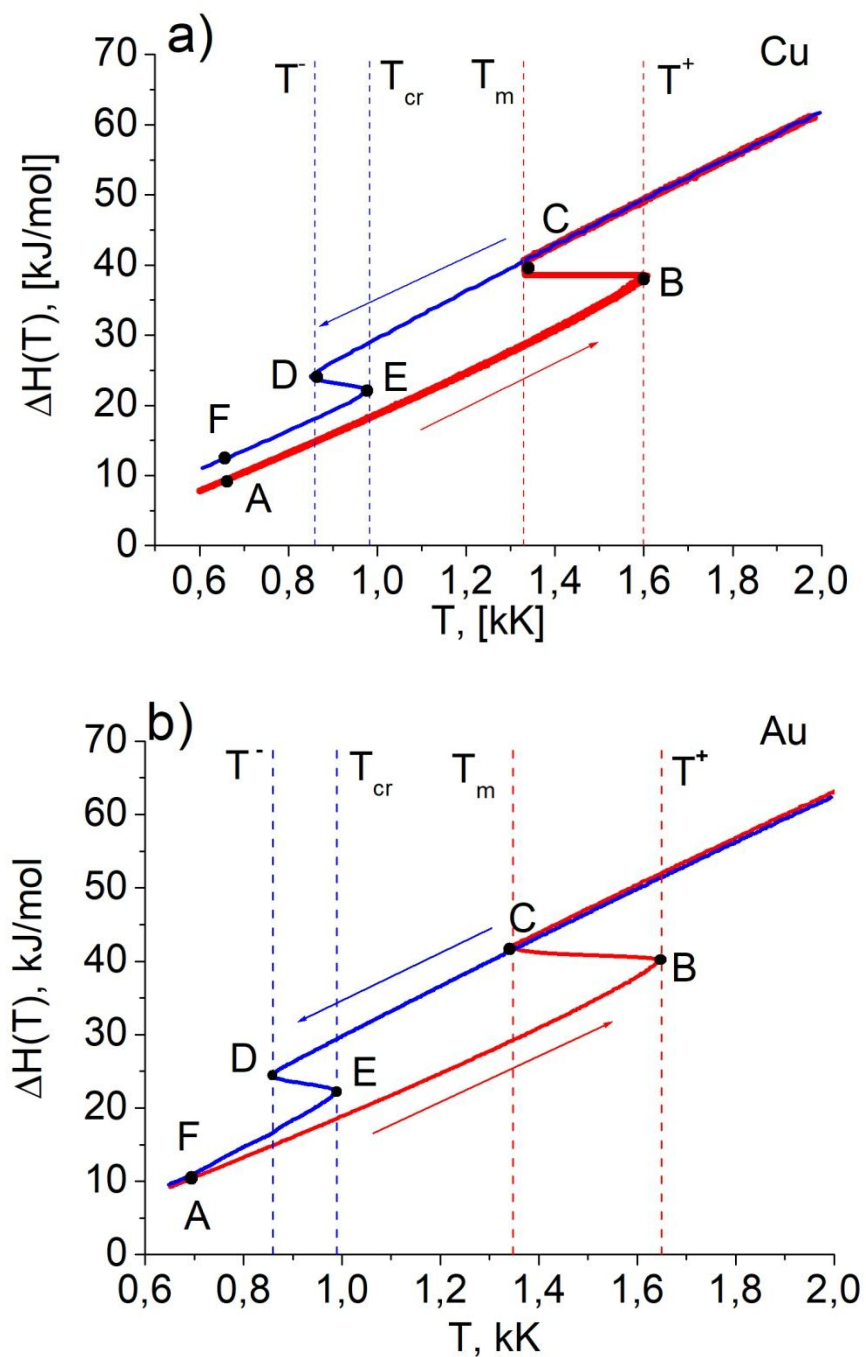


Fig. 1. Thermal hysteresis of enthalpy for a) copper, b) gold.

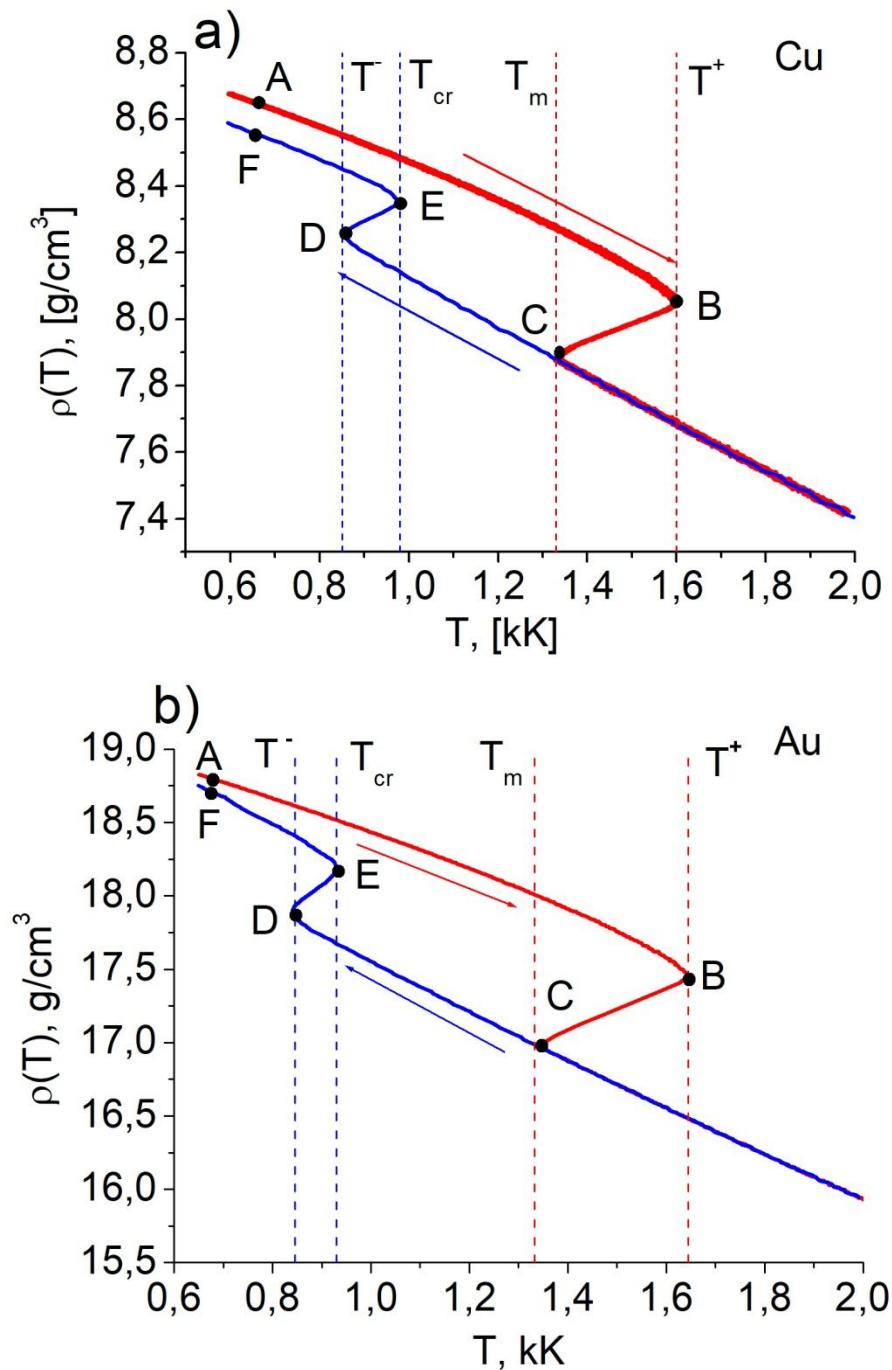


Fig. 2. Thermal hysteresis of density for a) copper, b) gold.

Cooling of copper and gold targets, unlike heating, occurs with the release of heat and is an isoprocess. Crystallization turns out to be much more sensitive to the cooling rate. The ultimate undercooling temperature T of the liquid phase, normalized to the melting point T_m , for gold and copper is shown in Table 1. The ultimate temperature of undercooling is the temperature of the beginning of crystallization, at which the formation of the first stable

nuclei of a new solid phase occurs. On the segment DE of the hysteresis contour (Fig. 1,2), there is a rapid growth of the formed nuclei of the new phase due to the rapid movement of their boundaries along the undercooled liquid phase, representing the crystallization fronts. In this case, the crystallization fronts are always undercooled relative to the equilibrium melting temperature T_m . At the point E (temperature T_{cr}), the liquid phase completely disappears.

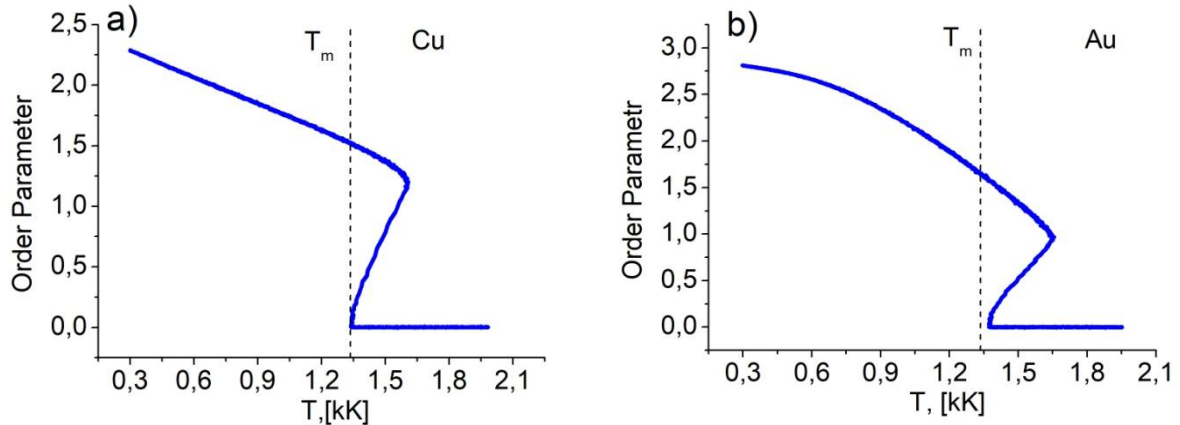


Fig. 3. Order parameter during heating of a) copper и b) gold.

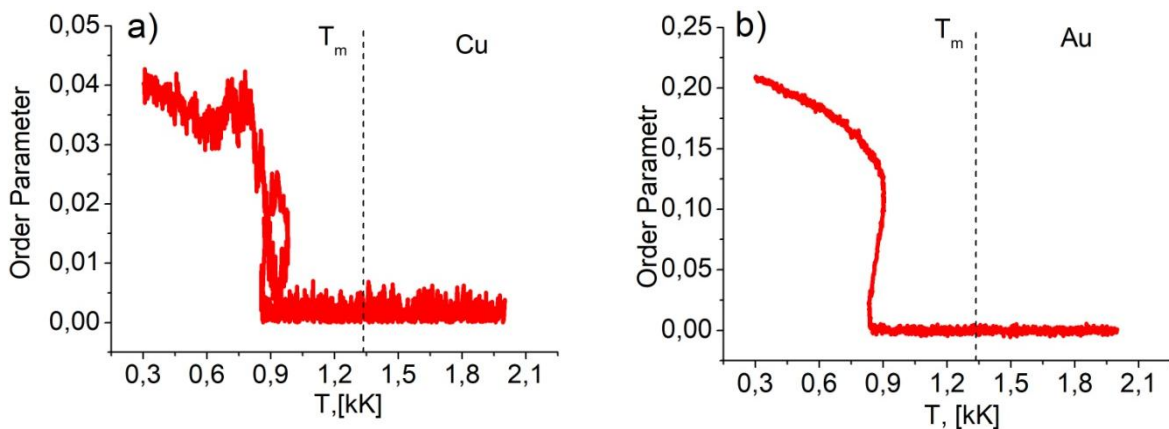


Fig. 4. Order parameter during cooling of a) copper и b) gold.

The end of crystallization occurs at the T_{cr} temperature given for copper and gold in Table 1 (point E in the hysteresis contour in Fig. 1, 2). In our calculation, due to the high cooling rate $V \sim 0.56 \times 10^9$ kK/s, the crystallization termination temperature T_{cr} is lower than the equilibrium melting temperature T_m , by $T_m - T_{cr} = 0.355$ kK for copper, and by $T_m - T_{cr} = 0.349$ kK for gold. Too high cooling rate in our calculation led to the fact that the density of the substance at the T_{cr} temperature turned out to be less by 1.7% in gold and 1.51% in copper than the density of the crystal when heated. The density of the new phase despite the constant increase of it (line EF in Fig. 2) remains less than the crystalline one (the line AB of the hysteresis contour in Fig. 2). This discrepancy is especially noticeable in copper, where the density of the new phase is less than the crystalline one at $T = 0.6$ kK by 1.06%, whereas in gold this difference is only 0.355%. Figure 4 (a) shows the temperature dependence of the

order parameter during cooling for copper. The order parameter of copper during cooling is by ~98.2% less than the order parameter of the crystal during heating (Fig. 3(a)), which indicates a strong undercooling of the melt, in which non-crystalline types of the solid phase (vitrification or amorphization) are realized. The order parameter of gold during cooling (Fig. 4 (b)) is about 10 times less than the order parameter of the crystal during heating (Fig. 3 (b)), which also indicates, although to a lesser extent, a strong undercooling of the melt and the formation of non-crystalline solid phase species.

Relative undercooling of the liquid phase $\theta^- = (T_m - T)/T_m$, which is observed in the enthalpy hysteresis (Fig.1) and densities (Fig.2), according to the results of MD modeling for gold and copper are presented in Table 1. Comparison with the results [20] obtained from MD calculations and from calculations using the classical theory of homogeneous nucleation, are respectively for copper $\theta_{md}^- \approx 0.3$, $\theta_{ns}^- \approx 0.24$ and for gold $\theta_{md}^- \approx 0.44$, $\theta_{ns}^- \approx 0.25$, which shows a good agreement with the presented results.

The maximum hysteresis value in this work was for gold $\Delta T_{\text{Hyst}} = T^+ - T^- \approx 0.589T_m$ and for copper $\Delta T_{\text{Hyst}} = T^+ - T^- \approx 0.56T_m$, which is consistent with the estimate of the hysteresis width for metals of $0.66T_m$ [17].

The resulting thermal hysteresis of enthalpy and density, as well as the order parameter for heating and cooling of gold and copper, demonstrate the formation of metastable regions and the non-equilibrium nature of melting-crystallization processes.

4. CONCLUSIONS

The hysteresis of the enthalpy and density of gold and copper in the range of $0.6 \text{ kK} \leq T \leq 2.0 \text{ kK}$ was obtained from a series of molecular dynamic calculations within the framework of one computational experiment. The resulting hysteresis demonstrates the formation of metastable regions and the nonequilibrium nature of the melting-crystallization processes of the studied noble metals. The analysis of the thermal hysteresis value at the heating and cooling rate $V \sim 0.56 \times 10^{12} \text{ K/s}$ allowed us to estimate the degree of superheating-undercooling of the condensed phase. The obtained limit temperature of superheating of the metastable state of the solid phase and relative superheating, as well as the limit temperature of undercooling and relative undercooling of the liquid phase of both metals are in good agreement with the results of alternative calculations [17,20,38]. The maximum hysteresis value for gold $\Delta T_{\text{Hyst}} \approx 0.589T_m$, for copper $\Delta T_{\text{Hyst}} \approx 0.56T_m$ is consistent with the estimate of the hysteresis width for metals of $0.66T_m$ [17].

REFERENCES

- [1] Q. Xu, I. D. Sharp, C. W. Yuan, D. O. Yi, C. Y. Liao, A. M. Glaeser, A. M. Minor, J.W. Beeman, M. C. Ridgway, P. Kluth, J. W. Ager, D. C. Chrzan, and E. E. Haller, "Large melting point hysteresis of Ge nanocrystals embedded in SiO₂", *PRL*, **97**(13), 155701 (2006).
- [2] Hugo K. Christenson, "Confinement effects on freezing and melting", *J. Phys.: Condens. Matter*, **13**, R95–R133 (2001).
- [3] A.L. Pirozerski, O.I. Smirnova, A.I. Nedbai, O.L. Pirozerskaya, N.A. Grunina, V.M. Mikushev, "Peculiarities of melting and crystallization of n-decane in a porous glass", *Phys. Let. A*, **383**, 125872 (2019).

- [4] K.K. Nanda, “Bulk cohesive energy and surface tension from the size-dependent evaporation study of nanoparticles”, *Appl. Phys. Lett.*, **87**, 021909 (2005).
- [5] V.D. Aleksandrov, V.A. Postnikov, “The effect of sample mass on the crystallization supercooling in bismuth melt”, *Tech. Phys. Lett.*, **29**, 287–289 (2003). Doi: 10.1134/1.1573293.
- [6] T.T. Järvi, Antti Kuronen, Kristoffer Meinander, Kai Nordlund, Karsten Albe, “Contact epitaxy by deposition of Cu, Ag, Au, Pt, and Ni nanoclusters on (100) surfaces: Size limits and mechanisms”, *Phys. Rev. B*, **75**(11), 115422 (2007). Doi: 10.1103/PhysRevB.75.115422.
- [7] J-P. Borel, “Thermodynamical size effect and the structure of metallic clusters”, *Surf. Sci.*, **106**, 1-9 (1981).
- [8] D.R. Uhlmann, “On the internal nucleation of melting”, *J. Non-Crystalline Solids*, **41**, 347-357 (1980).
- [9] R. Kofman, P. Cheyssac, A. Aouaj, Y. Lereah, G. Deutscher, T. Ben-David, J. M. Penisson, A. Bourret, “Surface melting enhanced by curvature effect”, *Surf. Sci.*, **303**(1-2), 231–246 (1994). Doi: [10.1016/0039-6028\(94\)90635-1](https://doi.org/10.1016/0039-6028(94)90635-1)
- [10] K.F. Kelton, “Crystal Nucleation in Liquids and Glasses”, *Solid State Phys.*, **45**, 75-177 (1991).
- [11] V.I. Mazhukin, A.V. Shapranov, M.M. Demin, and N.A. Kozlovskaya, “Temperature Dependence of the Kinetics Rate of the Melting and Crystallization of Aluminum”, *Bull. Lebedev Phys. Inst.*, **43**(9), 283–286 (2016). Doi: 10.3103/S1068335616090050
- [12] V.I. Mazhukin, A.V. Shapranov, V.E. Perezhigin, O.N. Koroleva, A.V. Mazhukin, “Kinetic melting and crystallization stages of strongly superheated and supercooled metals”, *Math. Models Comput. Simul.*, **9**(4), 448–456 (2017). Doi: 10.1134/S2070048217040081
- [13] Linggang Wu, Yiyang Zhu, Hao Wang, Mo Li, “Crystal/melt coexistence in fcc and bcc metals: a molecular-dynamics study of kinetic coefficients”, *Model. Simul. Mater. Sci. Eng.*, **29**(6), 065016 (2021).
- [14] V.I. Mazhukin, A.V. Shapranov, A.V. Mazhukin, O.N. Koroleva, “Mathematical formulation of a kinetic version of Stefan problem for heterogeneous melting/crystallization of metals”, *Math. Montis.*, **36**, 58-77 (2016).
- [15] Zhong-Li Liu, Jun-Sheng Sun, Rui Li, Xiu-Lu Zhang, Ling-Cang Cai, “Comparative Study on Two Melting Simulation Methods: Melting Curve of Gold”, *Commun. Theor. Phys.*, **65**, 613–616 (2016).
- [16] B. Rethfeld, K. Sokolowski-Tinten, D. von der Linde, S.I. Anisimov, “Ultrafast thermal melting of laser-excited solids by homogeneous nucleation”, *Phys. Rev. B*, **65**, 092103 (2002).
- [17] L.A. Boryniak, A.P. Chernyshev, “Temperaturny`i gisterezis pri plavlenii i kristallizatsii nanoobektov”, *Nauchny`i vestnyk NGTU*, **1**(54), 172-179 (2014).
- [18] V.D. Aleksandrov, O.A. Pokyntylytsia, A.Y. Sobolev, “Thermal hysteresis during the melting and crystallization of macroobjects”, *Tech. Phys.*, **62**, 741–744 (2017). Doi:10.1134/S1063784217050036
- [19] Laurent J. Lewis, Pablo Jensen, Jean-Louis Barrat, “Melting, freezing, and coalescence of gold nanoclusters”, *Phys. Rev. B*, **56**(4), 1-12 (1997). Doi: [10.1103/PhysRevB.56.2248](https://doi.org/10.1103/PhysRevB.56.2248)
- [20] S.-N. Luo, T.J. Ahrens, T. Çağın, A. Strachan, W.A. Goddard, D.C. Swift, “Maximum superheating and undercooling: Systematics, molecular dynamics simulations, and dynamic experiments”, *Phys. Rev. B*, **68**(13), 134206 (2003). Doi:10.1103/physrevb.68.134206
- [21] Q.S. Mei, K. Lu, “Melting and superheating of crystalline solids: from bulk to nanocrystals”, *Progr. Mater. Sci.*, **52**(8), 1175–1262 (2007). Doi: [10.1016/j.pmatsci.2007.01.001](https://doi.org/10.1016/j.pmatsci.2007.01.001)
- [22] D.V. Sivukhin, *Obshchiiy kurs fiziki: Termodinamika i molekuliarnaia fizika. Uchebnoe posobie. T.2.*, M.: Fizmatlit. Izd-vo MFTI, (2005)
- [23] A.K. Fedotov, *Fizicheskoe materialovedenie. Ch. 2. Fazovye prevrashcheniia v metallakh i splavakh*, Minsk : Vysh. shk., (2012)

- [24] V.D. Aleksandrov, V.N. Aleksandrova, A.A. Barannikov, *et al.*, “Melting and crystallization of copper, silver, and gold droplets”, *Tech. Phys. Lett.*, **27**, 258–259 (2001). Doi:10.1134/1.1359845.
- [25] S. Williamson, G. Mourou, J.C.M. Li, “Time-resolved laser-induced phase transformation in aluminum”, *Phys. Rev. Lett.*, **52**(26), 2364–2367 (1984). Doi:10.1103/physrevlett.52.2364
- [26] V.I. Mazhukin, A.V. Shapranov, O.N. Koroleva, “Atomistic modeling of crystal-melt interface mobility of fcc (Al, Cu) and bcc (Fe) metals in strong superheating/undercooling states”, *Math. Montis.*, **48**, 70-85 (2020). Doi: 10.20948/mathmontis-2020-48-7
- [27] V.V. Zhakhovskii, N.A. Inogamov, Yu.V. Petrov, S.I. Ashitkov, K. Nishihara, “Molecular dynamics simulation of femtosecond ablation and spallation with different interatomic potentials”, *Appl. Surf. Sci.*, **255**, 9592-9596 (2009).
- [28] Y. Mishin, M. J. Mehl and D. A. Papaconstantopoulos, A. F. Voter, J. D. Kress, “Structural stability and lattice defects in copper: Ab initio, tight-binding, and embedded-atom calculations”, *Phys. Rev. B*, **63**, 224106 (2001).
- [29] L. Verlet, “Computer “Experiments” on Classical Fluids. I. Thermodynamical Properties of Lennard-Jones Molecules”, *Phys. Rev.*, **159**, 98-103 (1967).
- [30] S. Plimpton, “Fast parallel algorithms for short-range molecular dynamics”, *J. Comput. Phys.*, **117**(1), 1-19 (1995).
- [31] H.J.C. Berendsen, J.P.M Postma, W.F. van Gunsteren, A. DiNola, J.R. Haak, “Molecular dynamics with coupling to an external bath”, *J. Chem. Phys.*, **81**, 3684 – 3690 (1984).
- [32] V.I. Mazhukin, A.V. Shapranov, “Matematicheskoe modelirovanie processov nagreva i plavleniia metallov. Chast I. Model i vychislitelnyi algoritm”, *KIAM Preprint №31*, (2012).
- [33] M.M. Demin, A.A. Aleksashkina, O.N. Koroleva, “Atomistic modeling of gold characteristics in the region of the meltingcrystallization phase transition”, *KIAM Preprint №1*, (2020).
- [34] M.M. Demin, O.N. Koroleva, A.A. Aleksashkina, V.I. Mazhukin, “Molecular-dynamic modeling of thermophysical properties of the phonon subsystem of copper in wide temperature range”, *Math. Montis.*, **47**, 137-151 (2020).
- [35] *Fizicheskie velichiny. Spravochnik*, I.S. Grigoriev, E.Z. Melihov [Ed.], M: Energoatomizdat (1991)
- [36] V.I. Mazhukin, M.G. Lobok, B.N. Chichkov, “Modeling of fast phase transitions dynamics in metal target irradiated by pico and femto second pulsed laser”, *Appl. Surf. Sci.*, **255**, 5112-5115 (2009).
- [37] V.I. Mazhukin, A.V. Shapranov, V.E. Perezhigin, “Matematicheskoe modelirovanie teplofizicheskikh svoistv, processov nagreva i plavleniia metallov metodom molekuliarnoi dinamiki”, *Math. Montis.*, **24**, 47-65 (2012).
- [38] K. Lu, Y. Li, “Homogeneous nucleation catastrophe as a kinetic stability limit for superheated crystal”, *Phys. Rev. Lett.*, **80**(20), 4474–4477 (1998). Doi:10.1103/physrevlett.80.4474

Received, February 2, 2022